

**INVESTIGATION INTO THE MOLECULAR
MECHANISMS OF INHERITED RENAL
CANCER**

By

Michael Stefan Nahorski

A thesis submitted to
The University of Birmingham
for the degree of
DOCTOR OF PHILOSOPHY

College of Medicine & Dentistry
The University of Birmingham
March 2012

UNIVERSITY OF
BIRMINGHAM

University of Birmingham Research Archive

e-theses repository

This unpublished thesis/dissertation is copyright of the author and/or third parties. The intellectual property rights of the author or third parties in respect of this work are as defined by The Copyright Designs and Patents Act 1988 or as modified by any successor legislation.

Any use made of information contained in this thesis/dissertation must be in accordance with that legislation and must be properly acknowledged. Further distribution or reproduction in any format is prohibited without the permission of the copyright holder.

Abstract

Birt Hogg Dubé (BHD) syndrome is an inherited cancer susceptibility syndrome characterised by the development of fibrofolliculomas on the face and upper torso, and increased risk of lung cysts, spontaneous pneumothorax and renal cancer. The findings presented in this thesis advance knowledge into how the mutations in the *FLCN* gene cause the phenotypes associated with BHD syndrome, and provides novel insights into the functions of folliculin within the cell. The results presented provide further evidence of the association between BHD syndrome and increased risk of colorectal cancer in a subset of BHD syndrome families, and suggest that this association appears restricted to those patients with an exon 11 mononucleotide tract mutation. Evolutionary conservation analysis across the *FLCN* sequence suggests that pathogenic mutations could be expected throughout the gene, and identifies a region between codons 100-230 of increased evolutionary significance. The experiments undertaken demonstrate a practical strategy for determining the pathogenicity of non-truncating folliculin variants *in vitro*, and indicate that loss of protein stability is the main mechanism of pathogenicity for the previously reported non-truncating mutations within *FLCN*. Finally, this thesis reports the first identification of p0071 as a folliculin interacting protein. Folliculin deficiency exerts a functional impact on previously reported p0071 functions inducing RhoA signalling upregulation, mitotic defects and disruption of cell junctions. These results demonstrate the potential efficacy of using inhibitors downstream of RhoA as therapeutic targets in BHD tumours with dysregulated RhoA signaling, and provide novel directions for research into BHD syndrome.

Acknowledgements

My great thanks to Professor Eamonn Maher for his support and guidance throughout the project. I would also like to thank all members of the Birt Hogg Dubé research group for all their help and suggestions, and to all member of the Medical and Molecular Genetics Department at the University of Birmingham for making it such an enjoyable place to work for the past four years.

I wish to thank Professor Mechthild Hatzfeld for hosting me at the University of Halle-Wittenburg for a month, and also members of her research group for making me feel so welcome while in Germany. I am very grateful to our collaborators, Professor Laurence Hurst, Dr Paul Gissen and Ania Straatman-Iwanowska for contributing data to this project, and also for their helpful discussions. Thanks also to the Myrovlytis Trust for funding the research.

Finally I would like the thank my family and friends for their continued encouragement, and particularly my girlfriend, Livia Oldland, for putting up with me while writing this beast!

Table of Contents

Chapter 1	Introduction	1
1.1	THE POST-GENOME ERA FOR CANCER RESEARCH.....	2
1.2	GENETICS OF FAMILIAL RENAL CANCERS	4
1.2.1	Classification of Renal Cell Carcinoma.....	5
1.2.1.1	Clear Cell Renal Carcinoma (ccRCC).....	5
1.2.1.2	Papillary Renal Cell Carcinoma (pRCC)	6
1.2.1.3	Chromophobe Renal Cell Carcinoma (chRCC)	6
1.2.1.4	Oncocytoma (OC)	6
1.2.2	Von Hippel-Lindau disease	7
1.2.2.1	Genetics of VHL.....	8
1.2.2.2	Function of the VHL protein pVHL.....	10
1.2.2.3	The impact of VHL research in the development of therapeutics for ccRCC	12
1.2.3	Hereditary leiomyomatosis and renal cell cancer (HLRCC).....	13
1.2.4	Succinate dehydrogenase mutations and renal cancer	14
1.2.5	Hereditary papillary RCC and germline MET mutations (HPRCC)	14
1.2.6	Familial RCC caused by constitutional chromosome 3 translocations.....	15
1.2.7	Tuberous sclerosis complex.....	16
1.3	BIRT HOGG DUBÉ SYNDROME.....	17
1.3.1	Introduction.....	17
1.3.2	Clinical manifestations of the Birt Hogg Dubé syndrome.....	18
1.3.2.1	Fibrofolliculomas	18
1.3.2.2	Kidney cancer	19
1.3.2.3	Spontaneous pneumothorax and pulmonary cysts	21
1.3.2.4	Other clinical findings	22
1.3.3	FLCN and the molecular genetics of BHD syndrome	23
1.3.3.1	The mapping of FLCN	23
1.3.3.2	FLCN mutation spectrum	24
1.3.4	Functions and associations of the folliculin protein	25
1.3.4.1	Folliculin.....	25
1.3.4.2	Folliculin interacting proteins.....	26
1.3.5	Animal models of BHD syndrome	30
1.3.5.1	BHD syndrome mouse models	30
1.3.5.2	Rat model of BHD syndrome	31
1.3.5.3	Canine model of BHD syndrome	32
1.3.5.4	Drosophila model of BHD syndrome.....	32
1.3.5.5	Yeast model of BHD syndrome	33
1.3.6	FLCN signalling pathways	34
1.3.6.1	mTOR signalling, cancer and folliculin	34

1.3.6.2 Raf-MEK-Erk signalling	37
1.3.6.3 JAK/STAT signalling.....	37
1.4 SUMMARY AND THESIS OBJECTIVES	38
Chapter 2 Materials and Methods	40
2.1 SEQUENCING ANALYSIS	41
2.1.1 DNA samples.....	41
2.1.2 Polymerase chain reaction	41
2.1.3 Agarose gel electrophoresis	44
2.1.4 Exosap/Clean up reaction	44
2.1.5 Sequencing.....	45
2.1.6 Ethanol precipitation.....	46
2.1.7 Mutation detection	47
2.1.8 DNA extraction from culture cells and tumour tissue	47
2.2 CELL CULTURE	48
2.2.1 Cell lines and growth conditions	48
2.2.1.1 Cell lines used.....	48
2.2.1.2 Cell maintenance	49
2.2.1.3 Cryopreserving cells.....	50
2.2.2 Serum starvation of cells.....	50
2.2.3 Transfection	51
2.2.3.1 Transient transfection	51
2.2.3.2 Transfection of stable mixed populations.....	53
2.2.4 Short interfering RNA transfection.....	54
2.3 RNA ANALYSIS	55
2.3.1 Extraction of RNA.....	55
2.3.2 cDNA synthesis	56
2.3.3 TaqMan quantitative real time PCR reaction	56
2.4 PROTEIN ANALYSIS	58
2.4.1 Protein extraction.....	58
2.4.2 Total cellular protein quantification	59
2.4.3 Co-immunoprecipitation.....	60
2.4.3.1 Antibody conjugation to beads	61
2.4.3.2 Immunoprecipitation	62
2.4.4 Western blotting.....	63
2.4.4.1 SDS-PAGE electrophoresis.....	63
2.4.4.2 Transfer to nitrocellulose membrane.....	63
2.4.4.3 Immunoblotting	64
2.4.4.4 Striping and re-probing of membranes.....	65
2.4.4.5 Densitometry	66

2.5 CLONING.....	68
2.5.1 Proofreading PCR	69
2.5.2 Gel extraction.....	70
2.5.3 Restriction digest	71
2.5.4 Ligation	72
2.5.5 Transformation.....	73
2.5.6 Purification of plasmid DNA.....	74
2.5.6.1 Screening of colonies	74
2.5.6.2 Miniprep	74
2.5.6.3 Maxiprep.....	75
2.5.7 Site directed mutagenesis.....	77
2.6 SOFT AGAR COLONY FORMATION ASSAY	80
2.7 IMMUNOFLUORESCENCE MICROSCOPY	83
2.7.1 Bimolecular fluorescence complementation analysis	84
2.8 G-LISA RHOA ACTIVATION ASSAY	85
2.8.1 Assay principle	85
2.8.2 Methodology	86
2.8.2.1 Cell culture	86
2.8.2.2 Cell lysis	86
2.8.2.3 G-LISA assay	87
2.9 <i>IN VITRO</i> CELL SCRATCH MIGRATION ASSAY	88
Chapter 3 Investigations of the <i>FLCN</i> gene in familial and sporadic colorectal cancer.....	89
3.1 INTRODUCTION AND OVERVIEW	90
3.1.1 Colorectal cancer	90
3.1.2 The genetic mechanisms of colorectal tumourigenesis	90
3.1.2.1 Inactivation of APC is characteristic of the majority of colorectal cancers.....	92
3.1.2.2 Wnt signalling and colorectal cancer	93
3.1.3 The chromosomal and microsatellite instability pathways of colorectal tumourigenesis	95
3.1.3.1 Chromosomal instability	95
3.1.3.2 Microsatellite instability.....	95
3.1.4 Hereditary colorectal cancer	96
3.1.4.1 Lynch syndrome/Hereditary non-polyposis colorectal cancer (HNPCC)	97
3.1.4.2 Familial adenomatous polyposis	98
3.1.4.3 MYH associated polyposis	99
3.1.5 The possible association between Birt Hogg Dubé Syndrome and increased risk of colorectal cancer	99

3.2 AIMS AND APPROACHES	101
3.3 PATIENTS AND SAMPLES	101
3.4 RESULTS	103
3.4.1 FLCN mutation analysis in individuals with familial, non-syndromic RCC and CRC	103
3.4.2 Genotype-phenotype correlations for colorectal cancer in BHD patients	105
3.4.3 FLCN C ₈ mononucleotide repeat mutation analysis in sporadic colorectal cancer tumours with microsatellite instability	108
3.5 DISCUSSION	115
Chapter 4 Birt Hogg Dubé syndrome-associated FLCN mutations disrupt protein stability	121
4.1 INTRODUCTION	122
4.2 AIMS AND APPROACHES	125
4.3 METHODS	126
4.3.1 Evolutionary Conservation of FLCN – Analysis performed by Professor Laurence D Hurst, University of Bath	126
4.3.2 Selection of FLCN mutations and variants	127
4.3.3 Characterisation of FLCN mutations in vitro	127
4.3.4 Extraction of DNA and protein from BHD renal tumour	128
4.3.5 Soft agar colony formation assay	129
4.3.6 Immunocytochemistry	129
4.4 RESULTS	132
4.4.1 Evolutionary constraint of FLCN	132
4.4.2 Pathogenic missense and inframe deletion mutations significantly affect the stability of the folliculin protein	135
4.4.3 Analysis of BHD tumour in patient with p.Arg239Cys	140
4.4.4 p.Val400Ile and p.Lys508Arg constructs retain anchor independent growth suppression	142
4.4.5 p.Val400Ile and p.Lys508Arg constructs do not affect protein intracellular distribution	145
4.4.6 No evidence for a dominant negative effect for pHis429ProfsX27 mutation	147
4.5 DISCUSSION	150
Chapter 5 Investigation of the molecular and cellular impact of the folliculin/plakophilin-4 interaction	159
5.1 INTRODUCTION	160

5.1.1 Plakophilin 4 (p0071/pkp4)	161
5.1.2 Cell-cell adhesion	161
5.1.2.1 Adherens junctions, Tight junctions and Desmosomes.....	161
5.1.2.2 Polarity and the apical junction complex	165
5.1.2.3 Loss of cell polarity and cell junction down regulation lead to cancer	165
5.1.3 RhoA signalling and cancer.....	166
5.1.3.1 Rho GTPases	166
5.1.3.2 RhoA.....	167
5.1.3.3 The role of RhoA in invasion and metastasis.....	171
5.1.3.4 The role of RhoA in cytokinesis.....	171
5.1.3.5 P0071 regulates RhoA activity.....	172
5.2 AIMS.....	176
5.3 METHODS	176
5.3.1 Co-immunoprecipitation.....	176
5.3.2 Immunofluorescence analysis.....	176
5.3.2.1 Bimolecular fluorescence complementation analysis	177
5.3.3 Analysis of Rho activity in folliculin isogenic cell lines	179
5.3.4 Multinucleation analysis	179
5.3.5 Cell migration analysis	180
5.3.6 Transepithelial electrical resistance assay and effect of folliulin/p0071 knockdown on epithelial cell polarisation	180
5.4 RESULTS	182
5.4.1 Yeast-2-hybrid Screen	182
5.4.2 Folliculin and p0071 interact in vitro	185
5.4.3 Folliculin and p0071 colocalise and interact at cell junctions during interphase	187
5.4.4 Folliculin and p0071 co-localise and interact at the midbody during cytokinesis.....	189
5.4.5 Loss of folliculin deregulates RhoA signalling/activity	192
5.4.6 Loss of FLCN causes cytokinesis defects resulting in multinucleation	195
5.4.7 Re-introduction of FLCN into null metastatic cells ameliorates migratory phenotype.....	197
5.4.8 Both knockdown of folliculin and p0071 disrupts cell junctional formation	200
5.5 DISCUSSION	205
Chapter 6 Discussion.....	210
6.1 SUMMARY OF THESIS	211
6.2 RECENT BREAKTHROUGHS IN ELUCIDATING FOLLICULIN FUNCTION (2008-2012).....	212
6.2.1 Folliculin and HIF signaling	212

6.2.2 Folliculin and TGF- β signaling	213
6.2.3 Further investigations of folliculin and mTOR.....	214
6.2.4 Folliculin interacts with p0071 – implications for further research.....	216
6.3 CONCLUSIONS.....	219
Chapter 7 Appendices	223
7.1 PLASMID MAPS	224
7.2 SITE-DIRECTED MUTAGENESIS PRIMERS.....	230
Chapter 8 References	231
Chapter 9 Peer Reviewed Publications	253

List of Figures

Figure 1.1. Morphology of the most common renal epithelial tumours.....	7
Figure 1.1 Regulation of HIF- α subunits by pVHL.....	11
Figure 1.2 Fibrofolliculomas on the face of a BHD patient	19
Figure 1.3 Schematic summary of FLCN-FNIP1/2 binding regions	30
Figure 1.4 Schematic diagram of mTOR/PI3K signaling detailing possible position of FLCN	36
Figure 2.1 Principle of co-immunoprecipitation with using Dynabeads Protein G.....	61
Figure 2.2 Diagram of transfer apparatus	64
Figure 3.1 Genetic model of colorectal tumourigenesis	91
Figure 3.2 Summary of the Wnt signaling transduction pathway	93
Figure 3.3 Summary of <i>FLCN</i> mutations detected	104
Figure 3.4 Age related risk of colorectal cancer (A) and neoplasia (B) in a cohort of 149 BHD patients from 51 families.	106
Figure 3.5 Comparison of the risks of colorectal neoplasia in <i>FLCN</i> c.1285dupC and c.610_611delGCinsTA mutation carriers.	107
Figure 3.6 Schematic diagram of p.His429ThrfsX39 and p.His429ProfsX27.	110
Figure 4.1 Schematic diagram describing the location of variants analysed within <i>FLCN</i>	130
Figure 4.2 Folliculin is a slower than average evolving gene.....	133
Figure 4.3 Folliculin while under purifying selection is less constrained 3' than 5'	134
Figure 4.4 FLCN mutations introduced using site-directed mutagenesis.....	137
Figure 4.5 Most <i>FLCN</i> missense and IFD mutations analysed significantly disrupted stability of the protein	138
Figure 4.6 Loss of heterozygosity and reduced folliculin expression in p.Arg239Cys RCC.....	141
Figure 4.7 Assessment of the tumour suppressive activity of FLCN mutant proteins. ..	144

Figure 4.8 The cellular localisation of the p.Val400Ile and p.Lys508Arg FLCN variants is similar to that of wild type FLCN.	146
Figure 4.9 No evidence of a dominant negative effect associated with the p.His429ProfsX27 mutation when introduced into DLD-1 cells.....	148
Figure 5.1 Schematic diagram of the location of p0071 in epithelial cell contacts	164
Figure 5.2 The RhoA GTPase cycle	168
Figure 5.3 The role of Rho in the interphase and mitotic cell	170
Figure 5.4 Localisation of p0071 in the mitotic cell.....	174
Figure 5.5 Principle of BiFC analysis.....	177
Figure 5.6 FLCN Venus constructs cloned for BiFC analysis.....	178
Figure 5.7 P0071 and FLCN interact in vitro	186
Figure 5.8 Folliculin and p0071 are co-localised and interact at cell junctions	188
Figure 5.9 FLCN and p0071 colocalise and interact at the midbody during telophase/cytokinesis	191
Figure 5.10 Loss of folliculin induces deregulation of RhoA signaling.....	194
Figure 5.11 Reintroduction of folliculin rescues multinucleation phenotype in FTC-133 cells	196
Figure 5.12 FTC-133 cells lacking folliculin are more migratory due to increased RhoA signaling.	199
Figure 5.13 TEER of cells with FLCN and p0071	202
Figure 5.14 Staining for junctional proteins in IMCD-3 cells treated with <i>FLCN</i> and <i>p0071</i> siRNA	204
Figure 7.1 p.Flag-CMV plasmid map.....	224
Figure 7.2 p.IRES2-AcGFP1 plasmid map.....	225
Figure 7.3 p.Ven1-flag-C plasmid map	226
Figure 7.4 p.Ven1-flag-N plasmid map	227
Figure 7.5 p.Ven2-HA-N plasmid map.....	228

Figure 7.6 p.Ven2-HA-C plasmid map.....	229
---	-----

List of Tables

Table 2.1 PCR conditions for FLCN exon amplification	42
Table 2.2 PCR reagents and volumes	42
Table 2.3 FLCN genomic primers	43
Table 2.4 Mononucleotide tract amplifying primers	43
Table 2.5 Exosap reagents and volumes	45
Table 2.6 Sequencing reaction reagents and volumes	45
Table 2.7 Sequencing reaction conditions	46
Table 2.8 TaqMan reaction reagents and volumes	57
Table 2.9 Quantitative real-time PCR reaction conditions	58
Table 2.10 Primary antibodies used.....	67
Table 2.11 Secondary antibodies used.....	68
Table 2.12 Proofreading PCR reagents and volumes	69
Table 2.13 Proofreading PCR reaction conditions	70
Table 2.14 Primers used for FLCN cloning into Venus vectors.....	70
Table 2.15 Restriction digest reagents and volumes.....	72
Table 2.16 Ligation reaction reagents and volumes	73
Table 2.17 Primers used for FLCN ORF sequencing.....	77
Table 2.18 Site-Directed mutagenesis reaction reagents and volumes.....	78
Table 2.19 Site-Directed mutagenesis reaction PCR conditions	79

Table 2.20 2 x DMEM reagents and volumes	80
Table 2.21 1 x DMEM reagents and volumes	81
Table 2.22 0.7% (v/v) DMEM agar constituents	81
Table 2.23 0.35% (v/v) DMEM agar constituents	82
Table 3.1 Details of FLCN mutation status and immunohistochemical status of mismatch repair proteins in MSI+ colorectal tumour DNA samples analysed, where information available.....	112
Table 3.2 Mutation profile of the mononucleotide repeat in four MSI+ target genes in 30 MSI+ colorectal tumours	114
Table 4.1 Clinical Information for FLCN variants selected	131
Table 4.2 In silico analysis predicting the possible functional consequences of missense and IFD mutations	139
Table 5.1 Yeast-2-hybrid results for folliculin	184
Table 7.1 Site-directed mutagenesis primers	230

Abbreviations

AJC	Apical Junction Complex
AMPK	AMP-activated Protein Kinase
BHD	Birt Hogg Dubé
BiFC	Bimolecular Fluorescence Complementation
ccRCC	clear cell Renal Cell Carcinoma
chRCC	chromophobe Renal Cell Carcinoma
CIN	Chromosomal Instability
CRC	ColoRectal Cancer
DBHD	Drosophila Melanogaster FLCN homologue
DMEM	Dulbecco's Modified Eagles Medium
DNA	DeoxyriboNucleic Acid
EMT	Epithelial to Mesenchymal Transition
FAP	Familial Adenomatous Polyposis
FBS	Foetal Bovine Serum
FH	Fumarate Hydratase
FLCN	Folliculin protein
GAP	GTPase Activating Protein
GDI	GDP Dissociation Inhibitor
GDP	Guanosine Di-Phosphate
GEF	Guanine Exchange Factor
GTP	Guanosine Tri-Phosphate
HNPCC	Hereditary Non-Polyposis Colorectal Cancer
HPRCC	Hereditary Papillary Renal Cell Carcinoma
IFD	InFrame Deletion
LOH	Loss Of Heterozygosity
LST7	Schizosaccharomyces pombe FLCN homologue
MMR	MisMatch Repair
MSA	Multiple Sequence Alignment
MSI+	MicroSattelite unstable
mTOR	mammalian Target Of Rapamycin
mTORC1	mTOR complex 1
mTORC2	mTOR complex 2
ORF	open reading frame
OC	Oncocytoma
p0071	plakophilin 4
PBS	Phosphate Buffered Saline
PCR	Polymerase Chain Reaction

pRCC	papillary Renal Cell Carcinoma
PSP	Primary Spontaneous Pneumothorax
pVHL	VHL protein
RCC	Renal Cell Carcinoma
	Renal Cystadenocarcinoma and Nodular
RCND	Dermatofibrosis
RNA	RiboNucleic Acid
ROCK	Rho-associated coiled-coil forming kinase
rpm	revolutions per minute
S6K1	ribosomal protein S6 kinase beta-1
siRNA	short interfering RNA
SNP	Single Nucleotide Polymorphism
TEER	Trans-Epithelial Electrical Resistance
TSC	Tuberous Sclerosis Complex
VHL	Von Hippel-Lindau syndrome

Chapter 1 Introduction

1.1 The post-genome era for cancer research

The field of cancer genetics has been transformed in the past decade. In the time previous to the sequencing of the human genome in 2001, and the subsequent burst of next generation genetic technologies becoming available, the major field limiting factor was the identification of genetic variants responsible for disease phenotype. The ‘next generation genetics’ undertaken within recent years has provided us with the tools to assess the complete diseased cancer genome in comparison with the normal genome, providing novel insights into the pathogenic landscape of cancer and cancer related syndromes.

However, the promise of new targeted therapies, believed by many to accompany these technological advances, has fallen into the next stumbling block; the incredible complexity of the cancer genome. The major field limiting factor is no longer that of variant identification, but in elucidating the precise role of these variants in the pathology of disease.

It has been suggested that there are around 80 DNA mutations that alter amino acids in a typical cancer, but that less than 15 are likely to be responsible for driving tumour initiation and the progressive pathway to metastasis (Wood, et al., 2007). Specific gene mutations are likely to occur infrequently, even among cancers of the same organ. This paints a depressing picture of the impact of genetic advances in eventual translation to the clinic. However, it appears logical for huge numbers of different proteins to become mutated in distinct cancer genomes, but that these alterations are likely involved in a far more manageable number of intracellular signalling pathways. There are six well

characterised hallmarks of cancer; sustained proliferative signalling, evasion of growth suppressors, induction of angiogenesis, resistance of cell death, replicative immortality and the activation of invasive and metastatic pathways (Hanahan and Weinberg, 2011). Functioning within these hallmark capabilities of a cancer cell, it is believed that not more than 20 signalling pathways are deregulated by the enormous number of potential driving mutations identified in next generation cancer genomic studies (Wood, et al., 2007). This represents a far more manageable and realistic aim of tailoring therapy against the specific signalling pathways disrupted in a given cancer, rather than against individual genes.

We are now therefore at the next stage in the road to personalised cancer therapy, namely the characterisation of the precise functional roles of genes mutated in cancer in the physiological setting, and the impact of their inactivation by mutation. It is in elucidating the molecular and biochemical processes associated with cancer causing mutations, that the daunting power of next generation genetics can be harnessed, with hope for revolutionising the efficacy of targeted cancer therapeutics in the near future.

I would argue that research into rare genetic cancer syndromes is a crucial component of these investigations. Rare cancer syndromes provide unequivocal evidence of a specific gene (or number of genes) with causative involvement in a particular pathology, often also reflected in sporadic forms of the disease. Research into the role of rare, syndrome associated proteins in pathogenesis of disease also informs potentially crucial aspects of cellular pathways, yet unidentified by traditional molecular biological methods and often overlooked by the broad brush of current genetic technologies (For example

identification of the role of the tumour suppressor protein VHL in regulation of hypoxia inducible factor (HIF) (Maxwell, et al., 1999)).

This thesis investigates the link between mutations in the *FLCN* gene, and the relationship with the phenotypes observed in the rare cancer susceptibility disorder Birt Hogg Dubé Syndrome (BHD). The study provides evidence of a potential genotype-phenotype correlation for a specific BHD phenotype, the probable mechanism of pathogenicity of most pathogenic *FLCN* variants and a novel function for the folliculin protein in a potentially drug sensitive, cancer related signalling pathway.

1.2 Genetics of familial renal cancers

The following section discusses a selection of rare cancer syndromes (with particular attention to hereditary renal cancers), and the impact the basic research into these syndromes has had on general cancer biology and therapeutics. The genetics of familial renal cancers is of strong relevance to this thesis, increased risk of renal cell carcinoma (RCC) being the most clinically problematic manifestation of BHD syndrome, and folliculin having a yet fully elucidated role in RCC pathogenesis.

Annually, kidney cancers account for close to 150,000 new cancer diagnoses and 78,000 cancer deaths worldwide (Maher, 2011). The most common renal malignancy is renal cell carcinoma (RCC) representing around 95% of all renal tumours (Hagenkord, et al., 2011). 75% of renal cancers are clear cell RCC (ccRCC), 10% papillary RCC (pRCC) and 5% chromophobe RCC (chRCC). The remaining 5% of kidney cancers observed are

oncocytoma (OC), a benign neoplasm (Hagenkord, et al., 2011). Only around 3% of renal malignancies are familial, however study into the familial cases has influenced and improved clinical practise for these at risk kindreds also providing important insights into sporadic forms of the disease. Inherited RCC is characterised by an earlier age at diagnosis compared with sporadic cases and is often bilateral and multicentric (Maher, 2011).

While most patients presenting with renal epithelial tumours have a good prognosis, the clinical manifestations can often remain hidden in early stages of disease resulting in around 30% presenting with metastasis at the time of initial diagnosis (Sadler, et al., 2007). Treatment of advanced kidney cancer with traditional therapies has a far reduced prognosis, and it is hoped that investigation of Medelian single gene cancer syndromes such as Von-Hippel-Lindau (VHL), hereditary papillary renal cell carcinoma (HPRCC), hereditary leiomyomatosis renal cell carcinoma (HLRCC) and Birt Hogg Dubé (BHD) syndrome can provide the key to developing pathway-specific therapies for renal cell carcinoma (Rosner, et al., 2009).

1.2.1 Classification of Renal Cell Carcinoma

1.2.1.1 Clear Cell Renal Carcinoma (ccRCC)

Clear cell renal cell carcinoma (ccRCC) is the most commonly presented renal cancer which accounts for around 75% of cases (Kovacs, et al., 1997). It is thought to originate from the proximal tubule of the nephron. ccRCC have a compact-alveolar or acinar cell

growth pattern. Cells display a clear cytoplasm, commonly filled with glycogen and lipids which dissolve upon processing for histologic analysis (Hagenkord, et al., 2011).

1.2.1.2 Papillary Renal Cell Carcinoma (pRCC)

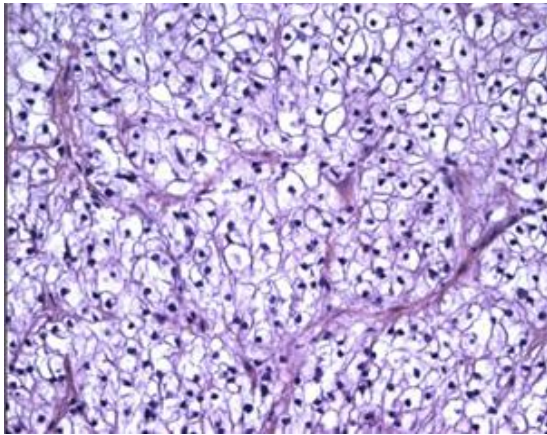
pRCCs are less frequently observed, making up around 10% of renal cell carcinomas, and are morphologically subdivided into small (type 1) and large (type 2) cell tumours. Type 1 pRCC are typically of lower stage and grade than type 2 tumours (Hagenkord, et al., 2011).

1.2.1.3 Chromophobe Renal Cell Carcinoma (chRCC)

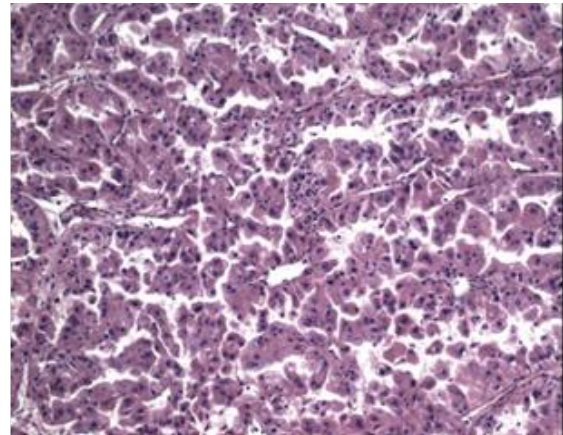
chRCC comprises approximately 5% of renal epithelial tumours. Tumour cells are large, polygonal and have prominent cell membranes and a clear cytoplasm (Stec, et al., 2009).

1.2.1.4 Oncocytoma (OC)

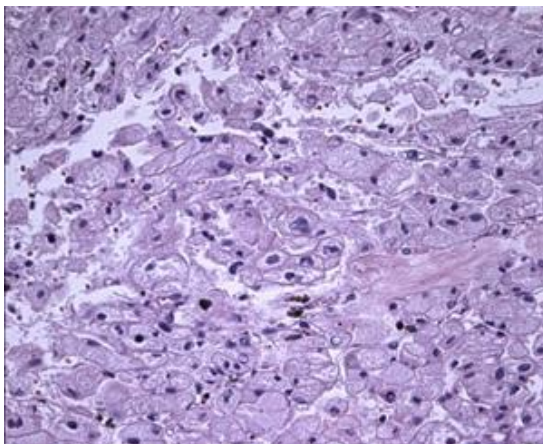
The final major group of renal tumours observed is oncocytoma, a benign neoplasm accounting for between 3 and 7% of all renal tumours. Oncocytoma tumour cells display abundant, granular eosinophilic cytoplasm, reflecting an abundance of mitochondria (Hagenkord, et al., 2011).



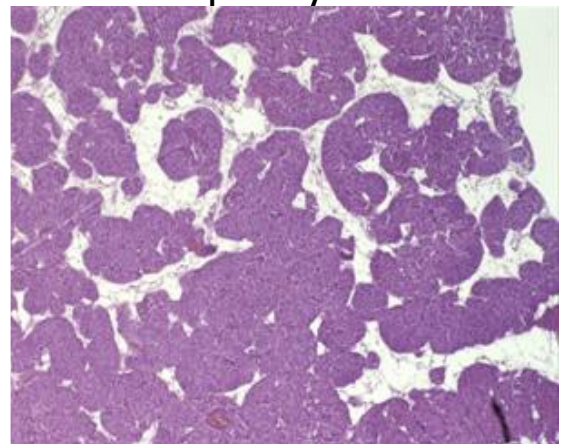
Clear Cell RCC



Papillary RCC



Chromophobe RCC



Oncocytoma

Figure 1.1. Morphology of the most common renal epithelial tumours - Adapted from (Hagenkord, et al., 2011)

1.2.2 Von Hippel-Lindau disease

Research into the Von Hippel-Lindau syndrome and elucidation of the functions of the *VHL* tumour suppressor gene function has provided important insights into the mechanism of pathogenesis of pVHL deficient renal cell carcinomas. Discoveries made in the last decade are now at the stage of translation into informing therapeutic strategies

for treating ccRCC. Understanding of the molecular mechanisms of the VHL protein (pVHL) is arguably a decade further forward than that of BHD syndrome, and thus VHL research provides an important template and realistic aim for the BHD syndrome field to achieve in the years to come.

1.2.2.1 Genetics of VHL

Von Hippel-Lindau is the most frequently identified familial RCC and is inherited in an autosomal dominant manner. VHL has a prevalence of approximately 1 in 36,000 live births (Maher, et al., 1991). Patients with VHL are at a greater than 70% lifetime risk of developing ccRCC, and also display increased risk of retinal and cerebral haemangioblastomas, pheochromocytomas and pancreatic, renal and epididymal cysts (Maher, 2004).

The cloning and characterisation of the VHL tumour suppressor gene (*VHL*) (Latif, et al., 1993) has facilitated early diagnosis of VHL increasing the chances of successful treatment and allowing targeted surveillance of RCC and other VHL associated manifestations in mutation carriers. The *VHL* gene is made up of 3 exons encoding two VHL proteins; a full length, 213 amino acid protein and a VHL protein lacking the first 53 amino acids, both believed to have very similar functional effects (Iliopoulos, et al., 1998). A wide range of mutations in *VHL* have been reported in over 900 VHL disease kindreds identified to date (Nordstrom-O'Brien, et al., 2010). The most common group of *VHL* mutations are deletions (0.5-250kb) that remove at least 1 *VHL* exon, mainly caused by Alu-mediated recombination (Franke, et al., 2009). The remaining mutations

are either non-truncating missense changes or mutations predicted to truncate the encoded protein product (nonsense, frameshift and splicesite mutations) (Maher, et al., 2011). Complex genotype-phenotype correlations have been described for *VHL*; for example, *VHL* truncation mutations are associated with a low risk of pheochromocytoma, which is conversely associated with certain missense mutations (Ong, et al., 2007). While the nature of the mutation identified in a *VHL* patient may therefore provide an indication of the likely risk of a *VHL* manifestation, the inter-familial variation in phenotype means there is little clinical impact on the management of *VHL* patients depending on mutation type. However the genotype-phenotype correlations described have informed research investigating the mechanisms of tumourigenesis in patients with *VHL* mutations (Maher, 2011).

The *VHL* gene is a classical tumour suppressor, with the identification of inactivation of the wildtype *VHL* allele in tumours from *VHL* patients. Reintroduction of wildtype p*VHL* into a *VHL*-null RCC cell line inhibited the ability of the cells to form tumours in nude mice (Iliopoulos, et al., 1995). The second hit can result from deletion of the wildtype *VHL* gene (3p loss is regularly reported in RCC), point mutations or hypermethylation of the *VHL* promoter region (Cheng, et al., 2009). While some cases of non-*VHL* related familial ccRCC have been reported due to chromosomal translocations of 3p and BHD syndrome (see section 1.2.6), a large number of patients with a familial risk of ccRCC have no known genetic cause (Woodward, et al., 2008).

Sporadic ccRCCs also display somatic inactivation and loss resulting in the loss of both copies of *VHL*, often due to deletion of the short arm of chromosome 3 (81-100% of cases) (Hagenkord, et al., 2011; Receveur, et al., 2005).

1.2.2.2 Function of the VHL protein pVHL

In the years since the identification of pVHL as a tumour suppressor, the protein has been reported to have multiple functions and influence numerous cellular pathways. The best defined function is the role of VHL in regulating proteolytic degradation of the α -subunit of the HIF-1 and HIF-2 transcription factors. A number of hypoxia-inducible mRNAs are regulated by the HIF-1 and HIF-2, heterodimeric transcription factors. Both HIF-1 and HIF-2 consist of a constitutively expressed β subunit, and a degradable α subunit (Woodward and Maher, 2006). Under normoxic conditions, the HIF- α subunits are rapidly degraded by the VHL containing, ubiquitin ligase protein complex (Maxwell, et al., 1999). Oxygen is essential for facilitating the binding of pVHL to HIF- α , thus in hypoxic conditions HIF-1 and HIF-2 are stabilised and activate between approximately 100 and 200 target genes, many involved in angiogenesis, apoptosis, proliferation and metabolism (Kaelin, 2009). These effects are mirrored by the loss of active pVHL by either deletion or mutational inactivation (Maher, et al., 2011). VHL tumours are highly vascular and display uncharacteristically high production of hypoxia-inducible mRNAs such as vascular endothelial growth factor (VEGF) (Woodward and Maher, 2006). The regulation of HIF- α subunits by VHL is displayed in Figure 1.1.

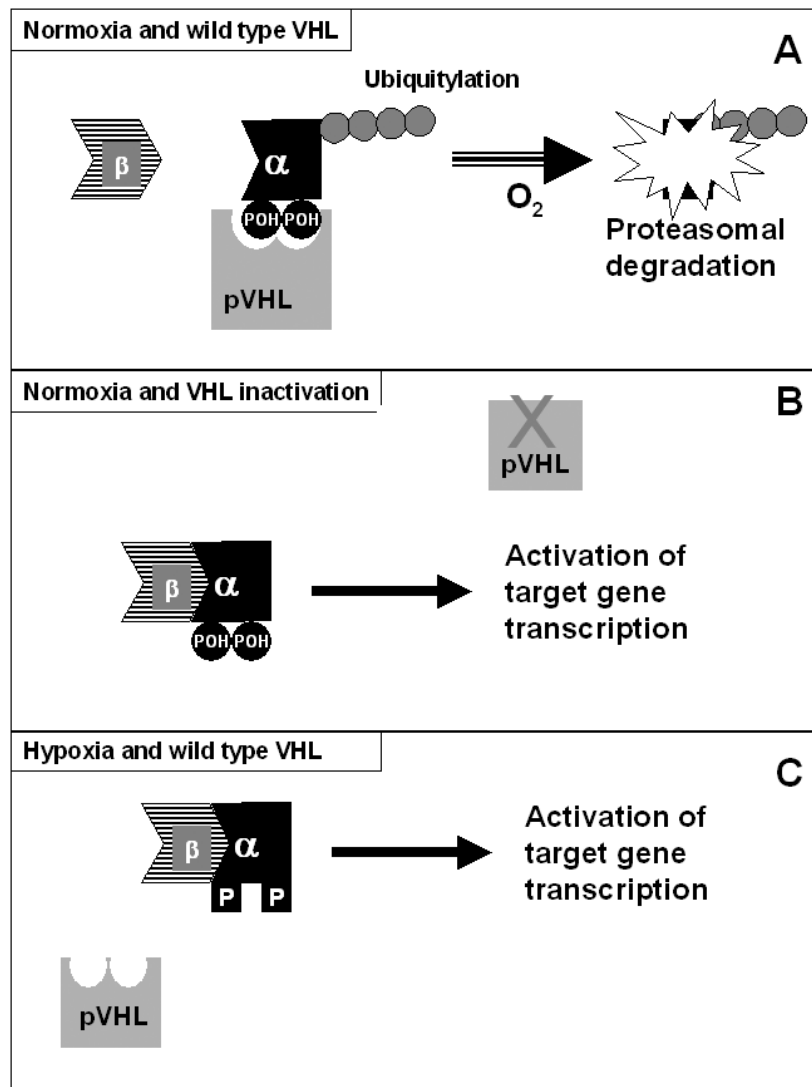


Figure 1.1 Regulation of HIF- α subunits by pVHL

(Woodward and Maher, 2006)

VHL mutation mimics the effects of hypoxia on HIF- α stabilisation, resulting in the activation of HIF target gene transcription. A: In normoxia, pVHL binds to the HIF- α subunits causing polyubiquitination and subsequent proteasomal degradation. B: When VHL is mutated and nonfunctional, HIF- α becomes stabilised and is able to bind HIF- β resulting in the activation of hypoxia inducible genes C: This is mimicked in hypoxia where two crucial proline residues in the HIF- α subunit are not hydroxylated, thus disrupting binding of pVHL to HIF- α . Hence hypoxia inducible genes are again activated

(VHL – Von-Hippel-Lindau gene, pVHL – Von-Hippel-Lindau tumour suppressor protein
HIF – Hypoxia inducible factor)

Research into the role of pVHL in renal tumourigenesis has provided the foundations for the development of targeted therapies for patients with advanced kidney cancer. Surgical excision is curative in the majority of ccRCC cases, but close to 30% of patients without detectable metastasis at the time of surgery, develop them after nephrectomy (Motzer, et al., 1996).

1.2.2.3 The impact of VHL research in the development of therapeutics for ccRCC

Understanding the role of pVHL in mediating the expression of HIF target genes has provided the opportunity for the development of many drugs targeted specifically against HIF gene targets. Sorafenib is a small-molecule protein kinase inhibitor that has more than one target (multikinase inhibitor) including the VEGF receptors, VEGFR-2 and VEGFR-3, and was approved in 2005 for treatment of metastatic ccRCC (Escudier, et al., 2007a). Sunitinib, an oral multikinase inhibitor that block activity of VEGF and PDGF receptors, has been associated with increased progression free survival and a 35% response rate in patients with advanced RCC over interferon. Bevacizumab is a humanised, recombinant anti-VEGF antibody that binds and neutralises the activity of all types of VEGF-A isoforms (Presta, et al., 1997). The most recent phase III trial of bevacizumab, examined treatment with either bevacizumab or placebo in combination with IFN- α in a study of 641 patients with metastatic clear cell RCC. Bevacizumab treated patients had a significantly longer progression-free survival and higher objective tumour response rate, compared with placebo treated controls (Escudier, et al., 2007b). Pazopanib, another multiple kinase inhibitor, with a broader spectrum of targets including

all VEGFRs, was approved in 2009 (Sternberg, et al., 2010). However despite the significant effects on progression free survival and quality of life associated with these drugs compared to placebo or interferon therapy, disease progression eventually occurs (Costa and Drabkin, 2007). The challenge is now to identify the factors which lead to resistance to anti-VEGF therapy by identifying informative biomarkers so the patients where these therapies will be most effective can be selected (Hagenkord, et al., 2011). These initial targeted therapeutic approaches, directly spawning from research into VHL, demonstrate the efficacy of targeting the VHL pathway in VHL deficient RCCs and provide scope for improving targeted therapies for RCC in the future.

1.2.3 Hereditary leiomyomatosis and renal cell cancer (HLRCC)

HLRCC is a rare, autosomal dominant syndrome caused by germline mutations in the fumarate hydratase gene (*FH*). Fumarate hydratase is a key enzyme functioning in the Krebs cycle catalysing the conversion from fumarate to malate (Tomlinson, et al., 2002). The disease is characterised by benign, cutaneous leiomyomas and also multiple uterine leiomyomas in women, developing at a young age (Tomlinson, et al., 2002). Only a minority of *FH* mutation carriers develop RCC, typically papillary RCC or collecting duct tumours, however they are particularly aggressive and require surgery as soon as they are detected (Maher, 2011). Age of onset is usually between 30-50 years of age, but cases as young as 11 years old have been described therefore renal screening from a young age is key to the clinical management of HLRCC patients (Morrison, et al., 2010).

1.2.4 Succinate dehydrogenase mutations and renal cancer

Succinate dehydrogenase is a complex made up of SDHA, SDHB, SDHC and SDHD subunits, and is bound to the inner mitochondrial membrane where it plays a crucial role in cellular energy metabolism by functioning in the Krebs cycle and as mitochondrial complex 2 in the electron transport chain (Maher, 2011). Germline *SDHB* mutations have been described in up to 5% of patients with inherited RCC susceptibility but no known causative syndrome (Ricketts, et al., 2008) with a lifetime risk of around 15% in *SDHB* mutation carriers (Ricketts, et al., 2010).

Interestingly, renal tumours derived from patients with *FH* or *SDHB* mutations also show upregulation of HIF-1 and HIF-2. This is hypothesised to be due to high levels of fumerate and succinate inhibiting hydroxylation of key proline residues on HIF α subunits. This prevents the binding of pVHL and thus HIF-1 and HIF-2 are not targeted for degradation and can activate hypoxic response genes, mimicking the response of *VHL* gene mutations (Isaacs, et al., 2005; Selak, et al., 2005). Therefore research into the molecular mechanisms of tumourigenesis in *FH* and *SDHB* mutation carriers has allowed the possibility of treating these patients with similar targeted therapies against HIF targets, described above in the treatment of metastatic RCC.

1.2.5 Hereditary papillary RCC and germline MET mutations (HPRCC)

HPRCC is a very rare (incidence of 1 in 10 million), autosomal dominant hereditary cancer syndrome. It is caused by germline missense mutations in the *c-MET* proto-

oncogene, first cloned in 1997 (Schmidt, et al., 1997). Affected individuals are at an increased risk of developing bilateral, multifocal pRCC (Rosner, et al., 2009). *c-MET* gain of function mutations promote cell proliferation, increase cell motility and neo-vascularisation (Hagenkord, et al., 2011). *c-MET* encodes the cell surface receptor for hepatocyte growth factor (HGF) and contains a tyrosine kinase domain (Bottaro, et al., 1991). Pathogenic mutations in *c-MET* constitutively activate the tyrosine kinase domain (Linehan, et al., 2009). Basic research into HPRCC has informed a number of approaches to target the MET pathway, which are currently in progress. One approach is to target the tyrosine kinase domain of MET using tyrosin kinase inhibitors (TKI's). Another is to produce antibodies that target HGF, the ligand of the MET cell surface receptor or the extracellular domain of MET itself to inactivate its receptor function (Linehan, et al., 2009).

c-MET mutations have also been reported in patients with sporadic type 1 pRCC (Linehan, et al., 2009). Both type 1 and type 2 pRCC characteristically display whole chromosome gains, often trisomy 7 (including the *HGF* and *MET* genes) and trisomy 17 (Kim, et al., 2009; Kovacs, et al., 1991).

1.2.6 Familial RCC caused by constitutional chromosome 3 translocations

Familial RCC can be caused by dominantly inherited chromosome 3 translocations, of which 12 have been described previously (Woodward, et al., 2010). In some cases, the translocations have been shown to have breakpoints within candidate tumour suppressor genes (eg. *LSAMP*, *FHIT*, *TRC8*, and *NORE1*), that have been demonstrated to be

deregulated, mutated or epigenetically inactivated in various sporadic RCCs and RCC cell models (Chen, et al., 2003; Gemmill, et al., 2002; Gemmill, et al., 1998; Ohta, et al., 1996). In contrast, other RCC associated translocations have been shown not to disrupt candidate genes and hence a “three hit” model has been proposed in such cases. In these cases it is proposed that the translocation is associated with chromosomal instability leading to loss of a derivative chromosome containing *VHL*, and somatic mutation of the remaining *VHL* allele (Schmidt, et al., 1995).

1.2.7 Tuberous sclerosis complex

Tuberous sclerosis complex (TSC) is a rare genetic disease caused by germline mutations in the *TSC1* or *TSC2* genes (1993; Borkowska, et al., 2011; van Slegtenhorst, et al., 1997). TSC can impact nearly every organ system in the body, with the most clinically problematic manifestations affecting the brain, heart, lung and kidney. The tumours in TSC are classified as hamartomas (similarly to fibrofolliculomas in BHD syndrome), which are benign and consist of a disorganised mass of cells and tissues normally found in the area of the body where the growth occurs. Regarding renal manifestations, TSC patients can develop RCC (in less than 3% of cases), and more usually benign angiomyolipoma in the kidney (~50% of cases) (Neuman and Henske, 2011). TSC is of relevance to BHD syndrome research as the proteins encoded by *TSC1* and *TSC2* (hamartin and tuberin respectively), function as part of the mammalian target of rapamycin (mTOR) signalling pathway (a pathway in which folliculin also functions), by

inhibiting Rheb upstream of mTORC1 (see sections 1.3.5.5 and 1.3.6.1) (Neuman and Henske, 2011).

1.3 Birt Hogg Dubé syndrome

The following section reviews the knowledge of Birt Hogg Dubé (BHD) syndrome as of 2008, at the start of this project. Research published in the in the last four years are discussed in relevant thesis chapters.

1.3.1 Introduction

BHD is an autosomal, dominantly inherited familial cancer syndrome characterised by the development of benign skin tumours on the face and upper torso, called fibrofolliculomas (Birt, et al., 1977). The syndrome also causes pre-disposition to kidney tumours, with clear cell, chromophobe or oncocytic features, pulmonary cysts and spontaneous pneumothorax (collapsed lung) (Schmidt, et al., 2005). The syndrome was first described in 1977 (Birt, et al., 1977), and the responsible gene, *FLCN*, identified in 2002 (Nickerson, et al., 2002). This marked a key discovery in BHD syndrome research, and has been the major driving force in studies trying to define the function of the *FLCN* encoded protein, folliculin, which has been shown to act as a tumour suppressor (Vocke, et al., 2005). In 2008, close to 200 BHD syndrome families had been identified (Toro, et al., 2008), although the syndrome is likely under-diagnosed due to the wide variability of

clinical symptoms, and this number is likely to increase as clinicians become more familiar with BHD syndrome and its manifestations.

1.3.2 Clinical manifestations of the Birt Hogg Dubé syndrome

1.3.2.1 Fibrofolliculomas

The appearance of benign hair follicle tumours on the head and upper torso, called fibrofolliculomas, are the characteristic phenotype of BHD syndrome, and develop after the age of 20. However, an estimated 25% of BHD patients do not manifest skin lesions (Schmidt, et al., 2005; Toro, et al., 2008). Fibrofolliculomas appear as dome-shaped, white papules and are displayed in Figure 1.2. The number of fibrofolliculomas a patient develops is highly variable, ranging from under 10 to over 100 (Toro, et al., 1999).



Figure 1.2 Fibrofolliculomas on the face of a BHD patient
(Menko *et al* 2009)

1.3.2.2 Kidney cancer

Individuals with BHD syndrome are also at increased risk of developing RCC (Toro, et al., 1999; Zbar, et al., 2002). The histology of BHD associated renal tumours is diverse, in contrast to the other familial kidney cancer syndromes described previously, for which a specific subtype of RCC was characteristic. Clear cell, chromophobe and papillary renal cell carcinoma, as well as oncocytoma have been described in BHD syndrome patients. Most common is a hybrid chromophobe and oncocytic renal tumour, occurring

in around half the cases of RCC in BHD syndrome (Pavlovich, et al., 2002). Chromophobe RCC presents in 33% of BHD patients, and renal oncocytoma in 5% (Hagenkord, et al., 2011). It is therefore likely that folliculin might play a universal role in the pathogenesis of RCC. Metastasis has also been reported in BHD renal tumours, all of papillary or clear cell histology (Claessens, et al., 2010b; Pavlovich, et al., 2005; Toro, et al., 2008).

The risk of developing kidney cancer in BHD patients is believed to be around seven-times increased compared with the general population (Zbar, et al., 2002). In one study, 34 of 124 (27%) individuals with BHD syndrome has renal tumours at a mean age of 50.4 years (Pavlovich, et al., 2005), and in another, 30 of 89 (34%) BHD patients had developed kidney tumours (Toro, et al., 2008). BHD patients often present bilateral renal tumours (60% reported frequency) (Pavlovich, et al., 2002). The earliest reported age of kidney tumour diagnosis in BHD patients is 20 years (Khoo, et al., 2002).

Folliculin loss is rare in sporadic RCCs (da Silva, et al., 2003; Khoo, et al., 2003) when compared with the frequency of VHL loss in sporadic ccRCC for example. However a low frequency of nonsense, frameshift and splice site mutations have been identified in sporadic chromophobe RCC and oncocytoma (Gad, et al., 2007). It is therefore likely that disruption of folliculin function does contribute to renal carcinogenesis, and that in some cases where *FLCN* is not mutated, folliculin related pathways are likely to be affected.

1.3.2.3 Spontaneous pneumothorax and pulmonary cysts

The presence of lung cysts in BHD patients was identified in 1999, and is now known to be the most common BHD manifestation, observed in up to 90% of patients (Zbar, et al., 2002). The same study reported a 50-times increase in the risk of pneumothorax in BHD patients, likely related to the presence of lung cysts (Toro, et al., 2007; Zbar, et al., 2002). Following an initial primary spontaneous pneumothorax (PSP), subsequent recurrent events are more common (Toro, et al., 2007). Pneumothorax has been reported to manifest in BHD patients as young as 7 and 16 years of age (Bessis, et al., 2006; Gunji, et al., 2007).

Patients with multiple pulmonary cysts and recurrent pneumothorax but no other BHD manifestations, have been found to harbour *FLCN* mutations (Gunji, et al., 2007), suggesting BHD syndrome should be considered in cases of multiple lung cysts even when other BHD symptoms are not present.

FLCN mutations have also been identified in patients with dominantly inherited PSP. A genome wide scan of a Finnish family with a dominant risk of PSP identified 17p11 as the candidate region. A 4-bp deletion in *FLCN* was identified, which was associated with bullous lung lesions and PSP displaying 100% penetrance (Painter, et al., 2005). While this family presented no other BHD associated phenotypes, the close connection between these conditions means such families are also monitored for renal/skin manifestations (Painter, et al., 2005).

1.3.2.4 Other clinical findings

As well as the widely accepted BHD phenotypes affecting the lungs, kidneys and skin, a small number of other clinical manifestations have been suggested to be associated with BHD syndrome.

Early studies suggested an increased risk of colorectal neoplasia to be part of the BHD phenotype, although this association has been subject to much debate (Khoo, et al., 2002; Rongioletti, et al., 1989; Zbar, et al., 2002). The risk of colorectal cancer and polyps in BHD patients is further investigated in Chapter 3.

BHD patients have also been reported with a range of tumours, both benign and malignant, however so far no causative association between BHD syndrome and increased risk of any tumour (but RCC) has been proven. These cases include the benign tumours, parotid-gland adenoma and oncocytoma, colorectal polyp and adenoma, multinodular goiter, neural-tissue tumour, connective-tissue nevus, trichoblastoma, focal-cutaneous mucinosis, lipoma, cutaneous leiomyoma and angioliipoma (Menko, et al., 2009). Malignant tumours include colorectal cancer, breast cancer tonsillar cancer, sarcoma of the leg, lung cancer, melanoma, dermatofibrosarcoma protuberans, basal and squamous-cell skin cancer and cutaneous leiomyosarcoma (Menko, et al., 2009). However it is likely that most of these cases represent sporadic cancers occurring by chance in BHD patients at the time of presentation, and further work is required to determine which, if any of these are causally linked to BHD syndrome. As well as these cancerous reports in BHD patients, a number of other abnormalities have been reported

including congenital cystic lung soft tissue mass, chorioretinopathy, internal carotid-artery aplasia and congenital chest deformation (Menko, et al., 2009).

1.3.3 FLCN and the molecular genetics of BHD syndrome

The field of BHD syndrome research was transformed with the identification of the causative gene *FLCN* in 2002 (Nickerson, et al., 2002). This discovery has provided the basis for all subsequent genetic and functional investigations into the syndrome in the past six years.

1.3.3.1 The mapping of FLCN

The *BHD* gene was mapped to the short arm of chromosome 17(17p11.2) by Khoo *et al.* (2001) and Schmidt *et al.* (2001). Khoo *et al.* (2001) used a genome wide scan on 17 individuals of a Swedish pedigree to identify the susceptibility locus of *BHD*. Using two-point LOD score linkage analysis, the group found a maximum LOD score between the disease locus and the microsatellite marker D1781852. Haplotype analysis showed a recombination event between D1781852 and D1781824, thus providing evidence for BHD to be located within a 35.5cM region on chromosome 17p12-q11.2 (Khoo, et al., 2001).

Schmidt *et al.* (2001) performed an initial genome wide scan on a three-generation family with 18 BHD affected members and, by linkage analysis, located the BHD locus to

region 17p. Further linkage analysis on another 8 BHD affected families produced a maximum LOD score of 16.06 for the most informative marker D17S2196. Haplotype analysis was used to narrow the minimal region of non-recombination to the location between D17S1857 and D17S805 (less than 4cM), which is within chromosomal band 17p11.2 (Schmidt, et al., 2001).

Subsequently Nickerson *et al.* (2002) used recombination mapping to, further narrow the BHD region to a 700kb section on 17p11.2. Within this region, the authors identified a novel candidate gene harbouring protein truncating mutations in BHD syndrome patients, named *BHD* (now named *FLCN*) (Nickerson, et al., 2002).

1.3.3.2 FLCN mutation spectrum

The *FLCN* gene is made up of 14 exons, with exons 4 to 14 being translated to the folliculin protein (Nickerson, et al., 2002). Since the cloning of the *FLCN* gene in 2002, numerous *FLCN* mutations have been identified, the vast majority of which prematurely truncate the protein product (Schmidt, et al., 2005). A mutation hotspot has been identified in the mononucleotide tract of 8 cytosine residues, in exon 11, with cytosine insertion or deletion thought to be responsible for close to 50% of the mutations within *FLCN* (Schmidt, et al., 2005). An in depth discussion and experimental investigation of the effects of *FLCN* mutations on folliculin function is located in Chapter 4.

The two-hit hypothesis proposed by Alfred G. Knudson suggested that two mutational events (within tumour suppressor genes) were necessary to cause cancer. In the

hereditary form, the initial mutation is inherited in the germline and the second occurs in somatic cells, thus increasing the risk of cancer in that individual. In the sporadic form, both mutations must occur in the same somatic cell thus reducing the risk of a specific cancer (Knudson, 1971). BHD syndrome patients harbour a mutation in one copy of the *FLCN* gene, inherited through the germline. Somatic mutations in the second, wild-type (WT) copy of the *FLCN* gene, or a loss of the WT region has been identified in the renal tumours of BHD patients, hence suggesting a role for *FLCN* as a tumour suppressor (Vocke, et al., 2005). However the role of *FLCN* in the skin phenotype seems to be more complex. In a study of five BHD patients, no evidence of loss of heterozygosity (LOH) or somatic mutations were found in fibrofolliculomas suggesting haplo-insufficiency may be enough to cause the formation of skin lesions (van Steensel, et al., 2007). In agreement, *FLCN* mRNA has also been reported to be strongly expressed in fibrofolliculomas (Warren, et al., 2004).

1.3.4 Functions and associations of the folliculin protein

1.3.4.1 Folliculin

The *FLCN* encoded protein produces a 579 amino acid protein, folliculin (FLCN), with a molecular weight of 64kDa (Nickerson, et al., 2002). The protein has no major homology to any other human protein, but is strongly evolutionarily conserved (Menko, et al., 2009). Two additional folliculin isoforms are predicted, which lack the C-terminal (342 and 197 encoded amino acids respectively) (Nickerson, et al., 2002). *FLCN* mRNA

expression was investigated by fluorescent *in situ* hybridisation techniques, displaying expression in a number of tissues including the skin, the kidney and lung. As aforementioned, fibrofolliculomas displayed strong *FLCN* mRNA expression, however mRNA was severely reduced in renal tumours derived from a patient with VHL disease, hereditary pRCC and BHD syndrome (regardless of tumour histology) (Warren, et al., 2004).

1.3.4.2 Folliculin interacting proteins

The folliculin protein has no known function, and the amino acid sequence of folliculin provides few clues as to potential function, with no transmembrane domains or organelle localisation signals identified with the folliculin sequence (Warren, et al., 2004). The identification of interacting proteins is likely to provide important insights into the function of the folliculin protein. Thus far, only two folliculin interacting proteins have been identified, FNIP1 and FNIP2/FNIPL, suggesting a link between folliculin and the mTOR signalling pathway (Baba, et al., 2006; Hasumi, et al., 2008; Takagi, et al., 2008).

FNIP1/AMPK

A fundamental study by Baba *et al.* (2006) made a number of key discoveries and the first insights into the role of folliculin in the cell. The first protein found to interact with folliculin was FNIP1, identified by immunoprecipitation and mass spectrometry. FNIP1

also binds to AMP-activated protein kinase (AMPK), a negative regulator of mammalian target of rapamycin (mTOR) signalling with a role in energy sensing (Baba, et al., 2006).

The proteins were shown to interact *in vitro* by co-immunoprecipitation, and also displayed a co-localised, reticular pattern by immunofluorescence of co-expressed folliculin and FNIP1 in HeLa Cells. Folliculin also showed a strong nuclear signal whereas FNIP1 was absent from the nucleus (Baba, et al., 2006).

A functional relationship between folliculin and AMPK/mTOR signalling was demonstrated by folliculin and FNIP1 being phosphorylated by AMPK. Folliculin phosphorylation was diminished by rapamycin and amino acid starvation suggesting folliculin may act downstream of mTOR and AMPK. Folliculin phosphorylation was also dependent on FNIP1 expression levels, leading the authors to hypothesise that FNIP1 may act as a scaffold regulator of folliculin (Baba, et al., 2006). Folliculin phosphorylation was reported to be both AMPK and mTOR dependent, however the functional relevance of folliculin phosphorylation is yet to be elucidated. In an investigation into the effects of *FLCN* knockdown on mTOR activation, the authors found that under amino-acid starvation, phosphorylation of ribosomal protein S6 kinase beta-1 (S6K1) (Thr389) was suppressed in BHD null cells but not in cells where folliculin had been stably re-expressed. Conversely, under serum starved conditions, pS6K1 was upregulated in BHD null cells but not those in which folliculin was re-expressed (Baba, et al., 2006). Further work into the role of folliculin in mTOR signalling is discussed in sections 1.3.6.1 and 6.2.3.

FNIP2/FNIPL

Two years after the identification of FNIP1 as a folliculin binding protein, a second closely related protein, FNIP2 (also reported as FNIPL) was identified by sequence homology (Hasumi, et al., 2008; Takagi, et al., 2008). FNIP2 is homologous to FNIP1 with a 49% identity and 74% similarity (Hasumi, et al., 2008). The protein was identified by bioinformatic searching of proteins closely related to FNIP1. Similarly to FNIP1, FNIP2 is reasonably conserved throughout evolution, although it contains no known functional domains. Like FNIP1, folliculin and FNIP2 co-localise in a reticular pattern in the cytoplasm but not in the nucleus (Takagi, et al., 2008). By subcellular fractionation analysis in HeLa cells, FNIP1 and FNIP2 were enriched in the membrane fraction, similarly to folliculin. Interestingly, folliculin was also significantly located in the cytoskeletal fraction (Takagi, et al., 2008). Takagi *et al.* (2008) reported folliculin/FNIP1 and folliculin/FNIP2 to positively regulate S6K1 phosphorylation, with phosphorylation of S6K and mTOR reduced when FNIP1 or FNIP2 was knocked down by siRNA (Takagi, et al., 2008).

Studies into the binding of FNIP1 and FNIP2 to folliculin have also mapped the region of interaction by immunoprecipitation of various deletion constructs of each protein. The C-terminus of folliculin is required for binding to FNIP1, with deletion of 63 amino acids from the C-terminus enough to disrupt FNIP1 binding. The full FNIP1 protein is required for optimal binding to folliculin, although there is still (albeit severely reduced) interaction when the first 300 amino acids in FNIP1 are deleted. This suggests that

optimal folliculin-FNIP1 interaction requires at least amino acids 300-1166 of FNIP1, likely required to form proper conformation of the protein (Baba, et al., 2006).

In respect of FNIP2-folliculin interaction, Takagi *et al.* (2008) reported that the C terminal of FNIP2 was required for folliculin binding, with deletion of 203 amino acids (of 1114) from the C terminal sufficient to disrupt FLCN-FNIP2 binding (Takagi, et al., 2008). The authors also reported that, like its interaction with FNIP1, the C terminus of folliculin was required for binding to FNIP2, with deletion of 217 amino acids from the C terminus enough to disrupt folliculin-FNIP2 binding (Takagi, et al., 2008). This finding was confirmed by Hasumi *et al* (2008), who reported that deletion of 63 amino acids from the folliculin C-terminus disrupted FNIP1 binding (Hasumi, et al., 2008). It is of interest that the C-terminal region of folliculin is required for FNIP1/FNIP2 binding as this is a region lost as a result of the vast majority of *FLCN* mutations, which prematurely truncate the protein. However it is currently unclear whether nonsense mediated decay mechanisms would result in absence of the full *FLCN* product in these cases, or produce a translated truncated protein. A broad schematic of the regions of binding for folliculin to FNIP1 and FNIP2 is displayed below.

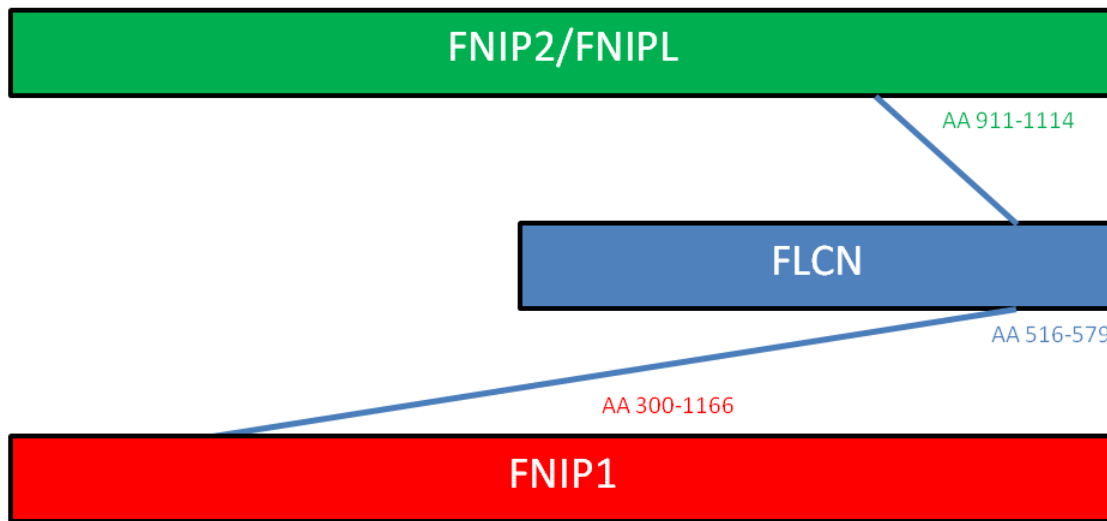


Figure 1.3 Schematic summary of FLCN-FNIP1/2 binding regions

1.3.5 Animal models of BHD syndrome

1.3.5.1 BHD syndrome mouse models

At the start of this project, two mouse models of BHD syndrome had been reported (Baba, et al., 2008; Chen, et al., 2008). Homozygous deletion of *FLCN* is embryonically lethal to the mouse, mutants dying between 3.5 and 8.5 days post conception (Chen, et al., 2008), therefore two conditional *FLCN*-knockout mouse were developed. The first was created using a *cre-lox* system, facilitating inactivation of *FLCN* specifically in the kidney by deleting exons 3 and 4 (Chen, et al., 2008). The second also used *cre*

technology to create conditional knockout in the kidney by deleting *FLCN* exon 7 (Baba, et al., 2008).

Baba *et al.* (2008) reported that BHD-knockout mice developed large, polycystic kidneys and died from renal failure at age 3 weeks (Baba, et al., 2008). The same results were confirmed in the mouse model developed by Chen *et al.* (2008). Both studies also reported up-regulation of mTOR signalling in the knockout mice, describing that rapamycin (mTOR inhibitor) had an ameliorating effect on kidney phenotype and extended mouse survival (Baba, et al., 2008; Chen, et al., 2008). Staining of BHD-inactivated kidneys also displayed elevated levels of phospho-c-Raf (Ser338), and downstream targets MEK1/2 and Erk1/2 in one study (Baba, et al., 2008).

1.3.5.2 Rat model of BHD syndrome

The ‘Nihon’ rat model of BHD is a naturally occurring model of mendelian, dominantly inherited, renal carcinoma susceptibility (Okimoto, et al., 2004a). It was found to harbour a germline frameshift mutation in the rat *FLCN* gene, and is thus an excellent model for studying BHD syndrome in the rat (Okimoto, et al., 2004b). Similar to the mouse models described, homozygous mutant rats are embryonically lethal; however in heterozygotes renal carcinomas develop at as early as 3 weeks of age. These carcinomas showed LOH at the *FLCN* locus or second hit mutation fitting the Knudson two hit model of *FLCN* as a tumour suppressor and confirming inactivation of *FLCN* as responsible for the “Nihon rat” phenotype (Okimoto, et al., 2004b). Further characterisation of the role of *FLCN* as a tumour suppressor in the Nihon rat was provided by Togashi *et al.* (2006),

who reported rescue of embryonic lethality in homozygote and suppression of renal carcinogenesis in heterozygote rats upon introduction of wildtype *FLCN* (Togashi, et al., 2006).

1.3.5.3 Canine model of BHD syndrome

First described in 1985, hereditary multifocal renal cystadenocarcinoma and nodular dermatofibrosis (RCND) is a kidney cancer susceptibility syndrome occurring naturally in dogs. The syndrome is characterised by nodules within the skin and bilateral, multifocal kidney tumours (Lium and Moe, 1985), displaying similar phenotype to BHD syndrome in humans. A causative *FLCN* mutation (H255R) was identified in exon 7 of canine *FLCN* in 2003, and similar to the rat and mouse models, homozygous inactivation of *FLCN* was embryonically lethal (Lingaas, et al., 2003). LOH was subsequently identified in renal cysts and tumours in both juvenile and adult dogs confirming the tumour suppressor function of *FLCN* in this BHD model (Bonsdorff, et al., 2008; Bonsdorff, et al., 2009).

1.3.5.4 Drosophila model of BHD syndrome

BHD syndrome has also been investigated in the fly model of *Drosophila melanogaster*. RNA interference was used to decrease the expression of the *FLCN* homologue in the fly (DBHD). DBHD was demonstrated to be required for male germline stem cell maintenance in the testis of the fly (Singh, et al., 2006). Reducing the DBHD activity in

the fly testis caused a loss of germline stem cells. DBHD was also linked to JAK/STAT and Decapentaplegic (DPP) signalling discussed in section 1.3.6.3.

1.3.5.5 Yeast model of BHD syndrome

The *FLCN* homologue in *Schizosaccharomyces pombe* (fission yeast) SPBC24C6.08c⁺ (BHD⁺, now called *LST7*), was identified in 2007 (van Slegtenhorst, et al., 2007). Homologous recombination was used to generate a strain of yeast in which BHD⁺ had been deleted. The authors were interested to see if knocking out BHD⁺ in *S. Pombe* produced similar effects to knocking down the tuberous sclerosis complex (TSC) homologues in yeast. TSC shares many clinical hallmarks of BHD in humans including skin hamartomas, lung cysts, pneumothorax and renal tumours, and it is thus likely they function in similar pathways. Mutations in the two TSC genes, *TSC1* and *TSC2*, inhibit mTOR via the small GTPase RHEB, a mechanism conserved in *S.Pombe* (van Slegtenhorst, et al., 2007). Interestingly, expression profiling in the BHD deleted strain showed an opposite profile compared to TSC1/2 deleted strains, and the authors concluded that BHD⁺ activates TOR2 (homologous mTOR protein in yeast) (van Slegtenhorst, et al., 2007). If this finding is replicated in human or mouse tissue, it would contrast with the studies of Chen *et al.* (2008) and Baba *et al.* (2008), who found folliculin loss to upregulate mTOR signalling (Baba, et al., 2008; Chen, et al., 2008).

1.3.6 FLCN signalling pathways

1.3.6.1 mTOR signalling, cancer and folliculin

In the non-cancerous cell, mTOR signalling is involved in regulating cell growth in response to extracellular growth factors and nutrients (Sabatini, 2006). mTOR functions in two complexes; the first and best understood, mTOR complex 1 (mTORC1), is a protein kinase which consists of the mTOR catalytic subunit and raptor and mLST8. The role of mTORC1 in controlling cell growth is achieved through modulating protein synthesis, autophagy and ribosome biogenesis (Sabatini, 2006). mTORC1 is activated in a high proportion of cancers. The TSC1-TSC2 (tuberous sclerosis 1-tuberin) tumour suppressor complex has been found to be the key upstream, negative regulator of mTORC1 (Gao, et al., 2002; Tapon, et al., 2001). This complex is a GTP-ase activating protein for the small GTPase Rheb which functions in activating mTORC1 (Garami, et al., 2003; Tee, et al., 2003). Inhibition of TSC1-TSC2 is responsible for the deregulation of mTOR signalling that occurs when cancer cells lose PTEN, LKB1, NF1 or p53 tumour suppressors (Sabatini, 2006), for example the loss of LKB1 suppresses AMPK, which is required for mediating the phosphorylation, and hence activation, of TSC1-TSC2 (Inoki, et al., 2003) see Figure 1.4.

mTORC1 controls cell growth through various downstream effectors, including S6K1 and 4EBP1 (eukaryotic translation initiation factor 4E binding protein 1) (Hay and Sonenberg, 2004). Upregulation of S6K1 promotes protein synthesis, but also represses the PI3K-Akt pathway by inhibiting the cellular levels of IRS1 (insulin receptor substrate 1) and IRS2, creating cross-talk between the two mTOR complexes (Shah, et al., 2004).

mTOR complex 2 (mTORC2) is less well characterised, but is known to contain mLST8, rictor and mSin1 as well as mTOR (Sabatini, 2006). The complex functions as part of the PI3K-Akt signalling pathway, directly phosphorylating AKT (Sarbasov, et al., 2005). Normally active AKT regulates cell survival, metabolism and proliferation by phosphorylating targets such as MDM2 and GSK3 β (Vivanco and Sawyers, 2002). Activation of AKT in the cancer setting is thought responsible for cellular transformation and apoptotic resistance by promoting growth, proliferation and survival while also inhibiting apoptotic pathways (Guertin and Sabatini, 2005).

As mentioned previously, folliculin has been linked to the regulation of mTOR signalling through its interaction with FNIP1/FNIP2 and indirect interaction with AMPK (Baba, et al., 2006; Takagi, et al., 2008). Although the exact role of folliculin in mTOR signalling is yet unknown, kidney specific knockout of folliculin in mice resulted in an increase in phosphorylated S6R (Baba, et al., 2008; Chen, et al., 2008), suggesting a role for folliculin in the downregulation of mTORC1 signalling. Activation of the PI3K-AKT-mTOR pathway was also observed in folliculin null kidneys, suggesting a role for folliculin in the mTORC2 branch of mTOR signalling (Baba, et al., 2008). However, the yeast model of BHD and different cell models showed opposite results, with mTOR signalling reported as being downregulated in the absence of folliculin (Takagi, et al., 2008; van Slegtenhorst, et al., 2007). Recent insights published during the period of current research, into the potential role of folliculin in mTOR signalling suggest a complex, context dependent role and are discussed in full in the discussion sections of this thesis. The predicted position of folliculin in the context of the mTORC1 and mTORC2 pathways is displayed in Figure 1.4.

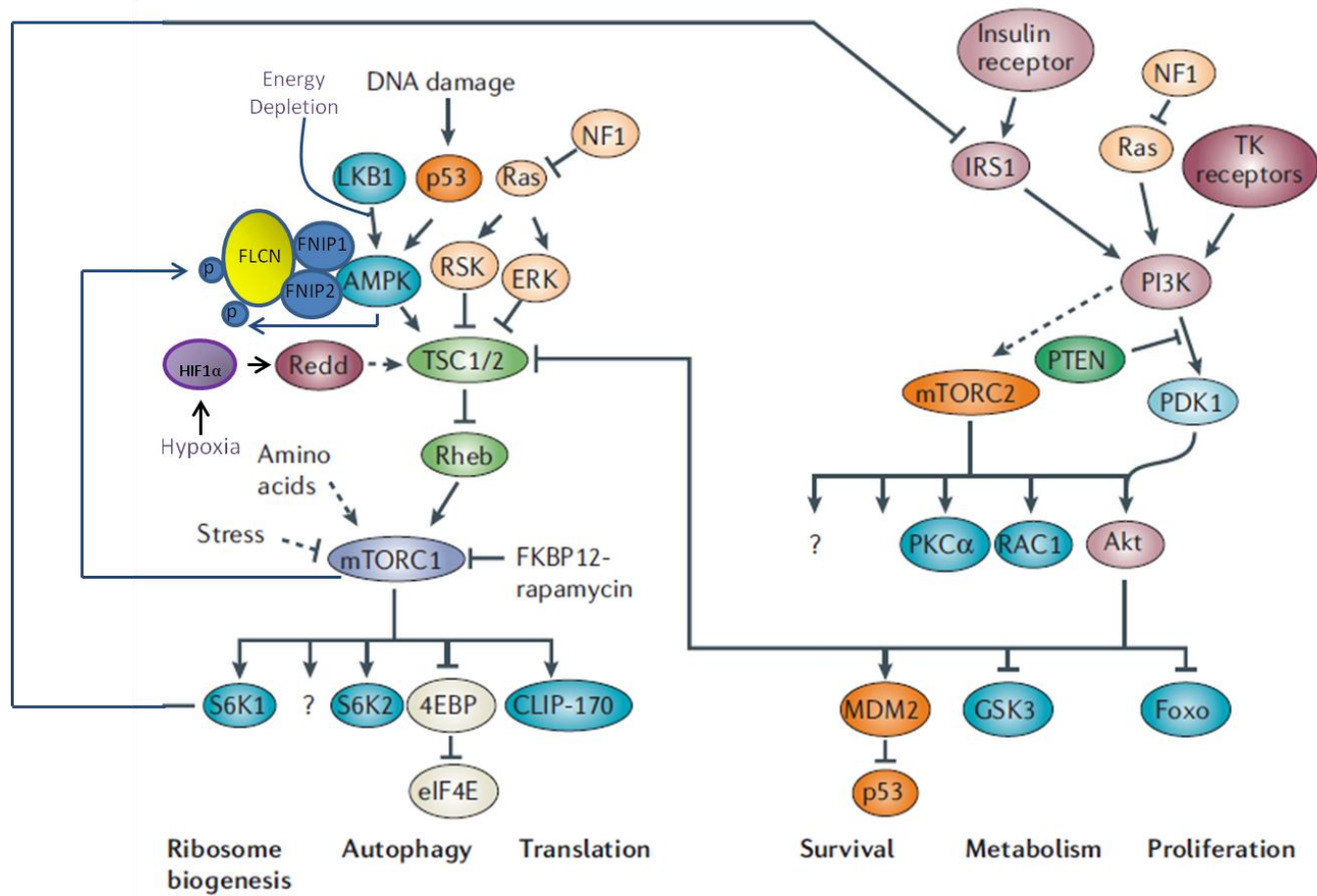


Figure 1.4 Schematic diagram of mTOR/PI3K signaling detailing possible position of FLCN

– adapted from (Sabatini, 2006)

1.3.6.2 *Raf-MEK-Erk signalling*

The Raf-MEK-Erk signalling cascade relays signals from cell surface receptors through the RAS GTPase switch, to transcription factors, thus regulating gene expression (Schubbert, et al., 2007). The pathway functions in regulating cell proliferation and is frequently activated in clinical cancers (Roberts and Der, 2007). Activation of Raf-MEK-Erk is also a marker of poor prognosis (McCubrey, et al., 2007). The mouse model of BHD syndrome created by Baba *et al.* (2008) displayed upregulation of Raf-MEK-Erk signalling in folliculin null kidneys. The authors hypothesised that, as PI3K-AKT-mTOR was also activated, folliculin loss might be activating a common upstream effector of Raf-MEK-Erk and PI3K-AKT-mTOR (Baba, et al., 2008).

1.3.6.3 *JAK/STAT signalling*

Singh *et al.* (2006) demonstrated that in *Drosophila Melanogaster*, the folliculin homologue DBHD regulates male germline stem cell maintenance and functions downstream, or in parallel with the JAK/STAT and Dpp signal transduction pathways. The authors hypothesised that this may be due to both signalling pathways synergising on downstream targets such as DBHD (Singh, et al., 2006). The JAK/STAT (Janus kinase/signal transducers and activators of transcription) pathway is a critical signalling mechanism for a wide range of growth factors and cytokines, and stimulates cell proliferation, differentiation, migration and apoptosis (Rawlings, et al., 2004).

Constitutive activation of JAK/STAT signalling has been linked to several cancers (Valentino and Pierre, 2006). However, links to this pathway have currently only been described in flies, and further research is required to identify possible relevance for the human DBHD homologue.

The studies described above provide a summary of some of the signalling pathways affected by folliculin loss, and give some clues as to the function of the folliculin protein. However, it is likely that there are numerous facets of folliculin function yet to be elucidated, and it can be argued that the causal link between *FLCN* mutation and BHD syndrome phenotype has yet to be identified. Further investigation into the role of this protein in the cell is required, with the ultimate aim to be able to target specific folliculin related pathways therapeutically when folliculin is mutated and non-functional.

1.4 Summary and thesis objectives

Research into rare hereditary renal cancer syndromes has greatly influenced the understanding and treatment of renal cell carcinoma. Birt Hogg Dubé syndrome is caused by germline mutations in the *FLCN* gene, and is characterised by the development of benign hair follicle tumours, lung cysts and renal cancer. Other manifestations have been described, including the possible increased risk of colorectal cancer in BHD patients. This association is investigated in Chapter 3.

Most *FLCN* mutations prematurely truncate the encoded protein, although a small number of non-truncating mutants have been described. The mechanism of pathogenicity of these mutants is currently unknown, and is investigated in Chapter 4.

The function of the folliculin protein is currently not well elucidated. Studies have linked folliculin to mTOR signalling through its association with FNIP1 and FNIP2 although a reliable functional consequence of these associations is currently unclear. It is possible that folliculin may bind to other proteins, exerting functional impact on yet unidentified pathways. The identification of a novel folliculin binding partner and signalling pathway is described in 0.

The identification of *FLCN* mutations in BHD syndrome patients, and loss of heterozygosity in BHD renal tumours highlights an important role for folliculin loss in renal tumourigenesis. The ultimate aim of research into BHD syndrome is to identify the physiological functions of the folliculin protein and how loss of this protein contributes to renal tumourigenesis. Elucidation of these functions may reveal mechanisms for potential therapeutics for BHD syndrome patients and could also provide important insights into the pathways deregulated in sporadic renal cancer.

Chapter 2 Materials and Methods

2.1 Sequencing analysis

2.1.1 DNA samples

2.1.2 Polymerase chain reaction

The Polymerase Chain Reaction (PCR) was used to amplify all coding exons and intron/exon boundaries in *FLCN*. Ten primer pairs were designed for the 11 coding exons of *FLCN* (exons 12 and 13 are encompassed by one reaction) using primer 3 software (Rozen and Skaletsky, 2000). Primers used for amplifying the mononucleotide tract sequences in *IGF2R*, *TGFBR2* and *MSH6* were designed in a similar way. The primers used are given in Table 2.3 and Table 2.4 (Alta Bioscience) and reagents and volumes for each reaction are displayed in Table 2.2 (Roche). A negative control reaction containing water in replacement of DNA was run in parallel for each PCR to confirm no DNA contamination in the PCR reagents. The thermal cycling profile of the PCR reaction is given in Table 2.1.

<i>Step</i>	<i>Temperature</i>	<i>Time</i>	<i>Number of Cycles</i>
Initial Melting	95°C	4 minutes	1
Melting	95°C	30 seconds	
Annealing	58°C	30 seconds	35
Extension	72°C	45 seconds	
Final Extension	72°C	7 minutes	1

Table 2.1 PCR conditions for FLCN exon amplification

The extension time was calculated based on the length of PCR product and rate of extension of *Taq* Polymerase.

<i>Reagent</i>	<i>Volume (μl)</i>
Faststart Taq DNA Polymerase (5 units/μl)	0.2
10x PCR buffer	5
MgCl ₂ (2nM)	4
dNTP mix (25 mM per dNTP)	1
Template DNA (100 ng/μl)	1
Forward Primer (20 pmol/μl)	1
Reverse Primer (20 pmol/μl)	1
Nuclease Free Water	36.8
Total	50

Table 2.2 PCR reagents and volumes

<i>Exon</i>	<i>Forward Primer (5'-3')</i>	<i>Reverse Primer (3'-5')</i>
4	GCAGGAAGTCCATGGCACC	CCTGAGAAGCAGTCTGTGTC
5	GCTTGAGTTTTCCGAGCTCAG	CCTGTGCTGTGCTGATCTGC
6	GCTGATTTGTGCCAGCTGAC	GCAAGCAAACACGGCTAAGG
7	GGACTGATCCTCCAGGAGTC	GCAAGCAAACACGGCTAAGG
8	GCTGGGTGAGCGTCAGGTTTGC	CGTTCTGGGCTGATTCAGAGC
9	CCATGAAGTATCTTGGGCTG	GCTGTCAGTCACTTCCTGC
10	CGCCTCCCTGAGAAGATAAG	CACAGCGGTTCTGTGCTG
11	ACAAGCTGGTGTGTGACTGG	TCCACAACCCATGACAGAGA
12+13	CACGGTGGGCTAGCGCAG	CAGCTCCAGGTTTTCTCCAGG
14	GGTGTGGATTCCAGCTCTGC	CCTTGCTGGGACACAGCTCC

Table 2.3 FLCN genomic primers

<i>Gene</i>	<i>Forward Primer</i>	<i>Reverse Primer</i>
<i>IGF2R</i> (exon 27)	CCCGAACCAAACCTTGTTTA	ATATGATCCCAGCAGCCTGA
<i>TGFBR2</i> (exon 3)	CCTCGCTTCCAATGAATCTC	TGCACTCATCAGAGCTACAGG
<i>MSH6</i> (exon 5)	CTGATAAAACCCCAAACGA	TAGGCTTTGCCATTTTCCTG
<i>FLCN</i> (exon 11)	TCCTCCTCAGACCATGCTTC	GGTTCCTTTGGGCCTGA

Table 2.4 Mononucleotide tract amplifying primers

2.1.3 Agarose gel electrophoresis

Amplified PCR products were resolved on an agarose gel to confirm successful, specific amplification. A 1.5% (w/v) agarose gel was made by dissolving 2.25 g agarose in 150 ml 1x TBE buffer (89 mM Tris Borate pH8.3, 2mM Na₂EDTA (Geneflow Ltd)) and 10 ng/ml ethidium bromide. Typically 8 µl of PCR product was mixed with 2 µl of 5x DNA loading buffer (33% (v/v) glycerol, 0.1% (w/v) orange G, in ddH₂O) and loaded onto the gel. To determine the size of amplified products, a 100 base pair ladder (Invitrogen) was also loaded for comparison. Electrophoresis was carried out at 180 volts for 20 minutes. Products were viewed under UV light and imaged using an Ingenius Syngene Bioimaging machine.

2.1.4 Exosap/Clean up reaction

Successfully amplified PCR products were cleaned using the Exosap reaction in order to remove unwanted primers by exonuclease and unwanted dNTP's by Antarctic phosphatase. The reaction mixture, displayed in Table 2.5, was heated at 37°C for 30 minutes then at 80°C for 20 minutes in PCR machine (G storm). Reagents were purchased from New England Biolabs.

<i>Reagent</i>	<i>Volume (μl)</i>
Antarctic phosphatase	1
Antarctic phosphatase buffer	1
Exonuclease	0.25
H ₂ O	1.75
PCR product	6

Table 2.5 Exosap reagents and volumes

2.1.5 Sequencing

Exosap cleaned PCR products were sequenced directly by dideoxy termination sequencing. Each product was sequenced in both forward and reverse directions, for confirmation of any alterations observed. The sequencing reaction mixture is displayed in Table 2.6, reagents purchased from Applied Biosystems.

<i>Reagent</i>	<i>Volume (μl)</i>
Big Dye	0.75
5x Big Dye buffer	2
Primer (20 pmol/ μ l)	1
Nuclease free water	2.25
PCR product	4

Table 2.6 Sequencing reaction reagents and volumes

Sequencing reaction conditions are displayed in Table 2.7

<i>Temperature</i>	<i>Time</i>
95°C	30 secs
50°C	30 secs
60°C	4 minutes

Table 2.7 Sequencing reaction conditions

2.1.6 Ethanol precipitation

After completion of the sequencing reaction, the DNA was purified by ethanol precipitation. DNA was precipitated by addition of 1 μ l of 250 mM EDTA and 35 μ l of 100% ethanol. Samples were centrifuged at 2254 x g for 30 minutes at 4°C to pellet DNA, and residual ethanol removed by centrifuging plates upside down on filter paper at 20 x g for 1 minute. The DNA pellet was washed with 200 μ l of 70% (v/v) ethanol, and the DNA re-pelleted at 2254 x g for a further 20 minutes at 4°C. The ethanol was removed as before, and the DNA mixed with 10 μ l of HiDi formamide (Applied Biosystems). The DNA was denatured at 95°C for 5 minutes, and then cooled on ice. Samples were then loaded onto an ABI 3730 capillary sequencer (Applied Biosystems).

2.1.7 Mutation detection

DNA sequences were analysed using the BioEdit Sequence alignment program (<http://www.mbio.ncsu.edu/bioedit/page2.html>) to compare patient sequence with a reference sequence. Traces were also checked by eye to identify heterozygous changes not detected by the alignment program. In the case of an identified variant, a second repeat of the PCR-Sequencing process was completed from the original DNA for confirmation of the result. Novel mutations were checked for absence in SNP databases (dbSNP, Ensembl, Exome variant server) and tested for absence in the sequence of more than 200 control chromosomes.

2.1.8 DNA extraction from culture cells and tumour tissue

DNA was extracted from cells and tissue using the DNA isolation kit for cells and tissues (Roche). For DNA isolation from tissue, the tissue was initially ground into a powder under liquid nitrogen. 10 ml Cellular lysis buffer was added to each 400 mg of ground tissue and mixed. 6.1 µl of proteinase K solution was added and the mixture incubated at 65°C for 1 hour. After incubation, 400 µl of RNase solution (10 mg/ml) was added to degrade unwanted RNA, and the sample placed at 37°C for 15 minutes. To precipitate unwanted protein, 4.2 ml protein precipitation solution was added and the sample incubated on ice for 15 minutes. The DNA was collected by centrifugation at 15600 x g for 20 minutes. The DNA was precipitated by addition of isopropanol and a

10 minute centrifugation at 500 x g, and washed with 10 ml of 70 % (v/v) ethanol. The DNA pellet was collected by centrifugation and resuspended in nuclease free water.

The same method was used for DNA extraction from cells in culture (see below for trypsinisation and preparation of cell pellet), with proportionally smaller volumes of reagent added depending on quantity of cells to be extracted from.

2.2 Cell Culture

2.2.1 Cell lines and growth conditions

2.2.1.1 Cell lines used

FTC-133 cells, derived from lymph node metastasis of a follicular thyroid carcinoma, were purchased from ECACC. The cell line is mutant for *FLCN* (p.His429ProfsX27) and produces no translated folliculin protein. FTC-133 cells were maintained in Dulbecco's modified Eagle's medium (DMEM) and Ham's F12 (vol:vol = 1:1), 10% (v/v) foetal bovine serum (FBS), 2mM L-glutamine and 1x penicillin-streptomycin. FTC-133 cell with stable transfection were grown in the same media supplemented with 500µg/ml G418 solution (PAA). ACHN cells with stable knockdown of *FLCN* (by shRNA) and a stable, scrambled control were kindly donated by Professor Arnim Pause (McGill University, Montreal, Canada) and have been described in (Hudon, et al., 2010). These cells were grown in DMEM, 10% (v/v) foetal bovine serum (FBS) and 2mM L-glutamine

supplemented with 1 µg/ml puromycin. MCF-7, HaCat, IMCD-3 and Hela cells were grown in DMEM (PAA) and Hek293 DMEM (Sigma), in addition to 10% (v/v) foetal bovine serum (FBS) and 2mM L-glutamine, all without selective antibiotic. All cell culture reagents were purchased from Sigma-Aldrich unless otherwise stated. Cell culture vessels were purchased from BD Falcon or Corning.

2.2.1.2 Cell maintenance

When the cells had grown to confluency, or were required for a specific experiment, the media was aspirated, and the cells washed with 5 mls of pre-warmed phosphate buffered saline (PBS) (1 PBS tablet per 100 ml ddH₂O, Gibco). The PBS was aspirated and replaced with 1 ml of trypsin (Gibco) (for a T75 flask), and the flasks placed in a 37°C incubator for ~ 5 minutes. Once the cells were completely detached, they were resuspended in 9 mls of media and either re-seeded at a suitable dilution (1/4 – 1/10) back into a T75 flask. If a specific cell seeding density was required, the trypsinised cells were placed in a 15 ml falcon tube and centrifuged at 280 x g for 3 minutes. They were then resuspended in 5 mls of media and counted using a haemocytometer, and the required dilution calculated before seeding.

2.2.1.3 Cryopreserving cells

Cells were trypsinised as described above then centrifuged at 280 x g for 3 minutes. Media was aspirated, the cell pellet resuspended in cold PBS and the cells re-centrifuged for a further 3 minutes at 280 x g. Cell pellets taken from a confluent T-75 flask, were resuspended in 4 mls of FBS containing 10% (v/v) dimethyl sulphoxide (DMSO, Sigma). Each 1 ml of cells was transferred into a 2 ml cryovial, placed in a Mr Frostie freezing container (Sigma) and left at -80°C overnight. Frozen cryovials were kept at -80°C or in liquid nitrogen for longer term storage.

2.2.2 Serum starvation of cells

Cells were serum starved in this project to determine basal levels of RhoA and mTOR signaling, and also to inhibit cell growth when testing the migratory ability of cells. Cells for serum starvation were first washed in serum free media, and then incubated in PBS for 10 minutes. The PBS was then replaced with serum free media and left over night.

2.2.3 Transfection

2.2.3.1 Transient transfection

Fugene HD

The majority of transfections within this project were undertaken using the Fugene HD method. Cells were plated the day before transfection at between 3×10^5 and 5×10^5 per well of a 6 well plate depending on the rate of growth of the cell line in question, to achieve a cell density of greater than 80% at the time of transfection. On the day of transfection, fresh media was placed on the cells. 2 μg of plasmid DNA was diluted in 100 μl of serum-free medium (Opt-MEM 1 - Invitrogen), and the transfection complex formed by adding 7 μl of Fugene HD transfection reagent (Roche, West Sussex, UK). The optimum ratio of plasmid to Fugene volume was determined by titration. The complex was mixed and incubated for 15 minutes at room temperature, before being added to the cells dropwise. The media was changed after 24 hours and transfection confirmed by western blot after 48 hours.

Calcium phosphate precipitation

Transfection by calcium phosphate precipitation was used to co-express the venus vectors into HeLa cells as part of the bimolecular fluorescence complementation (BiFC) analysis of the interaction between folliculin and p0071 (see section 2.7.1). HeLa cells were plated

on the day before transfection at 7.5×10^4 per ml, to reach close to 50% confluence by the time of transfection. On the day of transfection, 4 μg of each plasmid for co-transfection was diluted in 85.5 ml of nuclease free water. 12.5 μl of 2 M CaCl_2 was added to the diluted plasmids, and the transfection complex formed by adding 2xPP (50 mM Hepes pH7.05, 1.5 mM Na_2HPO_4 , 10 mM KCl, 280 mM NaCl, 12 mM glucose) dropwise to a gently swirling tube. The mixture was then incubated at room temperature for 20 minutes, before being added dropwise to the cells. After 6 hours of incubation at 37°C , the media was aspirated and the cells washed once in serum free media. The cells were then “shocked” by addition of glycerol to maximise transfection efficiency. 500 μl of glycerol mixture (150 μl Glycerol, 100 μl ddH₂O, 250 μl 2xPP) was added to each well, and incubated for exactly 2 minutes. After removal of the glycerol, the cells were washed 3 times in serum free media and finally left in normal serum media overnight. Transfection was confirmed by cell fixation and immunofluorescence analysis after 24 hours.

Lipofectamine 2000

Transfection using Lipofectamine 2000 reagent (Invitrogen) was used to co-express flag-tagged folliculin and dsRED-tagged p0071 constructs for exogenous co-expression, immunofluorescence analysis in Hela, HaCat, MCF-7, FTC-133 and ACHN cells.

Cells were seeded into 6 well plates with coverslips, at 3.75×10^5 cells per ml the day before transfection, to reach 95% confluence at the time of transfection. For each transfection sample, 2 μg of each DNA construct were pooled and diluted into 250 μl serum free media. At the same time, 10 μl of Lipofectamine 2000 were was diluted into a separate tube of 250 μl serum free media, and incubated for 5 minutes at room temperature. After this time, the diluted DNA and Lipofectamine 2000 tubes were pooled, mixed gently and incubated for 20 minutes at room temperature. After incubation, the mixture was added dropwise to a single well of a 6 well plate and incubated at 37°C for 6 hours. Media was replaced after 6 hours, and transfection confirmed by co-staining and immunofluorescence analysis after 24 hours.

2.2.3.2 Transfection of stable mixed populations

For transfection of a stable expressing pool of mixed clones, the initial transfection procedure was as described above using Fugene HD transfection reagent. After 48 hours, the media was aspirated, and replaced with media containing 500 $\mu\text{g}/\text{ml}$ G418 solution (PAA), which was used to select for cells expressing neomycin resistance gene, an indication of plasmid incorporation into the genome. An untransfected control well was also grown in G418 containing media to confirm a lack of resistance to G418 in the general cell population. Cells which stably expressed neomycin resistance gene were grown until confluent in a T75 flask and cryopreserved for future experiments.

2.2.4 Short interfering RNA transfection

Short interfering RNA (siRNA) transfection was used to transiently silence specific genes by degrading the encoded mRNA and thus reducing protein synthesis. For each well the required concentration of siRNA was diluted in 200 μ l of Opt-MEM 1 Reduced Serum Media (Invitrogen) and the transfection mixture formed by adding 10 μ l of INTERFERin transfection reagent (Polyplus). The mixture was then homogenized for 10 seconds and incubated at room temperature for 10 minutes. The transfection mixture was placed dropwise into each well of a 6 well plate. Cells were trypsinised, counted and seeded directly onto the siRNA transfection mixture at between 30-50% confluency ($\sim 1 \times 10^5$ cells/ml). The cells were incubated for 72 hours at 37°C, and gene silencing measured by western blotting and densitometry or TaqMan Real Time qPCR in comparison with luciferase siRNA transfected controls.

siRNA sequences were purchased from Applied Biosystems. Human flcn siRNA sequence was GGAAGGUGGCAUUCAGAUG. Mouse flcn siRNA sequence was CCUCAGCAAGUAUGAG, and mouse p0071 siRNA sequence was CAGACAGCAUUGUAUCGC.

2.3 RNA analysis

2.3.1 Extraction of RNA

RNA was extracted from cells and tissue using the TRIzol Plus RNA Purification Kit (Ambion). Cells were trypsinised and pelleted by centrifugation at 280 x g at room temperature as described in the cryopreservation section. Lysis was achieved by resuspending the cell pellet in TRIzol Reagent and incubating the lysate at room temperature for 5 minutes. The amount of TRIzol Reagent added was based on the culturing dish area (1 ml per 10 cm²). 0.2 mL of chloroform was added, mixed by shaking the tube for 15 seconds and incubated at room temperature for 3 minutes. The samples were then centrifuged at 12000 x g for 15 minutes at 4°C, after which the mixture had separated into a lower, red phenol-chloroform phase, an interphase and a colourless upper phase (which contained the RNA). The RNA containing phase was removed, mixed with an equal volume of 70% ethanol, vortexed, and added to a spin column. Tubes were centrifuged at 12000 x g for 15 seconds to bind RNA to the collection column. The column was washed and then centrifuged with 700 µl wash buffer I followed by two washes with wash buffer II. RNA was then eluted by addition of 30 µl nuclease free water, a 1 minute incubation and a centrifugation step of 12000 x g for 2 minutes. RNA was eluted 3 times to maximize the amount of RNA extracted and the 3 elutions pooled. Concentration and quality was determined using a Nanodrop spectrophotometer (NanoDrop Technologies, Wilmington, USA).

2.3.2 cDNA synthesis

For cDNA synthesis, 1 µg of total RNA was reverse transcribed using SUPERSCRIPT III reverse transcriptase (Invitrogen). 2 µl of 50uM random primers were added to 1 µg RNA and 1 µl 10mM dNTP mix (final volume 13 µl), mixed well and heated to 65°C for 5 minutes to destroy all secondary structure of mRNA. After this incubation, 4 µl 5x First-strand Buffer, 1 µl of 0.1 M DTT, 1 µl RNaseOUT inhibitor (40 units/ µl) and 1 µl SUPERSCRIPT II RT (200 units/ µl) were added to the mixture (final volume 20 µl), and mixed well in a PCR tube. The tubes were then incubated at 55°C for 90 minutes and heated to 70°C for 15 minutes to inactivate the enzyme. Finally the amount of cDNA was measured with a Nanodrop spectrophotometer and a working concentration of 200ng/ µl diluted using nuclease free water. Reagents were purchased from Invitrogen.

2.3.3 TaqMan quantitative real time PCR reaction

The TaqMan assay was used to determine gene expression by quantifying the amount of cDNA present in a given sample. It works based on the 5' nuclease activity of Taq DNA polymerase. Predesigned TaqMan probes hybridise to target DNA between two designed PCR primers (which span between different exons to inhibit amplification of genomic DNA). Fluorescent signal from the probe is quenched by the non-fluorescent quencher on its 3' end. When the PCR cycling commences, Taq polymerase extends the DNA

from each primer. When extension reaches the TaqMan probe, it cleaves the FAM dye from the quencher, thus releasing a fluorescent signal. With each cycle of PCR more dye is released exponentially, which is then detected in real-time by the qPCR machine. The amount of fluorescence detected can therefore be used to determine the amount of cDNA and hence mRNA in the original sample.

For each gene analysed, a TaqMan gene expression assay containing a pair of specific primers and MGB probes was ordered from Applied Biosystems. For each gene amplified, a plate of standard DNA concentrations was prepared at 100 ng, 250 ng, 500 ng, 650 ng, 850 ng and 1 µg, to determine a suitable concentration of cDNA to add to the reaction. Each concentration was carried out in duplicate. The reaction mixture is displayed in Table 2.8 and the reaction conditions given in Table 2.9. Reactions were run on an IQ5 multicolor real-time PCR machine (BioRad).

<i>Reagent</i>	<i>Volume per reaction (µl)</i>
TaqMan universal PCR master mix (2x)	10
20x gene expression assay Mix	1
cDNA (100ng/ µl) + water	9 (of differing cDNA concentrations)
Total	20

Table 2.8 TaqMan reaction reagents and volumes

<i>Step</i>	<i>Temperature (°C)</i>	<i>Time</i>	<i>Number of Cycles</i>
Initial Melting	95	10 minutes	1
Melting	95	15 seconds	40
Annealing/elongation	60	1 minute	

Table 2.9 Quantitative real-time PCR reaction conditions

An input cDNA concentration which produced quantitative amplification was determined from the standard curve, and that concentration used in subsequent assays.

Each assay consisted of amplification of the gene of interest and of *GAPDH* acting as an internal control for normalisation. The mRNA levels of the gene of interest in comparable samples were determined by the amount of cDNA amplification of the gene normalized by *GAPDH* control for each sample.

2.4 Protein analysis

2.4.1 Protein extraction

To extract protein for immunoblotting, the cells were first washed in PBS and scraped into 200 µl of RIPA lysis buffer (Tris pH7.4, NaCL 150mM, EDTA 0.5 mM, 1% Triton

(v/v) and protease inhibitor cocktail (Roche Applied Sciences)). For co-immunoprecipitation experiments, the same buffer was used, although to maximise the quantity of cell lysate produced, a T75 flask was scraped with 500 µl of lysis buffer. Protein extraction for G-LISA RhoA activation assay is described in detail in section 2.8.2.2. The cells were then centrifuged at 13300 x g and 4°C for 20 minutes and the supernatant transferred to a new tube for protein quantification. Cell lysates were stored at -20°C

2.4.2 Total cellular protein quantification

The concentration of protein within the lysate was determined using the DC Protein Assay Kit (BioRad). 5 µl of each sample in duplicate, and a standard curve with a serial dilution of bovine serum album (BSA) and lysis buffer (0 mg/ml to 2 mg/ml) were added to the wells of a 96 well plate. 20 µl of buffer S was mixed with 1 ml of reagent A to make reagent A' and 25 µl added to each well followed by 200 µl of reagent B. The plate was incubated at room temperature for 10 minutes before absorbance was measured using a Victor X3 Multilabel plate reader (PerkinElmer). The protein concentration was then determined using the standard curve as reference for each sample.

For western blot of total cellular lysate, equal concentrations of each sample were calculated and mixed with an appropriate volume of 5x protein loading buffer (250mM Tris HCl (pH6.8), 10% SDS (w/v), 0.5% Bromophenol Blue (w/v), 50% Glycerol (v/v),

5% DTT (v/v)). Samples were boiled for 5 minutes (>95°C) before being loaded onto SDS-PAGE gels for electrophoresis.

2.4.3 Co-immunoprecipitation

Co-immunoprecipitation using Dynabeads was used to confirm the interaction of folliculin and p0071 *in vitro* (see 0). The procedure used Dynabeads Protein G (Invitrogen), which are superparamagnetic polymer beads, covalently coupled to Protein G which binds to the Fc part of a wide range of immunoglobulins (Igs). The dynabeads were mixed with antibody, which bound to the Dynabeads protein G (protein G has been shown to have a strong affinity with both mouse IgG and rabbit IgG antibodies used in these experiments). The antibodies were covalently cross-linked to the beads to minimize heavy and light chain contamination. Finally the antibody conjugated dynabeads were incubated with protein lysate to pull down the specific antibody binding protein and also other proteins bound as part of a complex. As the dynabeads are magnetic, they can be separated from solution using a magnet, minimising contamination of unbound protein. Mixing steps were carried out at room temperature away from the magnet, and liquids removed from the beads after 30 seconds exposure to the magnet. Incubations were carried out using end-over mixing apparatus.

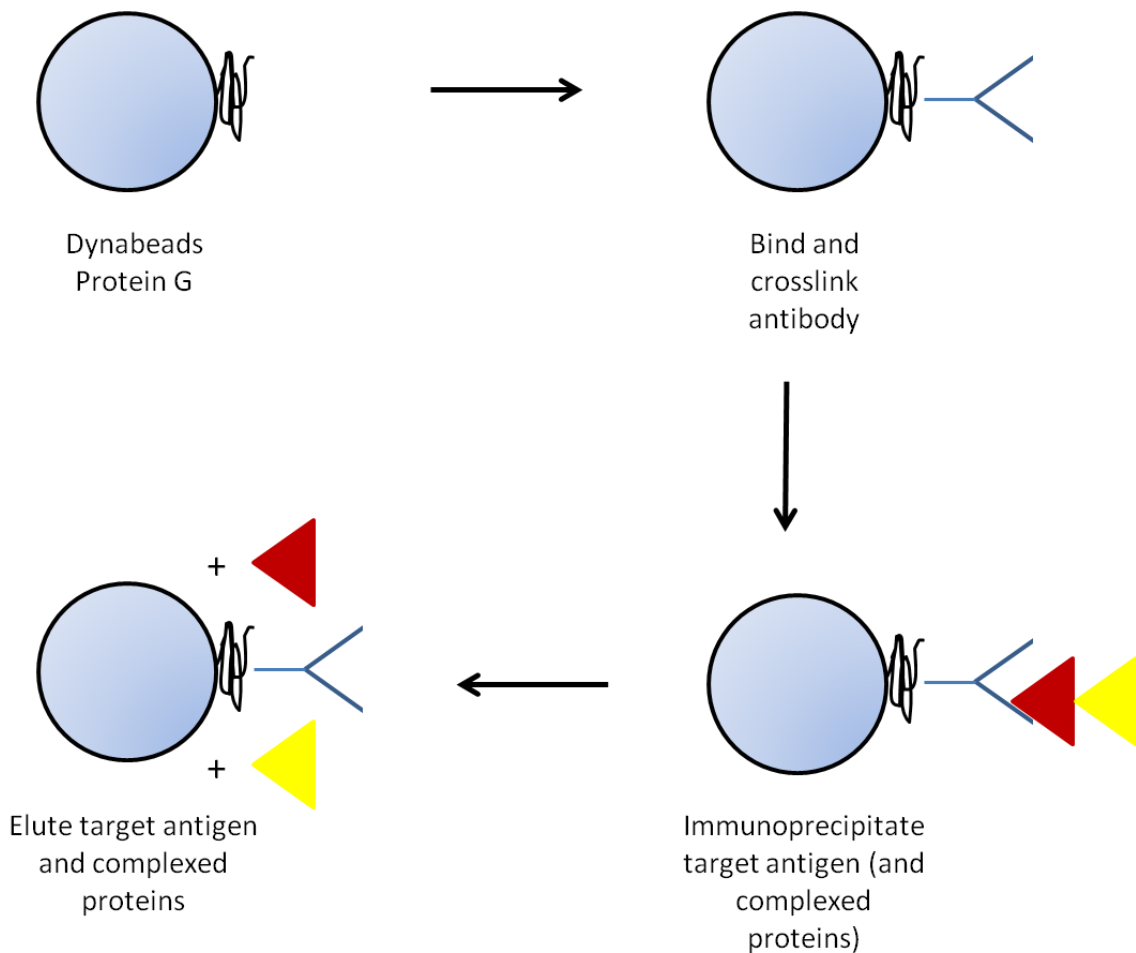


Figure 2.1 Principle of co-immunoprecipitation with using Dynabeads Protein G

2.4.3.1 Antibody conjugation to beads

Dynabeads were resuspended and 20 μ l of beads placed on the magnet per co-immunoprecipitation. Beads were washed twice with 500 μ l citrate phosphate buffer (24.5 mM citric acid and 51.7 mM dibasic sodium phosphate, pH 5.0) and mixed with 4 μ g of the required antibody diluted in 20 μ l of PBS (see Table 2.10), and incubated for

an hour at room temperature (except in the case of anti-FLCN rabbit monoclonal antibody, Cell Signaling, where 0.5 μ g was used). After a further 3 washes with 500 μ l citrate phosphate buffer, the beads were washed 3 times in 500 μ l 0.2 M triethanolamine (Sigma). Antibodies and beads were cross linked by incubation with 20 mM dimethyl pimelimidate (Sigma - dissolved in 0.2 M triethanolamine) for 30 minutes at room temperature. After removal of the dimethyl pimelimidate, the reaction was quenched by incubation with 1 ml of 50 mM Tris pH 7.5 for 15 minutes at room temperature. The antibody conjugated beads were washed 3 times with PBST (PBS and 0.1% tween) and re-suspended in 20 μ l PBST.

2.4.3.2 Immunoprecipitation

Dynabeads were first washed 3 times in citrate phosphate buffer and then resuspended in RIPA lysis buffer. For semi-exogenous co-immunoprecipitation 200 μ g and for endogenous co-immunoprecipitation 250 μ g of total cellular protein were added to 20 μ l of antibody bound dynabeads and incubated at 4°C for 3 hours. The lysates were then placed on the magnet and the supernatant removed as unbound fragment. The beads were washed 3 times with 500 μ l RIPA buffer (Tris pH 7.4, NaCl 300 mM, EDTA 0.5 mM, 1% (v/v) Triton-X-100, protease inhibitor cocktail (Roche)). Beads were resuspended in 20 μ l of 2x Laemmi sample buffer (Sigma) and transferred to a fresh eppendorf tube. Pulled down proteins were eluted by boiling for 10 minutes, and were then loaded onto 8% (w/v) SDS-PAGE gels for analysis.

2.4.4 Western blotting

2.4.4.1 SDS-PAGE electrophoresis

Proteins were resolved by SDS-PAGE electrophoresis. Gels were made up of 8 mls resolving gel and 2 mls stacking gel cast between two glass plates (1.5 mm). Gels of 6%, 8.5%, 10% and 12.5% (w/v) were used depending on the size of the protein of interest. Initially the resolving gel was poured and 1 ml of ddH₂O added to ensure a straight edge to the gel. Once the resolving gel was set, the ddH₂O was removed and 2 mls of stacking gel added on top of the resolving gel. In most instances a 15 well comb (occasionally a 10 well comb) was inserted into the stacking gel pre-setting to provide wells for lysate loading. Once set, gels were placed into an electrophoresis tank part filled with 1x SDS running buffer (25 mM Tris, 192 mM Glycine, 0.1% (w/v) SDS pH 8.3), and proteins separated using 150 Volts for one hour. 5 µl prestained protein marker (Fermentas) was loaded in the first and last lanes as a reference of protein size, and to separate experiments when more than one were run per gel.

2.4.4.2 Transfer to nitrocellulose membrane

The proteins separated by gel electrophoresis were then transferred onto PVDF (polyvinylidene difluoride) membrane (GE Healthcare), which was initially activated by 1 minute incubation in methanol. The transfer apparatus was set up as described in

Figure 2.2, and run in 1x transfer buffer (Geneflow) at 100V for 1.5 hours, with an ice pack.

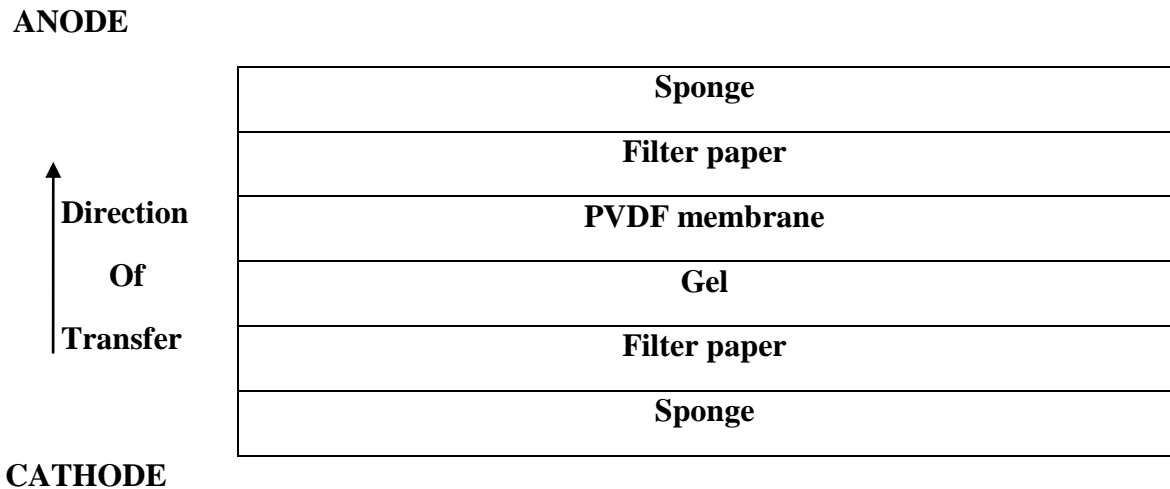


Figure 2.2 Diagram of transfer apparatus

2.4.4.3 Immunoblotting

Membranes were initially calibrated in PBST for five minutes, before being blocked with 5% (w/v) milk (5g powdered milk (Marvel) dissolved in 100 mls PBST) at room temperature for one hour. After blocking, the membrane was placed on a rocker in PBST for three 5 minute washes. Blocked membranes (proteins facing inwards) were left rolling in a 50 ml falcon containing 5 mls of diluted antibody overnight at 4°C. Primary

antibodies were diluted as described in Table 2.10. After incubation in primary antibody the membrane was washed three times with PBST for 5 minutes each time, before being incubated (on a roller) with corresponding secondary antibody for 1 hour at room temperature. Secondary antibodies had been conjugated to horse radish peroxidase to allow for their detection using autoradiography film (described in Table 2.11). After 3 final washes in PBST for 5 minutes, the membrane was incubated for 1 minute in enhanced chemiluminescence (ECL) reagent, and proteins detected using BioMax XAR film (Kodak).

2.4.4.4 Stripping and re-probing of membranes

In order to detect another protein of similar size to the protein initially detected, membranes were stripped and re-probed with an alternate primary antibody. ECL reagent was washed from the membranes by incubation with PBST on a rocker for five minutes. Proteins were incubated in ddH₂O for a further 5 minutes before being left in a beaker of boiling ddH₂O for 10 minutes. After stripping, membranes were incubated in PBST for 5 minutes before being blocked in 5% milk as before. They were then immunoblotted as described above as for the initial antibody.

2.4.4.5 Densitometry

Western Blots were quantified by densitometry using the Genetools, Syngene program. Blots were scanned as TIFF files and imported into the Syngene program (<http://www.syngene.com/genetools/>). Identical boxes were constructed around each band of interest, and one representing the background signal of the film. The intensity of signal within each box was calculated by the Syngene program. Using Microsoft Excel, the intensity of each band was calculated minus background signal, and normalized either to the corresponding loading control or, in the case of bicistronic vector, to the GFP transfection control.

<i>Antibody</i>	<i>Company</i>	<i>Species</i>	<i>Concentration</i>	<i>Application</i>
FLCN monoclonal	Cell Signalling	Rabbit	1 in 5000	Western Blot
FLCN monoclonal	Cell Signalling	Rabbit	0.5 µg	Immunoprecipitation
FLCN monoclonal	Cell Signalling	Rabbit	1 in 400	Immunofluorescence
FLCN polyclonal	Abnova	Mouse	1 in 2000	Western Blot
GFP monoclonal	Clontech	Mouse	1 in 5000	Western Blot
GFP monoclonal	Clontech	Mouse	1 in 200	Immunofluorescence
p0071 (clone 7.7.9) monoclonal	Progen	Mouse	1 in 20	Western Blot
p0071 (clone 7.7.9) monoclonal	Progen	Mouse	4 µg	Immunoprecipitation
p0071 monoclonal	(Wolf <i>et al</i> 2006)	Guinea Pig	1 in 100	Immunofluorescence
Flag monoclonal	Sigma	Mouse	1 in 1000	Western Blot
Flag monoclonal	Sigma	Mouse	4 µg	Immunoprecipitation
Flag monoclonal	Sigma	Mouse	1 in 1000	Immunofluorescence
β actin monclonal	Sigma	Mouse	1 in 5000	Western Blot
α Tubulin monoclonal	Sigma	Mouse	1 in 5000	Immunofluorescence
HA monoclonal	Roche	Rat	1 in 500	Immunofluorescence

Table 2.10 Primary antibodies used

<i>Antibody</i>	<i>Company</i>	<i>Species</i>	<i>Concentration</i>	<i>Application</i>
HRP conjugated anti-mouse	Dako	Rabbit	1 in 1000	Western Blot
HRP conjugated anti-rabbit	Dako	Goat	1 in 1000	Western Blot
anti-rabbit Alexa 594	Invitrogen	Goat	1 in 1000	Immunofluorescence
anti-mouse Alexa 488	Invitrogen	Goat	1 in 1000	Immunofluorescence
anti-mouse Dylight 649	Jackson	Donkey	1 in 250	Immunofluorescence
anti-rabbit Dylight 649	Jackson	Donkey	1 in 250	Immunofluorescence
anti-mouse Dylight 488	Jackson	Donkey	1 in 300	Immunofluorescence
anti-Guinea Pig Dylight 488	Jackson	Donkey	1 in 300	Immunofluorescence
anti-rabbit Dylight 488	Jackson	Donkey	1 in 400	Immunofluorescence
anti rabbit Cy3	Jackson	Donkey	1 in 400	Immunofluorescence
anti-mouse Cy3	Jackson	Donkey	1 in 300	Immunofluorescence
anti-Guinea Pig Cy3	Jackson	Donkey	1 in 400	Immunofluorescence

Table 2.11 Secondary antibodies used

2.5 Cloning

Plasmid cloning was used in two sections of this project. Initially *FLCN* cDNA was subcloned from the p.FLAG-CMV vector into the p.IRES2-acGFP1 vector, and patient mutations modeled in *FLCN* cDNA using site-directed mutagenesis.

FLCN was also cloned from human cDNA into the Venus vectors used in bimolecular fluorescence complementation analysis, to make fusion proteins of folliculin with each half of YFP, in both orientations (see section 2.7.1).

2.5.1 Proofreading PCR

To amplify the *FLCN* open reading frame from human cDNA, primers were designed which incorporated EcoR1 and BamH1 sites at the 5' and 3' end of *FLCN* respectively. It was confirmed by sequence analysis that *FLCN* contained no sites of recognition for these restriction endonucleases within its sequence. The primers were designed to include the restriction enzyme sites so that they were in frame with the preceding tag sequence and where appropriate the preceding Venus fusion protein. A cap of GCAG was added to the start of each primer to aid restriction digest. Primer sequences used for cloning *FLCN* into the Venus constructs are given in Table 2.14. The PCR reaction mixture and reaction profile are given in tables Table 2.12 and Table 2.13 respectively. Pfu enzyme was purchased from Stratagene, other PCR reagents were the same as used for PCR described in section 2.1.2.

<i>Reagent</i>	<i>Volume per reaction (μl)</i>
10x PCR buffer (2 mM Mg)	5
dNTP mix (25 μM/μl per dNTP)	2.5
Forward primer (20 pmol/μl)	1
Reverse primer (20 pmol/μl)	1
Pfu polymerase (5 units/μl)	1
DNA template	3
Nuclease free H ₂ O	37.5
Total	50

Table 2.12 Proofreading PCR reagents and volumes

<i>Step</i>	<i>Temperature (°C)</i>	<i>Time</i>	<i>Number of Cycles</i>
Initial melting	95	5 minutes	1
Melting	95	30 seconds	35
Annealing	56	30 seconds	
Extension	72	60 seconds	
Final extension	72	7 minutes	1

Table 2.13 Proofreading PCR reaction conditions

<i>Primer</i>	<i>Sequence</i>
FLCN forward	GCAGGAATTCATGAATGCCATCGTGGCTCT
FLCN reverse STOP	GCAGGGATCCTCAGTTCCGAGACTCCGAGG
FLCN reverse no STOP	GCAGGGATCCGTTCCGAGACTCCGAGGCTG

Table 2.14 Primers used for FLCN cloning into Venus vectors

FLCN Forward was used as the forward primer for all vectors. FLCN reverse STOP was used as the reverse primer for p.Ven2-HA-C and p.Ven1-Flag-C and FLCN reverse no STOP used for p.Ven1-Flag-N and p.Ven2-HA-N

2.5.2 Gel extraction

The amplified PCR products were electrophoresed on a 1% (w/v) agarose gel as in section 2.1.3, using a 1 kb DNA ladder (New England Biolabs) for a DNA fragment size

reference. The gel was visualised under UV light, and the correct sized band excised using a clean scalpel. To purify the DNA, the surrounding gel was digested using the QIAGEN QIA quick spin kit. The gel slice was weighed and 3 volumes of QG buffer added per 1 volume of gel (100 µl per 100 mg gel), and the tubes incubated at 50°C for 10 minutes until the gel was completely dissolved. 1 gel volume of isopropanol was added to the sample to maximize DNA yield, the sample added to a collection column and centrifuged at 15600 x g for 1 minute at room temperature. To remove all traces of agarose, the DNA bound to the collection column was washed by addition and centrifugation of 0.5 ml buffer QG. To wash the DNA 0.75 ml of buffer PE was added, incubated for 3 minutes then centrifuged. Flow through was discarded, and the column re-centrifuged at 15600 x g to remove residual PE buffer. Finally the DNA was eluted by addition of 30 µl of nuclease free water to the centre of the column, incubation for 1 minute and centrifugation at 15600 x g for 1 minute.

2.5.3 Restriction digest

Gel extracted PCR products and corresponding vectors were digested with restriction enzymes EcoR1 and BamH1, respectively, to create complimentary, cohesive ends on both. Digestion mixtures were set up as in Table 2.15 and incubated at 37°C for 4 hours. Reagents were purchased from Promega.

<i>Reagent</i>	<i>Volume per Digest (μl)</i>
10 x Buffer E	2
BSA	0.2
BamH1	0.5
EcoR1	0.7
DNA	Volume for 1 μ g
Nuclease free water	Up to 20
Total	20

Table 2.15 Restriction digest reagents and volumes

Digested products were then loaded in full onto a 1% (w/v) agarose gel and electrophoresed and gel extracted as described previously. Estimation of the quantity of DNA digested was determined by comparison with a 1kb DNA ladder.

2.5.4 Ligation

To ligate the digested insert into the digested plasmid, the following reaction mixture was prepared and incubated at room temperature over night. Reagents were purchased from Promega.

<i>Reagent</i>	<i>Volume per Ligation (μl)</i>
2x ligation buffer	5
T4 DNA ligase (3 units/ μl)	1
Insert digested DNA	3
Vector digested DNA	1
Total	10

Table 2.16 Ligation reaction reagents and volumes

2.5.5 Transformation

The ligated plasmids were then transformed into *E. Coli* for propagation. 7 μl plasmid was added to 30 μl competent *E. Coli* cells, and the mixture incubated on ice for 30 minutes. The bacteria were heat-shocked at 42°C for 45 seconds and immediately cooled back on ice. 500 μl of SOC medium (Invitrogen) was added to each transformation mixture, and the cells incubated at 37°C for 90 minutes with 220 rpm shaking, to allow antibiotic resistance genes located in the plasmids to be expressed. Cells then were collected in a pellet by centrifugation at 2254 x g for 3 minutes, and the pellet resuspended in 100 μl of SOC medium (Invitrogen). The bacteria containing medium was then transferred to LB agar plates containing either 100 μg/ml of ampicillin or 50 μg/ml of kanamycin, and the plated incubated over night at 37°C.

2.5.6 Purification of plasmid DNA

2.5.6.1 Screening of colonies

Only bacteria which had been transformed were able to grow on the selective bacterial plates. Single colonies were picked and transferred into 5 ml of LB broth containing the same concentration of appropriate antibiotic. The cultures were left to propegate overnight at 37°C in a shaking incubator (220 rpm). After > 16 hours of growth, the cells were collected by centrifugation and the plasmid purified by either miniprep (small scale) or maxiprep (large scale).

2.5.6.2 Miniprep

Minipreps were carried out using a QIAGEN miniprep kit. Cells were pelleted by centrifugation at 6000 x g for 15 minutes at 4°C. The cell pellet was resuspended in 250 µl of buffer P1, and cells lysed in 250 µl of buffer P2. The lysis reaction was neutralized by addition of 350 µl of buffer N3. Cells were then centrifuged for 10 minutes at 13,000 rpm to separate the cell debris. The plasmid containing supernatant was transferred to a spin column and the DNA bound by centrifugation. The DNA was washed initially with 500 µl of Buffer PB and then 750 µl of Buffer PE, with a 1 minute, 15600 x g centrifugation step after each wash. The column was then transferred to a clean tube and 50 µl of nuclease free water added to the column. After 2 minute incubation, the DNA was eluted by centrifugation at 15600 x g for 1 minute.

A restriction digest was set up as before for 5 μ l of the DNA, and the digested product run on a 1% (w/v) agarose gel to check for which plasmids had ligated the correct sized insert. When a correctly ligated plasmid was identified the miniprep DNA was then sequenced directly for the complete *FLCN* sequence including primers covering the boundaries between insert and vector. Primers are given in Table 2.17, and the reaction profile and ethanol precipitation was the same as for genomic DNA sequencing. If the plasmid was proved by sequencing to include the insert in frame, and un-mutated, the DNA was propagated in large bacterial cultures and purified by maxiprep for use in cell transfections.

2.5.6.3 Maxiprep

For the large scale preparation of plasmid DNA, the Genopure Plasmid Maxi Kit (Roche Applied Science) was used. Colonies were initially picked and grown in 5 mls of LB broth containing the appropriate antibiotic for 6 hours in a shaking incubator at 37°C. This culture was then added to 100 ml of the same LB broth, and grown over night with the same conditions. The following day, the cells were centrifuged at 1400 x g for 5 minutes and the supernatant disposed of. The pellet was resuspended in 12 mls of suspension buffer and the cells lysed by addition of 12 mls of lysis buffer and incubation for 3 minutes. The lysis was neutralised by addition of 12 mls of neutralisation buffer and mixing inverting the tube 6-8 times until a homogenous suspension had formed. The tube was then incubated for 5 minutes on ice. The lysate was cleared of SDS precipitates

by filtration, and the filtered solution loaded onto a pre-equilibrated column. The lysate was allowed to run through the column by gravity flow, and the flowthrough discarded. The column was then washed twice with 16 ml of wash buffer and the flowthrough discarded. To maximize yield the plasmid was eluted into a fresh tube by addition of 15 ml of pre-warmed elution buffer (50°C) to the column. The eluted plasmid DNA was then precipitated by addition of 11 ml of isopropanol, and collected by centrifugation at 1400 x g for 30 minutes at 4°C. The DNA pellet was then washed with 4 mls of ice cold 70% ethanol and re-centrifuged for 10 minutes at 1400 x g. After removal of the 70% ethanol by pipette, the DNA pellet was allowed to air dry for 10 minutes, before being dissolved in 200 µl of nuclease free water.

After both plasmid preparation procedures, the DNA concentration was measured using a nanodrop spectrophotometer and the quality of DNA can be determined by ratio of absorbance at 260nm vs 280nm.

<i>Primer</i>	<i>Sequence</i>
EcoR1	GCGAATTCAATGAATGCCATCGTGGCTCTCTGC
Primer1	GCACCCGGGATATATCAGCCATG
Primer2	AGCGTGCTCAGAGGATGAACACAG
Primer3	TCTTCAAGTCCCTCCGGCACATG
Primer4	GCTCAGCAAGTACGAGTTTGTG
BamH1 Reverse	GATGGATCCTCAGTTCCGAGACTCCGAGGC
EcoR1 Reverse	GCGCACGCATCCGACTGTTCATCT

Table 2.17 Primers used for FLCN ORF sequencing

EcoR1 primer designed from the EcoR1 site encompassing the FLCN ATG start site
 BamH1 reverse primer designer from the reverse BamH1 site encompassing the FLCN
 stop codon

EcoR1 reverse primer designed to sequence from within FLCN back into the vector

2.5.7 Site directed mutagenesis

Site-directed mutagenesis using the QuikChange Lightning Site-Directed Mutagenesis Kit (Stratagene) was used to introduce a number of patient mutations into *FLCN* cDNA for expression in FTC-133 cells. *FLCN* had been previously cloned into the pFLAG-CMV vector by Dr Anne Reiman, which acted as a template for construction of the *FLCN* mutants. Primers for site-directed mutagenesis are displayed in Table 7.1. Mutant constructs were subsequently sub-cloned into the p.IRES2-AcGFP1 vector described in Appendix 7.1.

Complimentary primers were designed according to the manufacturer's instructions to contain the appropriate mutation surrounded by between 15 and 20 base pairs of wild type sequence in each direction. A proofreading PCR was carried out to synthesis the mutant DNA. Reaction components are given in Table 2.18, reaction thermal profile given in Table 2.19.

<i>Reagent</i>	<i>Volume (μl)</i>
10 x Reaction Buffer	2.5
dsDNA template (100ng)	2.8
Primer 1 (50 ng/ μ l)	0.5
Primer 2 (50 ng/ μ l)	0.5
dNTP mix	0.5
Quiksolution reagent	0.75
Nuclease free water	16.95
QuikChange lightning enzyme	0.5
Total	25

Table 2.18 Site-Directed mutagenesis reaction reagents and volumes

<i>Step</i>	<i>Temperature</i>	<i>Time</i>	<i>Number of Cycles</i>
Initial melting	95°C	2 minutes	1
Melting	95°C	20 seconds	18
Annealing	60°C	10 seconds	
Extension	68°C	4 minutes	
Final Extension	68°C	5 minutes	1

Table 2.19 Site-Directed mutagenesis reaction PCR conditions

After completion of the PCR reaction, 2ul of *Dpn I* restriction enzyme was added to each amplification reaction to digest the methylated, non-mutated parental DNA (DNA isolated from almost all *E. coli* strains is dam methylated and therefore susceptible to Dpn I digestion), but leaving the PCR amplified (mutant DNA) intact. The mixture was then spun down, and incubated at 37°C for 5 minutes.

Transformation was achieved using XL10-Gold ultra competent cells as described in section 2.5.5, and colonies processed and sequenced as described previously.

Plasmids used in this project are given in Appendix 7.1.

2.6 Soft Agar Colony Formation Assay

The soft agar colony formation assay tests the ability of cells to grow unadhered to a surface suspended in soft agar, which measures cell proliferation in a semisolid culture media. The assay is considered a simple yet stringent assay for detecting malignant transformation *in vitro* and was used in this project to test the potential tumour suppressor function of a number of mutant folliculin constructs.

Firstly 1 x DMEM and 2 x DMEM solutions were made up as described in Table 2.20 and Table 2.21.

<i>Reagent</i>	<i>Volume (mls)</i>
Fetal calf serum	50
Pen/strep solution	5
L-Glutamine	5
10 x DMEM	50
7.5% Sodium bicarbonate	25
Sterile nuclease free water	115
Total	250

Table 2.20 2 x DMEM reagents and volumes

<i>Reagent</i>	<i>Volume (mls)</i>
Fetal calf serum	20
Pen/strep solution	2
L-glutamine	2
10 x DMEM	20
7.5% sodium bicarbonate	10
Sterile nuclease free water	146
Total	200

Table 2.21 1 x DMEM reagents and volumes

1.4% (w/v) noble agar was dissolved in sterile, distilled water and mixed with the DMEM mixtures as described in Table 2.22 and Table 2.23, to form 0.7% (v/v) DMEM agar and 0.35% (v/v) DMEM agar.

<i>Reagent</i>	<i>Volume (mls)</i>
2 x DMEM	150
1.4 % Agar	150
Total	300

Table 2.22 0.7% (v/v) DMEM agar constituents

<i>Reagent</i>	<i>Volume (mls)</i>
1 x DMEM	40
2 x DMEM	20
1.4 % agar	20
Total	80

Table 2.23 0.35% (v/v) DMEM agar constituents

Both DMEM agar mixtures were kept at 42°C to maintain a liquid state. 2 mls of 0.7% DMEM agar was added to each well of a 6 well plate to make the base agar level, and was left to set at room temperature. FTC-133 cells expressing various *FLCN* mutants as stable mixed populations were released from flasks using trypsin as described in section 2.2.1, and were counted. Per well, 3×10^4 cells were combined with 1 ml of 0.35% agar and laid on top of the 0.7% base layer. This layer was then left to set at room temperature. Finally a further 2 mls of 0.7% agar was place on top of the cells and left to set at room temperature. The plates were left in and incubator for up to four weeks, with 200 µl of G418 selective media added per well twice weekly. At day 27 the plates were blinded and colonies over 100 microns in size were counted (indicative of loss of growth suppression). Experiments were carried out in 6 wells for each construct. Reagents were purchased from Sigma unless otherwise stated.

2.7 Immunofluorescence Microscopy

Immunofluorescence microscopy was used to determine if apparent non-pathogenic *FLCN* variants might be influencing the cellular distribution of folliculin and also to define the cellular context of the interaction between folliculin and p0071.

Cells were grown on poly-L-Lysine covered cover slips for at least 24 hours before fixation. Media was aspirated and the cells washed 3 times with ice cold PBS. To fix the cells, ice cold 3.7% (w/v) formaldehyde (dissolved in PBS pH 7.0) was added to each well and the plate left for 10 minutes on ice. After this time, formaldehyde was aspirated and the slides washed a further 3 times with ice cold PBS. To permeabilise cell membranes, 1 ml of 0.5% Triton-X-100 (Sigma) diluted in PBS was added to each well, and incubated on ice for 15 minutes. The cells were then blocked to prevent non-specific antibody binding, by incubating with pre-centrifuged 1% (w/v) milk (diluted in PBS) at 4°C for 2 hours.

After blocking, the coverslips were washed 3 times with PBS, and placed upturned onto a 50 µl drop of primary antibody diluted in milk for 1 hour at room temperature. After incubation with primary antibody, the coverslips were washed three times in PBS and placed onto a 50 µl drop of corresponding, fluorophore conjugated secondary antibody, and incubated in the dark also for 1 hour at room temperature. Antibodies and concentrations used are given in Table 2.10 and Table 2.11. Finally, coverslips were washed twice in PBS, once in distilled water and once in 70% ethanol before being left to

dry in the dark. Coverslips were mounted onto glass microscopy slides using ProLong Gold Antifade Reagent with DAPI (4',6-diamidino-2-phenylindole) (Invitrogen).

2.7.1 Bimolecular fluorescence complementation analysis

Bimolecular fluorescence complementation analysis enabled the direct visualization of the interaction between follinulin and p0071 in living cells. The principles of the assay in the context of this thesis are discussed in section 5.3.2.1.

Full length *FLCN* was amplified from human cDNA by PCR, and cloned into both Venus 1 and Venus 2 BiFC vectors, in both N-terminal fusion and C-terminal fusion orientation respectively (For plasmid maps for Venus constructs see Appendix 7.1). Venus constructs expressing p0071 fused to both the N terminal half (Venus 1 - amino acids 1-115) and C terminal half (Venus 2 - amino acids 115-238) of YFP respectively, were co-expressed with *FLCN* constructs cloned into the complimentary Venus vector.

All various combinations of *FLCN* and p0071 complimentary Venus constructs were co-transfected into HeLa cells using calcium phosphate precipitation (see section 2.2.3.1). After 24 hours, the cells were fixed using formaldehyde fixation at 4°C, and were stained for HA, Flag and DAPI. Cells in which both *FLCN* and p0071 Venus-fusion constructs were expressed at close to endogenous levels (identified by HA and Flag staining), were imaged using a Nikon Eclipse 600 microscope. BiFC signal was detected at 495 nanometers, and it was determined that the combination of pVen1-Flag-p0071 and p.Ven2-HA-*FLCN* produced the most easily detectable signal. To determine potential

interaction at cytokinesis, α -tubulin was stained instead of Flag so that midbodies could be identified. Folliculin was predicted by yeast-2-hybrid to bind to the head domain of p0071, so a p.Ven1-Flag-p0071 repeats fusion of only the armadillo repeats of p0071 (head domain of p0071 lacking) was used as a negative control.

2.8 G-LISA RhoA activation assay

2.8.1 Assay principle

The small GTPase RhoA, is a molecular switch which operates by alternating between an active, GTP bound state and an inactive, GDP bound state. The mechanisms of RhoA activation are discussed in detail in Section 5.1.3.2. The G-LISA RhoA activation assay (cytoskeleton inc.) was used to determine the amounts of active RhoA in various isogenic cell models, and hence the differences in the signaling intensity through the RhoA pathway.

The G-LISA kit contains a protein which specifically binds to the GTP-bound form of RhoA, linked to the wells of a 96 well plate. When lysates are added to the plate, only active RhoA is bound, and the inactive RhoA removed during washing steps. The amount of GTP-bound RhoA is detected with a RhoA specific antibody, and the signal absorbance quantified using a microplate spectrophotometer.

2.8.2 Methodology

2.8.2.1 Cell culture

Cells were grown in 100 mm dishes for 3 days to reach a confluency of 50-60% by the time of harvesting. In experiments including siRNA treatment, cells were seeded on top of the siRNA mixture, and left for 3 days to reach the required 50-60% confluency at harvesting. In primary experiments, cells were grown in both normal and serum starved media, which had no impact on the experimental outcome. Subsequent experiments were therefore undertaken in normal serum media.

2.8.2.2 Cell lysis

The binding of RhoA to GTP is a transient occurrence, and is liable to dissociate rapidly if exposed to temperatures of greater than 4°C for a prolonged period. Therefore in lysing the cells, every effort was made to work as quickly as possible, keeping the cells lysates as cold as possible. Lysate collection was undertaken sequentially to allow rapid processing. After three days of culture, the cells were lysed. Media was immediately aspirated from the 100 mm dish, and the cells rinsed with 10 ml of ice cold PBS. All PBS was carefully removed and 250 µl of ice cold lysis buffer added to the cells. Lysates were harvested with a cell scraper, transferred to an ice-cold 1.5 ml tube and clarified by centrifugation at 11180 x g at 4°C for 2 minutes. 60 µl of lysate was removed for protein

quantification and western analysis, and the remaining lysate snap frozen in liquid nitrogen and stored at -80°C.

Equalised protein lysates were immunoblotted for p0071, folliculin, β -actin and RhoA to confirm equal loading and successful knockdown where appropriate.

2.8.2.3 *G-LISA assay*

Frozen lysates were thawed in a room temperature water bath, and placed on ice once thawed. 70 μ l of lysate was mixed with an equal volume of binding buffer by vortexing, and 50 μ l added to duplicate wells of the Rho plate. A buffer blank negative control and 1 ng of GTP bound RhoA positive control were also mixed with binding buffer and added to duplicate wells. The plate was then incubated at 4°C on an orbital microplate shaker (20 g) for 30 minutes. Lysate was then vigorously removed and the wells washed twice with 200 μ l of wash buffer. 200 μ l of antigen presenting buffer was added to each well and incubated at room temperature for 2 minutes. After 3 more washes with 200 μ l of wash buffer, the wells were incubated with 50 μ l of anti-RhoA primary antibody on a microplate shaker for 45 minutes at room temperature. After incubation, the antibody was vigorously removed and the wells washed 3 times in wash buffer, before being similarly incubated with 50 μ l HRP coupled, secondary antibody for 45 minutes at room temperature. Secondary antibody was removed after the incubation; the wells were washed 3 times with wash buffer and 50 μ l of HRP detection reagent added to each well.

The plate was then left in a 37°C incubator for 15 minutes at which point 50 µl HRP stop buffer was added to each well to quench the reaction. The luminescence absorbed from each well was immediately measured at 490 nm using a microplate spectrophotometer, and the levels of active RhoA calculated in Microsoft Excel according to the G-LISA manufacturing instructions.

2.9 *In vitro* cell scratch migration assay

The *in vitro* cell scratch assay was used to study the effects of folliculin loss on cell migration. Cells were grown to full confluency in 6 well plates, and serum starved as described in section 2.2.2. The following day, a scratch in the cell monolayer was made with a p200 pipette tip, with a perpendicular scratch for reference. The cell scratch was imaged at the same point (using the perpendicular scratch) at 0 hours and every 24 hours until the scratch had healed. The percentage of scratch healed at each time point was determined using ImageJ software. In the experiments investigating the effects of Rock inhibitor Y-27632 (Sigma) on cell migration, 10 µM (dissolved in 20 µl ddH₂O) was added dropwise to each well every 12 hours though out the experiment (media changed before each treatment). In the untreated samples, the same volume of distilled water was added to the cells in a similar manner.

Chapter 3 Investigations of the *FLCN* gene in familial and sporadic colorectal cancer

3.1 Introduction and overview

3.1.1 Colorectal cancer

Colorectal cancer (CRC) is a major worldwide health risk with over 800,000 new patients being diagnosed with colorectal carcinomas each year, making up approximately 8.5% of all new cancer cases. Of these, approximately 30% of patients will have a first or second degree relative affected by the cancer (Gatalica and Torlakovic, 2008). While the molecular mechanisms of colorectal tumourigenesis are increasingly well understood, the prognosis, particularly for more advanced forms of the disease has not dramatically improved (Li and Lai, 2009). It is crucial to try and catch colorectal cancer as early as possible, with over a 90% five year survival rate for those cases caught at Dukes stage A (currently only around 9%) (O'Connell, et al., 2004). This can be achieved by identifying groups at increased risk of colorectal cancer (especially if earlier onset), and subsequently tailoring their colonoscopy surveillance to this information. The interaction between a person's genetics and environmental factors play an important role in colorectal carcinogenesis, and it is through insights into both these mechanisms that these at risk groups can be identified.

3.1.2 The genetic mechanisms of colorectal tumourigenesis

Colorectal tumorigenesis is a multistep process of genetic alterations that cause the progressive transformation from normal colorectal mucosa into benign adenomas and

eventually highly malignant carcinomas. This progression is driven by the accumulation of mutations; each one providing a growth advantage to the mutated cells. The mutated cancer cells acquire various advantageous properties including uncontrolled proliferation, the loss of intracellular adhesion, the ability to digest the basement membrane, enhanced motility and the ability to survive in remote locations (Tejpar and Van Cutsem, 2002).

E. Fearon and B. Vogelstein proposed the following model for colorectal tumourigenesis. It has since been confirmed and expanded, and is considered a classic genetic model of tumourigenesis (Fearon and Vogelstein, 1990).

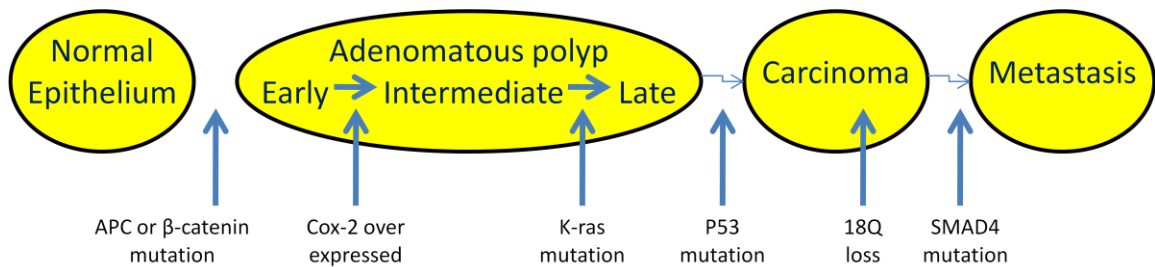


Figure 3.1 Genetic model of colorectal tumourigenesis

Adapted from (Tejpar and Van Cutsem, 2002)

While more recent studies have confirmed the model proposed by Fearon and Vogelstein, there are many additional genes which have been demonstrated to also be involved

(Lynch and de la Chapelle, 2003). Colorectal cancers progress through the accumulation of additional genetic instability which drives the accumulation of other cancerous mutations. This instability is achieved either through chromosomal instability (as in Familial Adenomatous Polyposis) or microsatellite instability (as in Lynch syndrome/HNPCC), observed in both sporadic and familial colorectal cancers and is discussed in more depth in section 3.1.3. As a consequence of these molecular alterations, tumour suppressor genes can be inactivated (by mutation, deletion or epigenetic mechanisms) or proto-oncogenes activated.

3.1.2.1 Inactivation of APC is characteristic of the majority of colorectal cancers

APC is a tumour suppressor gene that is inactivated in more than 80% of colorectal cancers, a common feature of colon cancers driven by chromosomal and microsatellite instability. One of the functions of *APC* is to prevent the accumulation of catenins that can lead to the accumulation of oncogenes *c-myc* and *cyclinD1* (Su, et al., 1993). The cellular levels of β -catenin, a mediator in the wnt/wingless signalling pathway, are regulated by the *APC* gene product. The wnt signalling transduction pathway is a complex network of proteins that regulates the transcription of certain genes in response to extracellular glycoprotein ligands, often in conjunction with other pathways notably the transforming growth factor-B (TGF-B) and fibroblast growth factor (FGF) pathways (Tejpar and Van Cutsem, 2002). A brief summary of Wnt signalling in the physiological and cancer setting is displayed in Figure 3.2.

3.1.2.2 Wnt signalling and colorectal cancer

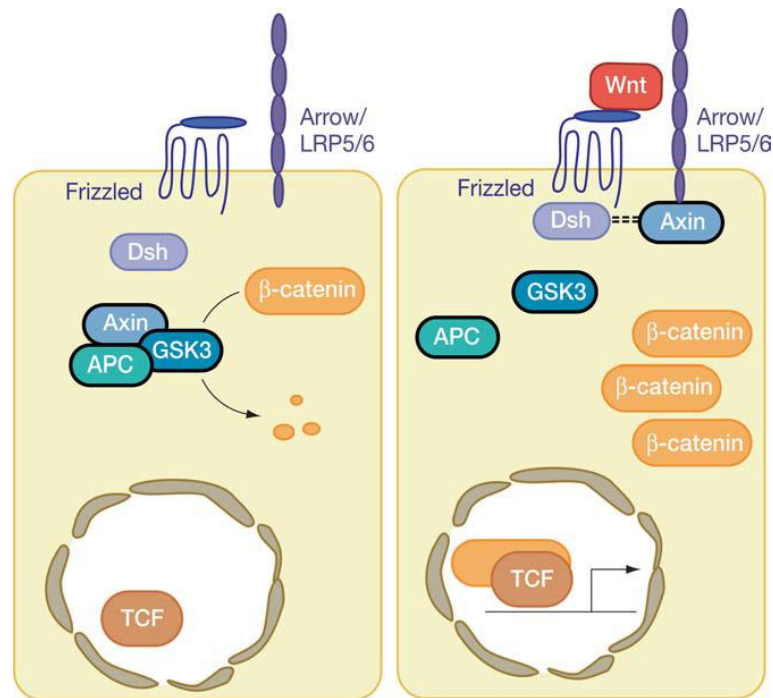


Figure 3.2 Summary of the Wnt signaling transduction pathway

(Logan and Nusse, 2004)

In the absence of Wnt signalling, a cytoplasmic degrading complex including APC, glycogen synthase kinase 3B and β -Catenin, causes the phosphorylation of both β -catenin and Axin by GSK-3B. This initialises the interaction of β -catenin with β -TrCP, leading to the ubiquitination of β -catenin and hence its degradation in the proteosome. Therefore the Wnt target genes remain off.

When the Wnt signal is present, it interacts with its co-receptors Frizzled and LRP, which causes the modular protein, dishevelled (Dsh), to be activated. Dsh interacts with Axin to

antagonise GSK3, halting the ubiquitination of β -catenin. Therefore β -catenin accumulates in the nucleus, interacts with TCF/LEF transcription factors and leads to the activation of Wnt target genes as an essential co-activator of transcription (Alberici and Fodde, 2006). Numerous TCF target genes have been identified and appear to be cell type specific, *MYC* (c-myc) and *CCND1* (Cyclin D1) being of major interest for cancer research (Clevers, 2006).

Although this pathway is a normal developmental pathway, its deregulation is a fundamental event in the initiation of colorectal cancer. 80% of colorectal adenomas have mutations in *APC* and of the other 20%, half harbour activating *CTNNB1* (β -catenin) mutations (Sparks, et al., 1998). Other genes encoding key members of the Wnt signalling pathway are also altered in colorectal cancer albeit less frequently, e.g. mutations in the genes *AXIN1*, *AXIN2* and *TCF7L2* (T-cell factor 4 a β -catenin binding transcription factor) and also the epigenetic silencing of genes such as sFRPs (secreted frizzled-related proteins). Despite the wnt pathway being known to activate alternate pathways including activation of Rho GTPase, Jun kinase and calcium dependent effectors, and wnt ligands being able to bind to alternate receptors such as Ryk and ROR2, activation of the wnt pathways has proved to be the key action for developing colorectal cancer cells (Polakis, 2007).

3.1.3 The chromosomal and microsatellite instability pathways of colorectal tumourigenesis

The progression to more advanced colorectal cancer occurs by adenoma cells acquiring additional genetic instability via either the chromosomal instability pathway or the microsatellite instability pathway.

3.1.3.1 Chromosomal instability

Chromosomal instability (CIN) is found in approximately 90% of colorectal cancers (Yim, 2011). CIN tumours develop gains or losses of whole chromosomes at a rate that is up to 100 times higher compared with normal cells. *BUB1* was the first gene reported that when mutated, lead to CIN (Cahill, et al., 1998), although loss of function of *APC* itself has been implicated in producing chromosomal instability (Fodde, et al., 2001). The progression to invasive colorectal carcinoma is achieved through the deregulation of numerous signalling pathways including, Wnt signalling, TGF- β signalling, and the p53 and K-ras pathways (Tejpar and Van Cutsem, 2002).

3.1.3.2 Microsatellite instability

Microsatellites are short, repetitive DNA tracts, and are mostly found in non-coding sections of the genome. However certain genes associated with promoting cancer,

including *APC* and *K-ras*, contain coding microsatellites. Mutations in one of the main mismatch repair (MMR) genes *MLH1*, *MSH2*, *MSH3* *MSH6* (*MSH2* and *MLH1* are responsible for 90% of cases) lead to deficiency in mismatch repair proteins, promoting mutations in genes harbouring coding microsatellites (Yim, 2011). These genes accumulate frame-shift mutations and hence become non-functional, fuelling the progression of colorectal cancer. However it is often unclear which microsatellite mutations are driving tumourigenesis and which mutations represent background microsatellite instability, not contributing to the progression of cancer. Microsatellite instability can be caused by sporadic inactivation of MMR genes, or due to a germline mutation in a MMR gene causing Lynch syndrome (discussed below). Interestingly, *APC* is one of numerous genes at increased risk of mutation in the background of mismatch-repair gene deficiency, and thus MMR genes are thought to represent “caretaker” genes which increase the mutation rate, whereas *APC* is believed to be a “gatekeeper” where mutation initiates neoplasia directly (Gryfe, 2009).

3.1.4 Hereditary colorectal cancer

The risk of developing colorectal cancer in the general population is between 5-6%. Patients with a familial risk (one or more first or secondary degree relatives with the disease) make up around 20% of all colorectal cancer cases, with 5-10% of all cases displaying a mendelian pattern of inheritance (Lynch and de la Chapelle, 2003).

The fraction of familial cancers related to high penetrance, predisposition alleles is relatively modest. The best understood colorectal syndromes, Familial Adenomatous Polyposis (FAP) and Hereditary non-polyposis colorectal cancer (HNPCC or Lynch Syndrome), together account for less than 5% of colorectal cancers, the remaining familial risks are likely due to lower penetrance alleles (de la Chapelle, 2004).

Identifying genes associated with familial cancers can help to identify at risk families, facilitating early detection, but can also provide important insights into the pathogenesis of both the familial and sporadic forms of the disease. For example, the discovery that mutations in the *APC* gene cause FAP, identified *APC* as a key gene to be mutated in the majority (>80%) of sporadic colorectal cancers (see FAP section below).

3.1.4.1 Lynch syndrome/Hereditary non-polyposis colorectal cancer (HNPCC)

Lynch syndrome is the most common heritable colon cancer syndrome and is dominantly inherited. Multiple generations are affected with the cancer with an early age of onset (mean approximately 45 years). Lynch syndrome also exhibits accelerated carcinogenesis, whereby a small colonic adenoma may become a carcinoma in 2 to 3 years as opposed to the 8 to 10 years seen in the general population (Lynch and de la Chapelle, 2003). The syndrome is caused by a lack of functional mismatch repair proteins due to germline mutations in mismatch repair (MMR) genes *MSH2*, *MLH1*, less frequently in *MSH6* and rarely in *PMS2* (Imai and Yamamoto, 2008). Germline MMR

gene mutations are implicated in the development of various cancers, with a penetrance of approximately 80% for colorectal cancer, 60% for endometrial cancer and less than 20% for a number of other organs. The lack of functional MMR proteins reflects in high microsatellite instability and the accumulation of mutations in the exonic microsatellites of multiple cancer driving genes (see microsatellite instability section). Lynch syndrome makes up approximately 3-5% of the total cancer burden in the USA (Gatalica and Torlakovic, 2008).

3.1.4.2 Familial adenomatous polyposis

Familial adenomatous polyposis (FAP) is another hereditary colorectal cancer syndrome which, like Lynch syndrome, presents autosomal dominant inheritance. The syndrome is characterised by a large number (>100) of adenomatous colorectal polyps usually presenting in adolescence (de la Chapelle, 2004). FAP makes up less than 1% of all new colorectal carcinomas observed, and is caused by a germline mutation in the *APC* gene (Kinzler, et al., 1991). In fully developed cases, the colonic mucosa is carpeted by hundreds of polyps, evenly distributed along the whole large bowel. At mean age of 40, second hit mutations/deletions result in adenocarcinoma development in a small proportion of these adenomas, with malignant degradation in most patients by the age of 50 (Lynch and de la Chapelle, 2003).

3.1.4.3 MYH associated polyposis

A second genetic pre-disposition to colorectal adenomatous polyposis and cancer, caused by mutations in the *MYH* gene, was identified in 2002 (Al-Tassan, et al., 2002). The polyposis in *MYH* mutation carriers is generally less severe than for FAP patients. *MYH* functions in DNA proofreading (base-excision repair) and inactivation of *MYH* leads to somatic mutations, in particular, a specific G:C to T:A transversion mutation in the *APC* gene. Thus *MYH*, similarly to MMR genes, can also be described as a “caretaker” gene (Gryfe, 2009).

3.1.5 The possible association between Birt Hogg Dubé Syndrome and increased risk of colorectal cancer

Birt Hogg Dubé syndrome is characterised by the development of fibrofolliculomas on the face and upper torso, renal cell carcinoma, lung cysts and pneumothorax, however the association with increased risk of colorectal cancer is more controversial.

Early reports of BHD syndrome described colorectal cancer as being part of the BHD phenotype (Birt, et al., 1977; Chung, et al., 1996; Hornstein, 1976; Rongioletti, et al., 1989; Schachtschabel, et al., 1996; Schulz and Hartschuh, 1999). However a large study of 111 BHD patients by Zbar *et al.* (2002), found only 3 to have colon cancer compared with 0 of the 112 non-BHD-affected control group ($p=0.12$) and regarding neoplasia, 8 of 45 BHD-affected persons compared with 7 of 38 non-affected-controls had colon polyps

by colonoscopy ($p=1.00$). The study concluded that colonic neoplasms were not associated with BHD syndrome (Zbar, et al., 2002).

Nevertheless, Khoo *et al.* (2002) described a large BHD syndrome family in which 6 of 20 affected family members had developed colonic polyposis and 2 had died of probable gastrointestinal cancer. These observations suggest that the association between BHD and colonic neoplasia may only relate to certain BHD families and that the interfamilial differences described may relate to allelic heterogeneity or modifier effects (Khoo, et al., 2002).

A small number of studies have examined the role of *FLCN* inactivation in colorectal tumorigenesis. Da Silva *et al.* (2003) reported a germline missense substitution (p.Arg320Gln) and a somatic missense substitution (p.Arg392Gly) in a study of 29 primary colorectal tumours, although the pathogenicity of these variants is unclear. Shin *et al.* (2003) identified frameshift mutations in the *FLCN* exon 11 mononucleotide tract, in 5/32 sporadic, microsatellite unstable colorectal tumours. Kahnoski *et al.* (2003) reported two novel missense variants Ser79Trp and Ala455Thr in 30 microsatellite stable CRCs, also of unknown pathogenicity (da Silva, et al., 2003; Kahnoski, et al., 2003; Shin, et al., 2003)

3.2 Aims and Approaches

Previously, members of our laboratory had identified unsuspected germline *FLCN* mutations in ~5% of patients with inherited RCC (familial RCC, multiple tumours or early onset) but no known causative syndrome (Woodward, et al., 2008). To further investigate the potential role of folliculin in the pathogenesis of colorectal cancer it was investigated (1) whether individuals with non-syndromic, familial colorectal cancer may harbour germline *FLCN* mutations (and how this compared with mutation rates in a new cohort of non-syndromic familial RCC patients), (2) whether there were potential genotype-phenotype correlations for CRC in BHD patients and (3) the frequency and clinicopathological associations of exon 11 mononucleotide repeat mutations in *FLCN*, in microsatellite unstable CRC.

3.3 Patients and samples

Four cohorts of patients were used for this study. (1) Blood DNA samples from 50 unrelated patients with familial colorectal cancer and no evidence of germline MMR gene mutations or FAP, were sequenced for germline *FLCN* mutations. *FLCN* was also sequenced in DNA extracted from five colorectal cell lines available in the laboratory (HCT-116, DLD-1, SW480, LoVo and HT29). (2) Similarly blood DNA from 39 unrelated patients with a familial risk of RCC (2 or more relatives with the disease), but no clinical diagnosis of VHL disease, BHD syndrome, familial leiomyomatosis or a

germline *VHL* mutation, and no evidence of a 3p chromosomal translocation were also analysed for germline *FLCN* mutations. All 11 coding exons and exon/intron boundaries were amplified by PCR and sequencing carried out directly from PCR products. (3) Clinical data for colorectal neoplasia (colon cancer or adenomatous polyps) was collected from 149 BHD syndrome affected patients from 51 families (*FLCN* mutation positive or clinically diagnosed according to European BHD consortium criteria (Menko, et al., 2009)). A subset of these patients (15 British and Dutch kindreds harbouring one of two recurrent, germline *FLCN* mutations) were analysed to identify possible genotype phenotype correlations for colorectal neoplasia. (4) DNA extracted from paraffin embedded tumour samples from 30 patients with microsatellite unstable colorectal cancer was analysed for somatic mutations in the mutation hotspot, C₈ mononucleotide tract in *FLCN* exon 11, and in the mononucleotide tracts in *TGFBR2*, *IGF2R* and *MSH6* genes.

Mutations analysis was performed as described in methods 2.1 using the primers in Table 2.3 and Table 2.4.

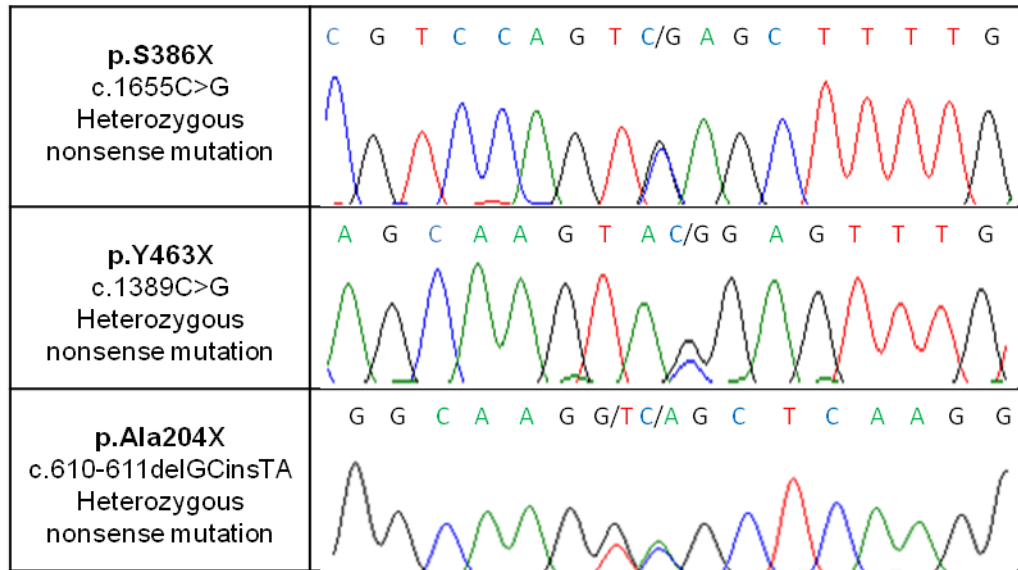
3.4 Results

3.4.1 FLCN mutation analysis in individuals with familial, non-syndromic RCC and CRC

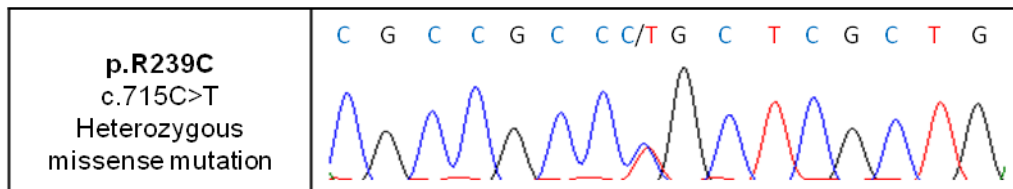
FLCN mutations were identified in 3 of 39 patients with familial RCC (see Figure 3.3). The study also included a positive control patient whose *FLCN* mutation had been previously reported. This mutation was correctly identified in the study. The p.S386X nonsense mutation identified in exon 10 is novel and has not been previously reported. It was not present in 164 normal control DNA samples also tested (Figure 3.3), nor was it found to be present in dbSNP (<http://www.ncbi.nlm.nih.gov/projects/SNP/>) or Exome Variant Server (evs.gs.washington.edu).

No *FLCN* mutations were detected in the cohort of patients with familial colorectal cancer, although one heterozygous variant of unknown significance (p.R362C) was identified in the LoVo cell line (Figure 3.3).

A



B



C

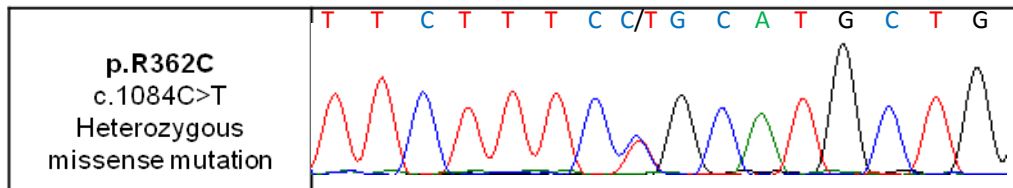


Figure 3.3 Summary of *FLCN* mutations detected

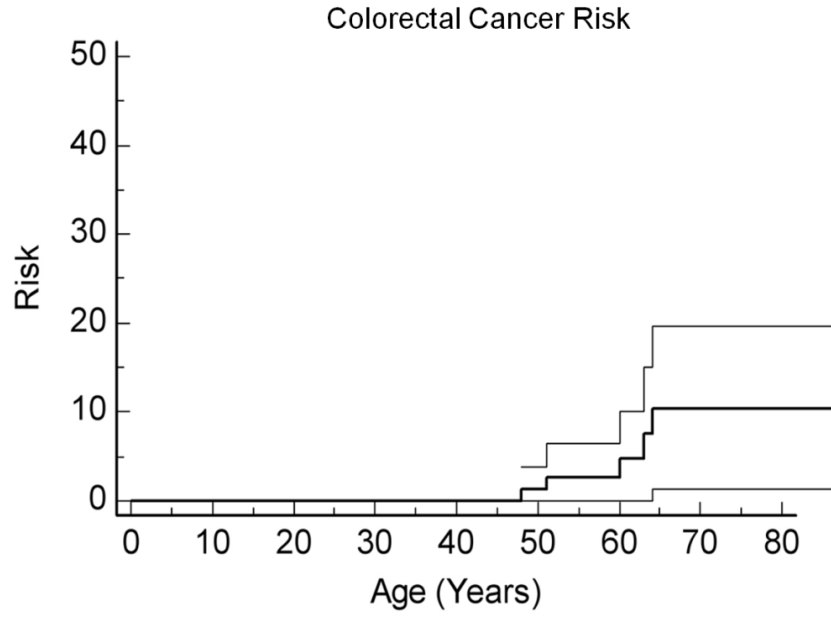
- (A) Diagram of electropherograms displaying three previously unidentified mutations, p.S386X in exon 10, p.Y463X in exon 12 and p.Ala204X in exon 6
(B) Previously identified, control mutation (p.R239C) in exon 7
(C) Mutation detected in colorectal cell line LoVo

3.4.2 Genotype-phenotype correlations for colorectal cancer in BHD patients

The cohort of 149 BHD patients were analysed for age related risk of colorectal cancer and colorectal neoplasia (cancer or neoplastic polyps). The risk of colorectal cancer and colorectal neoplasia are shown in Figure 3.4. Five members of the cohort had developed a CRC (mean age 57.4 years, range 48-64 years) and five patients had been diagnosed with colorectal polyps (mean age 52.0 years, range 42-68 years) (Figure 3.4).

Of this cohort, germline *FLCN* mutations had been described in 32 of the 51 families (104 affected individuals). Six mutations were found in two or more families, only two mutations present in more than 5 patients. The frameshift mutation c.1285dupC in exon 11, was present in 37 patients from 9 families and the c.610delGCinsTA nonsense mutation in exon 6, was present in 32 patients from 6 families. 5 patients harbouring the c.1285dupC mutation developed a colorectal neoplasm (3 of which were malignant) in contrast, none of the exon 6 mutation carriers developed a colorectal polyp or cancer. Comparison of the risks of colorectal neoplasia in c.1285dupC and c.610delGCinsTA mutation carriers displayed a significantly higher risk of colorectal neoplasia in the mononucleotide tract mutation carriers ($\chi^2=5.78$, $p=0.016$) (Figure 3.5).

A



B

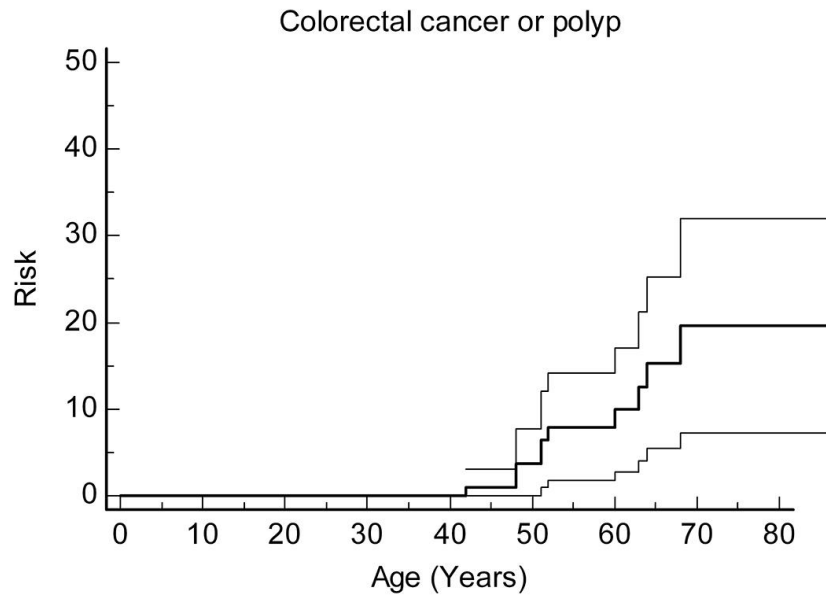


Figure 3.4 Age related risk of colorectal cancer (A) and neoplasia (B) in a cohort of 149 BHD patients from 51 families.

Error bars represent 95% confidence intervals

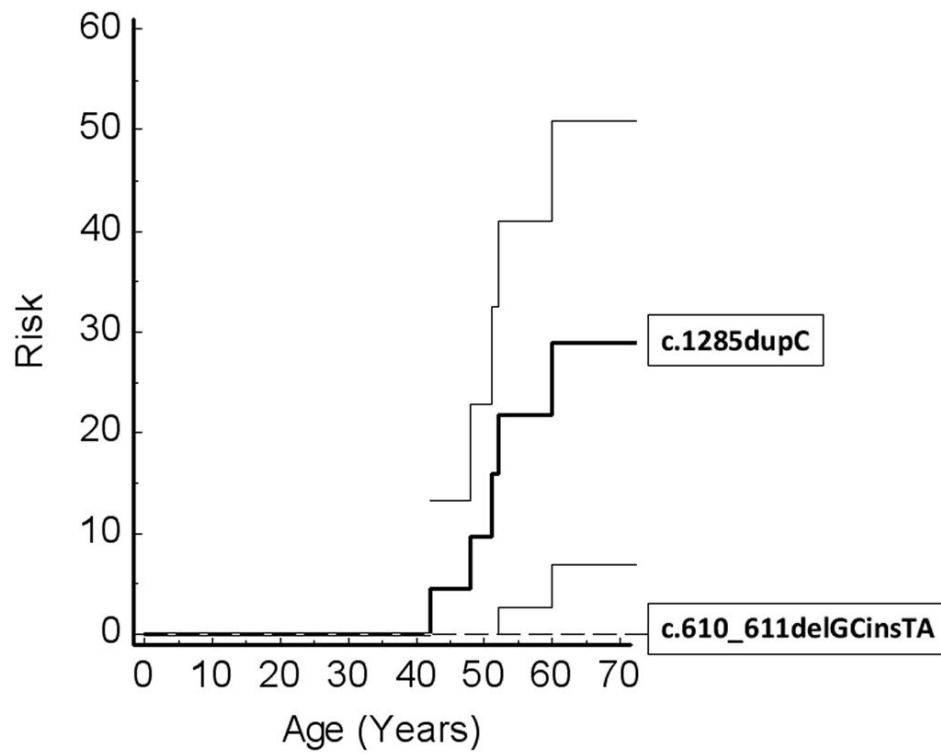


Figure 3.5 Comparison of the risks of colorectal neoplasia in *FLCN* c.1285dupC and c.610_611delGinsTA mutation carriers.

Error bars represent 95% confidence intervals

3.4.3 FLCN C₈ mononucleotide repeat mutation analysis in sporadic colorectal cancer tumours with microsatellite instability

The genotype-phenotype correlation identified suggested allelic heterogeneity in *FLCN* might be responsible for the differing risks of colorectal neoplasia in BHD patients, specifically at the exon 11 mononucleotide tract. Exonic mononucleotide tracts, such as that in *FLCN*, may be at increased risk of accumulating mutations under microsatellite unstable conditions. To test if this region might be mutated in sporadic colorectal cancers, the *FLCN* mononucleotide tract was sequenced in 30 microsatellite unstable colorectal tumour DNAs. Seven of 30 (23%) microsatellite unstable CRCs were identified to have heterozygous frameshift mutations within the *FLCN* mononucleotide repeat region in exon 11 (C₈). In five cases, the mutation was a single cytosine deletion (c.1285delC) and in two cases a single cytosine insertion (c.1285dupC) (Figure 3.6). Mean % (+standard deviation) of microsatellite instability (i.e. % of microsatellite markers showing instability divided by number of microsatellite markers tested) was similar in *FLCN* C₈ mutated and non-mutated tumours (83.5 (+8.38) and 64.2 (+5.86) respectively (t=1.57 P=0.128 – 2 tailed, independent Student's T Test. The mean % of mononucleotide microsatellite instability (tested using BAT25, BAT26 and/or BAT40 (Lynch and de la Chapelle, 2003)) was similar for *FLCN* mutated and non-mutated tumours (77.8 (+16.47) and 69.6 (+8.76) respectively (t=0.434 P=0.667 – 2 tailed, independent Student's T Test)). Results of MSH2 and MLH1 protein expression (by routine immunohistochemistry) were available for 26 tumours. The frequency of *FLCN* C₈

mutations was significantly higher in tumours that demonstrated loss of MLH1 or MSH2 protein expression than in those with no loss (43% (6/14) and 0% (0/12) respectively (P=0.017 – Fisher’s exact test)) (Table 3.1). To give an indication of the relative frequency of *FLCN* mutations compared with other known colorectal cancer MSI+ target genes, the mononucleotide tracts in *TGFBR2*, *IGF2R* and *MSH6* were also sequenced in the same samples. All tumours tested demonstrated a mutation within the A₁₀ tract in *TGFBR2* and 2/30 (7%) harboured a mutation within the G₈ tract in *IGF2R*. The two tumours with *IGF2R* mutations demonstrated instability for all microsatellite markers tested (6/6 and 7/7 markers). Immunohistochemistry for MSH2 and MLH1 expression was available for one of the *IGF2R* unstable cancers and loss of MLH1 expression was detected. No tumour demonstrated a mutation in both *FLCN* and *IGF2R*. *MSH6* mononucleotide tract mutations were detected in 7/30 (23%) of the colorectal cancers tested (28.5% and 8% respectively of those with and without MSH2 or MLH1 protein expression loss; P=0.17 – Fisher’s exact test) (Table 3.2).

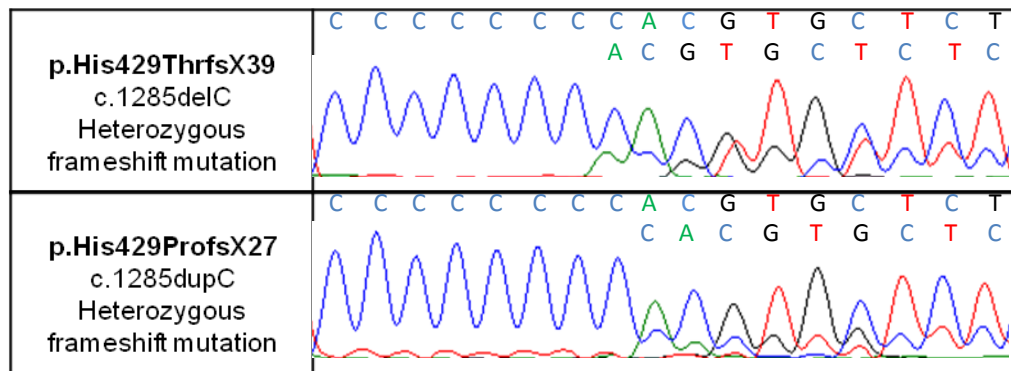


Figure 3.6 Schematic diagram of p.His429ThrfsX39 and p.His429ProfsX27.

Electropherograms showing the two mutations detected in 30 microsatellite unstable colorectal cancers, affecting the mononucleotide tract in exon 11 of FLCN

<i>Tumour</i>	<i>Folliculin</i>	<i>MSI</i>	<i>Immunohistochemical analysis</i>
1	no mutation	4 of 4 (3/3BATs)	Loss of MLH1
2	no mutation	4 of 4 (3/3BATs)	n/a
3	no mutation	2 of 4 (1/3BATs)	No loss of MLH1/MSH2
4	mutation	7 of 7 (3/3BATs)	Loss of MLH1
5	no mutation	6 of 6 (3/3BATs)	n/a
6	no mutation	2 of 7 (0/3BATs)	No loss of MLH1/MSH2/MSH6/PMS2
7	no mutation	3 of 7 (2/3BATs)	No loss of MLH1/MSH2/MSH6
8	no mutation	2 of 7 (0/3BATs)	No loss of MLH1/MSH2
9	no mutation	4 of 4 (0/0BATs)	Loss of MLH1
10	mutation	4 of 5 (2/2BATs)	Loss of MLH1/PMS2
11	no mutation	3 of 6 (2/2BATs)	No loss of MLH1/MSH2
12	no mutation	2 of 7 (0/3BATs)	No loss of MLH1/MSH2
13	no mutation	3 of 7 (3/3BATs)	No loss of MLH1/MSH2
14	mutation	7 of 7 (3/3BATs)	Loss of MSH2
15	no mutation	7 of 7 (3/3BATs)	Loss of MLH1
16	no mutation	3 of 7 (3/3BATs)	Loss of MLH1
17	no mutation	4 of 6 (3/3BATs)	n/a
18	no mutation	2 of 4 (1/3BATs)	No loss of MLH1/MSH2
19	no mutation	3 of 7 (0/3BATs)	No loss of MLH1/MSH2
20	no mutation	6 of 7 (3/3BATs)	Loss of MLH1
21	no mutation	7 of 7 (3/3BATs)	No loss of MLH/MSH2
22	no mutation	3 of 7 (3/3BATs)	No loss of MLH1/MSH2
23	mutation	3 of 6 (0/3BATs)	n/a

24	no mutation	5 of 7 (1/3BATs)	Loss of MSH2
25	mutation	5 of 7 (2/3BATs)	Loss of MLH1
26	no mutation	2 of 7 (2/3BATs)	No loss of MLH1/MSH2
27	no mutation	7 of 7 (3/3BATs)	Loss of MLH1/PMS2
28	mutation	Unknown	Loss of MLH1/PMS2
29	mutation	7 of 7 (3/3BATs)	Loss of MLH1
30	no mutation	5 of 7 (3/3BATs)	Loss of MSH2

Table 3.1 Details of FLCN mutation status and immunohistochemical status of mismatch repair proteins in MSI+ colorectal tumour DNA samples analysed, where information available

<i>Tumour</i>	<i>FLCN</i>	<i>IGF2R</i>	<i>MSH6</i>	<i>TGFBR2</i>
1	-	-	-	+
2	-	-	-	+
3	-	-	-	+
4	+	-	-	+
5	-	+	+	+
6	-	-	-	+
7	-	-	-	+
8	-	-	-	+
9	-	-	+	+
10	+	-	-	+
11	-	-	-	+
12	-	-	-	+
13	-	-	-	+
14	+	-	-	+
15	-	-	-	+
16	-	-	-	+
17	-	-	+	+
18	-	-	-	+
19	-	-	-	+
20	-	-	-	+
21	-	-	+	+
22	-	-	-	+
23	+	-	-	+

24	-	-	-	+
25	+	-	+	+
26	-	-	-	+
27	-	+	-	+
28	+	-	-	+
29	+	-	+	+
30	-	-	+	+

Table 3.2 Mutation profile of the mononucleotide repeat in four MSI+ target genes in 30 MSI+ colorectal tumours

3.5 Discussion

Cumulatively, the lifetime risk of developing colorectal cancer in the USA is high, close to 6% (Bazensky, et al., 2007). Assessing the precise tumour risks associated with rare familial cancer syndromes is a problem for geneticists, because of the limited number of patients available and the possible ascertainment bias associated with this.

The risks of colorectal neoplasia in this cohort (cohort (3) described in the methods section to this chapter) of BHD patients was around 20% and is notably higher than that in the general population (~6%) (Jemal, et al., 2002), however much larger numbers of patients would be required to obtain statistically significant results.

The results presented in this chapter differ from that of (Toro, et al., 1999), who found no colorectal neoplasms in 152 BHD syndrome patients. In a subsequent study from the same group, 3 colorectal tumours were detected in 111 patients with BHD syndrome, which was not statistically different from the number (0) in unaffected members of BHD families, leading the authors to conclude that there was no increased risk of colorectal neoplasia in BHD syndrome (Zbar, et al., 2002). Our findings are more similar to those of Khoo *et al.* (2002) who described a large French family with BHD syndrome, and an increased risk of colorectal neoplasia.

Differences in risk of colorectal neoplasia between different studies and BHD families may be the result of interfamilial differences in environment, or genetic modifier effects. The results presented in this chapter suggest that it is probable the differences observed

are due to *FLCN* allelic heterogeneity; different mutations within *FLCN* being associated with differing risks of colorectal cancer. This study identified that BHD patients with a mutation in the mononucleotide tract in exon 11 had a significantly higher risk of colorectal neoplasia than those with a c.610_611delGCinsTA nonsense mutation. It is also interesting to note that the high risk family described by Khoo *et al.* (2002) also affected the same locus (c.1285delC (previously reported as c.1733delC)). In the absence of nonsense mediated decay, exon 11 mononucleotide mutations with a single cytosine deletion would be predicted to result in a protein with p.His429ThrfsX39 (lacking 114 amino acids) and a single cytosine duplication p.His429ProfsX27 (lacking 126 amino acids). A possible explanation for the genotype-phenotype correlation observed is that if p.His429ThrfsX39 and p.His429ProfsX27 were produced in colorectal cells, they might exert a dominant negative effect on endogenous folliculin function not associated with the c.610delGCinsTA mutation (p.Ala204X (lacking 377 amino acids)). Alternatively, the shorter protein produced from the c.610delGCinsTA mutation may have differential effects on as yet undetermined folliculin functions (both mutations lack the FNIP1/FNIP2 binding domain). However Toro *et al.* (2008) reported 19 patients with exon 11 mononucleotide frameshift mutations who did not develop colorectal neoplasia, and hence further studies are required to confirm this finding in a larger dataset. If proven, it will be very useful to determine a functional explanation for the genotype-phenotype correlation observed, with an overall aim of providing better surveillance for those BHD patients at increased risk of CRC, and potentially influencing therapeutic strategies in the future.

Familial cancer genes are often also somatically inactivated in sporadic forms of the disease. Such examples include the finding of *VHL* and *APC* somatic mutations in most clear cell RCC and colorectal cancers respectively (Gallou, et al., 1999; Miyoshi, et al., 1992). Conversely, genetic studies into *FLCN* have revealed a low frequency of mutations in sporadic colorectal cancer. Three studies have previously investigated *FLCN* in sporadic colorectal cancer, reporting *FLCN* heterozygous mutation frequencies of 2/30 microsatellite stable CRC (p.Ser79Trp and p.Ala455Thr), 5/32 microsatellite unstable CRC, and 2/29 CRC (germline p.Arg320Gln and somatic p.Arg392Gly) (da Silva, et al., 2003; Kahnoski, et al., 2003; Shin, et al., 2003) respectively. The pathogenicity of the missense changes is unclear, and having never been reported as germline mutations in BHD patients, it is impossible to determine if they represent “passenger” mutations or those driving cancer progression.

Having identified an association between the germline *FLCN* c.1285dupC mutation and colorectal neoplasia, the potential link between colorectal neoplasia and exon 11 mononucleotide mutations was further investigated by analysing the region for somatic mutations in 30 microsatellite unstable (MSI+) CRCs. As aforementioned, mononucleotide repeat regions are known to be hypermutable in MSI+ CRC. Kahnoski *et al.* (2003) did not detect C₈ mutations in 8 MSI+ CRC analysed (Kahnoski, et al., 2003), however Shin *et al.* (2003) detected two c.1285dupC, two c.1285delC and one c.1285delCC in 32 sporadic MSI+ CRC's (5/32 = 16%) (Shin, et al., 2003). In this study, *FLCN* C₈ tract mutations were identified in 23% of MSI+ CRC analysed. In addition to

the mutant sequence, WT sequence was also detected (Figure 3.6), suggesting either the absence of loss of heterozygosity (no second hit mutation was identified in 4 MSI+ tumours for which every exon was sequenced) and a possible dominant negative effect, or perhaps the presence of normal tissue in the tumour sample.

Evolution of tumours to a more advanced and aggressive state (including the microsatellite unstable tumourigenesis pathway) is reliant on the selection of mutations within genes driving neoplastic growth. These driver mutations occur in the background of a large number of random mutations having no impact on cancer progression. It was therefore important to try and identify if the somatic mutations we observed in *FLCN* were likely to be driver or passenger mutations. A number of criteria have been suggested to distinguish driver mutations in MSI, including (a) a high mutation frequency, (b) biallelic inactivation, (c) involvement in a growth suppressor pathway, (d) inactivation of the same pathway in MSS tumours and (e) functional studies (Boland, et al., 1998). Despite points (b) and (c) proving controversial (Perucho, 1999), mutation frequency and functional studies, are argued to be the simplest parameters for defining the likelihood of mutations being drivers (Woerner, et al., 2003). The functions of *FLCN* beyond its role as a general tumour suppressor are not yet well defined. We were unable to confirm biallelic inactivation in our samples, and so chose to compare the frequency of *FLCN* mutations in our samples to those of other previously reported, functional colorectal MSI+ target genes.

The frequency of *FLCN* mutations (23%) was less than that of *TGFBR2* (100%), similar to that of *MSH6* (23%) and greater than that of *IGF2R* (7%) (Table 3.2). Somatic mutations in *IGF2R* and *MSH6* have been considered to contribute to tumorigenesis in MSI+ CRC's (Malkhosyan, et al., 1996; Souza, et al., 1996), suggesting that the frequency of *FLCN* mononucleotide mutations in MSI+ CRC may be consistent with mutations in the gene undergoing selection during tumorigenesis.

Folliculin has been reported to have a role in mTOR signalling (Baba, et al., 2006) (See section 1.3.6.1). Interestingly, deregulation of the mTOR pathway has been previously linked to intestinal tumorigenesis; Cowden syndrome presents a gastrointestinal polyposis phenotype (Umemura, et al., 2008) and rapamycin (inhibitor of mTORC1) is able to suppress polyp formation in a mouse model of human FAP (Fujishita, et al., 2008). However, folliculin is likely to have multiple functions and, thus to properly determine the role of *FLCN* in colorectal cancer, it will first be necessary to better characterise the function of the folliculin protein.

Mutations in *FLCN* have been previously identified in individuals with non-syndromic RCC (Woodward, et al., 2008). This study reports a comparative frequency of *FLCN* germline mutations identified in a similar group of familial RCC patients (7.7%). The p.S386X, c.1655C>G, is a novel nonsense mutation that has not been previously reported in *FLCN*. The c.610delGCinsTA is a recurrent mutation in BHD syndrome and this study therefore excludes the possibility that a distinct set of *FLCN* mutations are responsible for the “non-syndromic” RCC susceptibility phenotype.

In contrast we did not identify any germline mutations in 50 patients with “non-syndromic” inherited CRC. The difference between the involvement of *FLCN* in these two situations may have several explanations. BHD is a rare disorder and familial CRC is more frequent than familial RCC, hence it may be necessary to test a larger group of familial CRC patients to identify a causative *FLCN* mutation. Also, whereas BHD is associated with early onset RCC, this study reports the mean age of colorectal cancer to be 57.4 years. As many diagnostic criteria for familial CRC include early onset tumours, it is therefore less likely that BHD patients may present in this group. The missense variant (p.Arg362Cys) identified in the colorectal cell line LoVo is of unknown significance, and is further investigated in Chapter 4.

In summary, the identification of a genotype-phenotype correlation for colorectal neoplasia risk in BHD is a potential explanation for the heterogeneity reported in the literature. It does appear that the increased risk of colorectal neoplasia is restricted to a subset of BHD families. Further studies are required to confirm this finding, with the potential for using *FLCN* mutation type to determine the need for colonic surveillance in BHD patients.

In light of these findings, it was decided to investigate the mechanism of pathogenicity of previously reported germline *FLCN* mutations, with the aims of providing insights into wildtype folliculin function, investigating the cellular effects of pathogenic *FLCN* mutations and trying to elucidate the basis for the genotype-phenotype correlation reported in this chapter, at a functional level.

Chapter 4 Birt Hogg Dubé syndrome-
associated FLCN mutations disrupt
protein stability

4.1 Introduction

Twenty four years after the syndrome was first described, the gene locus for Birt Hogg Dubé syndrome was localised to chromosome 17p11.2 by linkage analysis (Khoo, et al., 2001; Schmidt, et al., 2001). The following year, truncating mutations were identified in a novel gene at that locus, *FLCN*; a gene with an encoded protein product, folliculin, which had no known function (Nickerson, et al., 2002). Subsequently, *FLCN* mutations have been identified in patients with familial primary spontaneous pneumothorax (PSP) and in familial renal cell carcinoma patients lacking the other classical BHD manifestations (Frohlich, et al., 2008; Graham, et al., 2005; Gunji, et al., 2007; Painter, et al., 2005; Ren, et al., 2008; Woodward, et al., 2008).

The *FLCN* gene consists of 14 exons (transcription commencing in exon 4) encoding a protein of 579 amino acids, folliculin (Nickerson, et al., 2002). Close to 85% of patients with BHD syndrome have been found to harbour germline *FLCN* mutations (Nickerson, et al., 2002; Schmidt, et al., 2005) and recent work by Benhammou *et al* (2011) has identified large intragenic gene duplications and deletions in seven BHD families previously found to be *FLCN* mutation negative by sequencing. These duplications and deletions are thought to account for at least 5% of cases of BHD syndrome (Benhammou, et al., 2011).

In 2010, a *FLCN* mutation database was collated to identify and pool all previously reported *FLCN* mutations (Lim, et al., 2010). At the time of writing, 147 unique *FLCN* variants are listed on the database, of which 132 are reported as pathogenic. Mutations

have now been identified in all coding exons, with a mutation hotspot of eight cytosine residues in exon 11 where close to 50% of mutations are reported to occur (Schmidt, et al., 2005). Consistent with the putative tumour suppressor function for *FLCN*, the vast majority of pathogenic *FLCN* mutations are predicted to prematurely truncate the encoded product, in the absence of nonsense mediated decay. The *FLCN* mutation database describes 52.9% frameshift, 20% splice site and 14.3% nonsense mutations (Lim, et al., 2010).

In addition, a small number of potential *FLCN* non-truncating, missense or in-frame deletion mutations have been described (see Table 4.1). These mutations are of particular interest as they could indicate the importance of specific domains within the protein which result in BHD syndrome phenotype when disrupted. However unless a missense substitution is detected in a large kindred and shown to segregate with disease status or affect protein function, the pathogenicity of rare, non-truncating variants can be difficult to determine.

Most human genetic variation is represented by single nucleotide substitutions, accounting for about 90% of sequence differences (Wang and Moulton, 2001). It is estimated that 60,000 to 87,600 substitutions occur in coding regions causing an alteration of the wildtype amino acid (Cargill, et al., 1999; Livingston, et al., 2004). These are most often neutral changes (benign single nucleotide polymorphisms), but in rare cases are pathogenic. In an age of high-throughput sequencing methods, the numbers of such reported variants is rapidly increasing and the ability to discriminate

between benign and pathogenic variants is therefore of great importance. An amino acid substitution or deletion may disrupt critical sites for the function of the protein, such as ligand binding pockets or catalytic residues, causing either a loss or inappropriate gain of function (Thusberg and Vihinen, 2009), or more frequently may affect the structure and stability of the protein product thereby preventing the protein from functioning correctly (Wang and Moulton, 2001). A less frequently observed effect of missense mutations is to disrupt the cellular localisation of the mutant protein. Proteins are normally directed to the correct location by short peptide sequences. Missense changes in the signal peptide can lead to alteration of the signal and a pathogenic response through mislocalisation of the protein (Laurila and Vihinen, 2009).

Great efforts are being deployed to develop computer software to accurately predict the pathogenicity of non-truncating variants, using structural and/or evolutionary information about the mutated sites. This study utilised 2 computational methods to predict the phenotypic effects of the missense variants investigated. SIFT (Sorting Intolerant From Tolerant) is a program which uses evolutionary information to predict tolerance of variants, by constructing a multiple sequence alignment (MSA) and mathematically considering the position and type of amino acid change (Ng and Henikoff, 2001; Thusberg and Vihinen, 2009). PolyPhen (Polymorphism Phenotyping) uses a combination of functional and/or protein structural parameters as well as MSA information in making predictions of pathogenicity (Sunyaev, et al., 2001). The program

characterises a given missense variant using multiple other sequence, structure and phylogeny based descriptors (Thusberg and Vihinen, 2009).

To give an indication of domains of particular importance within the folliculin protein (where mutations are most likely to be pathogenic), an evolutionary analysis was undertaken both at an inter- and intra-gene level. This is a useful technique, as the debilitating effects of mutations create selective pressures which result in sequence conservation over evolutionary time. Thus disease-associated missense/IFD mutations occur more often at residues that have been strongly, evolutionarily conserved (Pal, et al., 2006).

In this study I have used both computational software and have modelled 10 previously described *FLCN* mutations *in vitro*, to determine the pathogenicity of these mutations, and the effects on folliculin stability and tumour suppressor activity.

4.2 Aims and Approaches

In order to gain insights into potential functional domains of the folliculin protein and indicate the pathogenicity of the missense and in frame deletion mutations reported in *FLCN*, the aims of this chapter are to analyse the patterns of evolutionary conservation of folliculin and study 10 *FLCN* mutations *in vitro*.

4.3 Methods

4.3.1 Evolutionary Conservation of FLCN – Analysis performed by Professor Laurence D Hurst, University of Bath

The patterns of evolutionary conservation of *FLCN* at both the inter and intra-gene level was analysed using computational techniques by Prof Laurence D Hurst. A summary of the methods used is located below. For complete methodology, see (Nahorski, et al., 2011).

Orthologues of human Folliculin isoform 1 were identified using Homologene at NCBI, and the sequences for chicken, cow, dog, mouse, rat, xenopus and chimp extracted from GenBank. The sequences were aligned using Muscle (Edgar, 2004) on the translated sequence, with the nucleotide aligned being reconstructed from the aligned protein sequences using the program AA2NUC. Ka and Ks were estimated using the method of Li (Li, 1993), and K4 estimated using the Tamura-Nei protocol (Tamura and Nei, 1993).

Using this data, the overall rate of evolution of the gene was compared with a comparator set of previously defined set of 5,056 orthologs (Parmley, et al., 2007). To look at the evolutionary constraints across the *FLCN* gene, a sliding window analysis was undertaken using 102 codon windows and a three codon jump between windows (using the program SLIDERKK).

4.3.2 Selection of FLCN mutations and variants

The great majority of reported *FLCN* mutations are predicted to prematurely truncate the encoded protein. To investigate the consequences of non-truncating *FLCN* variants, the six missense and in-frame-deletion (IFD) mutations that were available in the BHD database (www.lovd.nl/flcn) at the start of the study (representing all such changes at the time), an unpublished germline variant (p.His255Pro) and a variant detected in the LoVo colorectal cell line (p.Arg362Cys – reported in section 3.4) were selected for analysis (see Figure 4.1). In the previous chapter, a genotype-phenotype correlation for colorectal cancer risk was reported. Patients harbouring the c.1285dupC (p.His429ProfsX27) mutation were at significantly higher risk of colorectal neoplasia than those with the c.610delGCinsTA (p.Ala204X) nonsense mutation. To continue this investigation, both of these mutations were also selected for study. The location of each mutation studied within the *FLCN* gene is displayed in Figure 4.1, and associated clinical information is summarised in Table 4.1.

4.3.3 Characterisation of FLCN mutations in vitro

FLCN was expressed *in vitro* by amplifying the coding region of *FLCN* from human cDNA, and cloned into the EcoR1-BamH1 sites of the pFlag-CMV vector (available at the start of the study, with thanks to Dr Anne Reiman). Mutations were introduced into *FLCN* using the Quik-Change Site-Directed Mutagenesis kit (see methods 2.5.7). The

mutant constructs were subsequently subcloned into the pIRES2-AcGFP1 vector (see Appendix 7.1) and confirmed by sequencing. Primer sequences are displayed in table.

FTC-133 cells with no folliculin expression (Lu, et al., 2011) were transiently transfected with the ten mutant constructs as well as wild type *FLCN* and empty vector expressing controls. Cells were lysed, electrophoresed and blotted as described in methods 2.4.4. The cellular levels of exogenous folliculin, transfected GFP (a marker of transfection efficiency) and β -actin were determined by densitometry of western blots. The cellular levels of folliculin were divided by that of GFP to give a value of folliculin steady state levels for each *FLCN* construct. Experiments were carried out in triplicate.

4.3.4 Extraction of DNA and protein from BHD renal tumour

Tumour and normal tissue from the kidney of a BHD patient was ground into a powder under liquid nitrogen. DNA was extracted using the DNA Isolation Kit for Cells and Tissues (Roche) and protein extracted by resuspension of the tissue in RIPA buffer (as for protein extraction from culture cells). *FLCN* sequence was determined as described previously and protein expression determined by western blotting.

4.3.5 Soft agar colony formation assay

Soft agar colony formation assays were carried out to identify if selected *FLCN* mutants had lost their ability to suppress cell growth, *in vitro*. Assays were also utilised to investigate a potential dominant negative effect, testing whether the p.His429ProfsX27 mutant disrupted endogenous *FLCN* function, in a colorectal cancer background. Complete methodology is located in methods 2.6.

4.3.6 Immunocytochemistry

FTC-133 cells transfected were transfected with *FLCN* mutants which had no impact on protein stability, to identify possible alterations to intra-cellular distribution of FLCN. Full methodology is located in methods 2.7

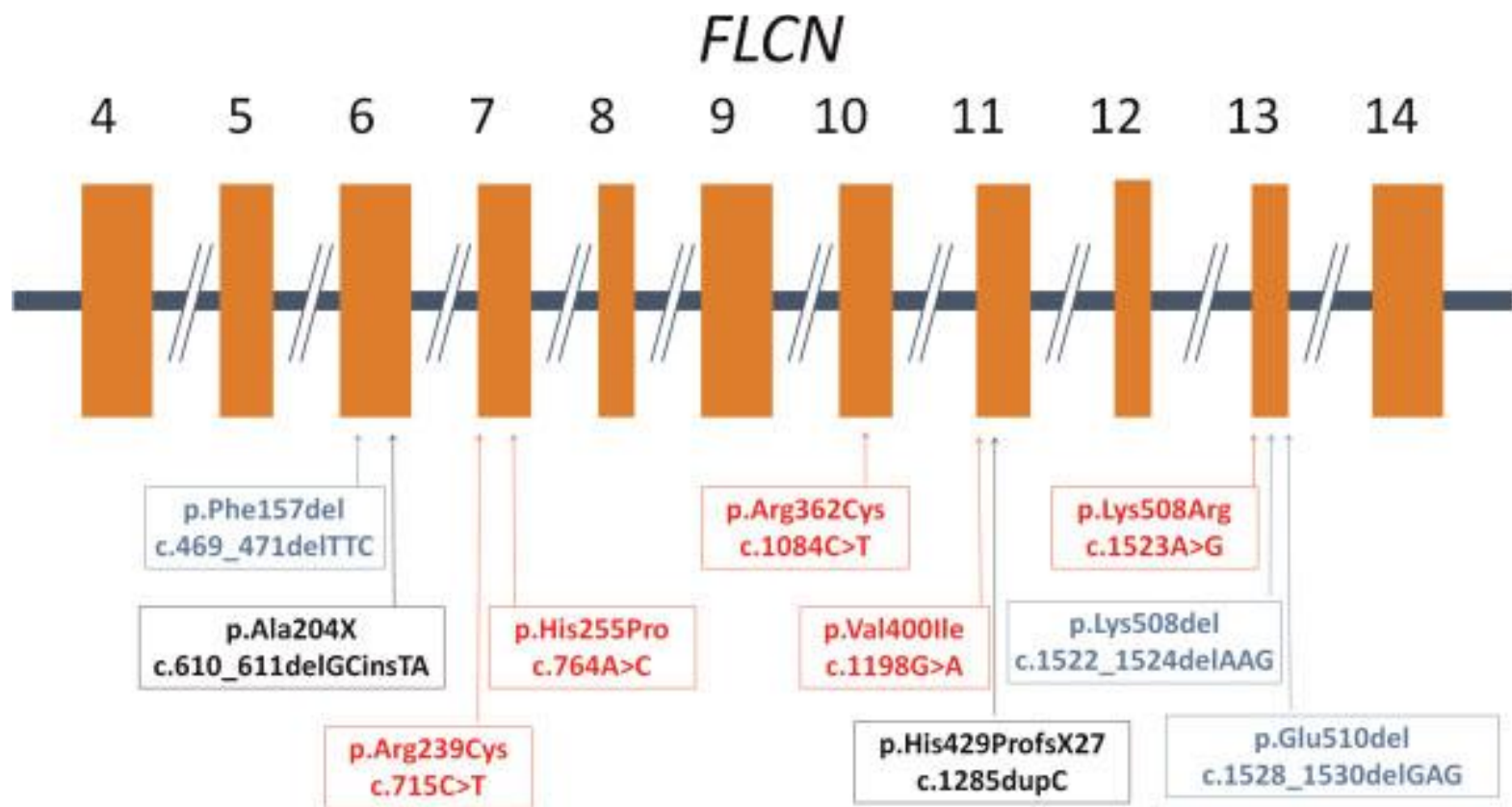


Figure 4.1 Schematic diagram describing the location of variants analysed within *FLCN*

Mutation		Exon	Mutation type	BHD syndrome features	Reference
c.469_471delTTC	p.Phe157del	6	Inframe deletion	PSP	Ren <i>et al</i> 2008
c.610_611delGCinsTA	p.Ala204X	6	Nonsense	Fibrofolliculomas, PSP, lung cysts, RCC	Toro <i>et al</i> 2008, Leter <i>et al</i> 2008
c.715C>T	p.Arg239Cys	7	Missense	RCC	Woodward <i>et al</i> 2008
c.764A>C	p.His255Pro	7	Missense	Multiple skin lesions (biopsy proven trichodiscoma)	Unpublished
c.1084C>T	p.Arg362Cys	10	Missense	Detected in colorectal cell line LoVo	Unpublished
c.1198G>A	p.Val400Ile	11	Missense	Variant of unknown significance	Lim <i>et al</i> 2010
c.1285dupC	p.His429ProfsX27	11	Frameshift	Fibrofolliculomas, PSP, lung cysts, RCC	Nickerson <i>et al</i> 2002
c.1522_1524delAAG	p.Lys508del	13	Inframe deletion	PSP, fibrofolliculomas	So <i>et al</i> 2009
c.1523A>G	p.Lys508Arg	13	Missense	RCC	Toro <i>et al</i> 2008
c.1528_1530delGAG	p.Glu510del	13	Inframe deletion	Fibrofolliculomas, PSP, lung cysts	Toro <i>et al</i> 2008

Table 4.1 Clinical Information for FLCN variants selected

4.4 Results

4.4.1 Evolutionary constraint of FLCN

By comparing the evolutionary conservation of the complete *FLCN* gene with over 5000 other mouse-human orthologues, Professor Hurst found that folliculin is slower evolving at the protein level than the average gene (Figure 4.2) and under slightly stronger purifying selection compared with the average gene (Figure 4.3). Analysis within the gene identified a domain from approximately codons 100-230 that is both slower evolving (Figure 4.3a) and under especially strong purifying selection (Figure 4.3b) compared with the rest of the gene. This finding was repeatable across independent comparisons. Thus, all non-synonymous mutations here are extremely likely to be deleterious. However, given the high level of constraint operating throughout the rest of the *FLCN* sequence, deleterious mutations could be expected anywhere.

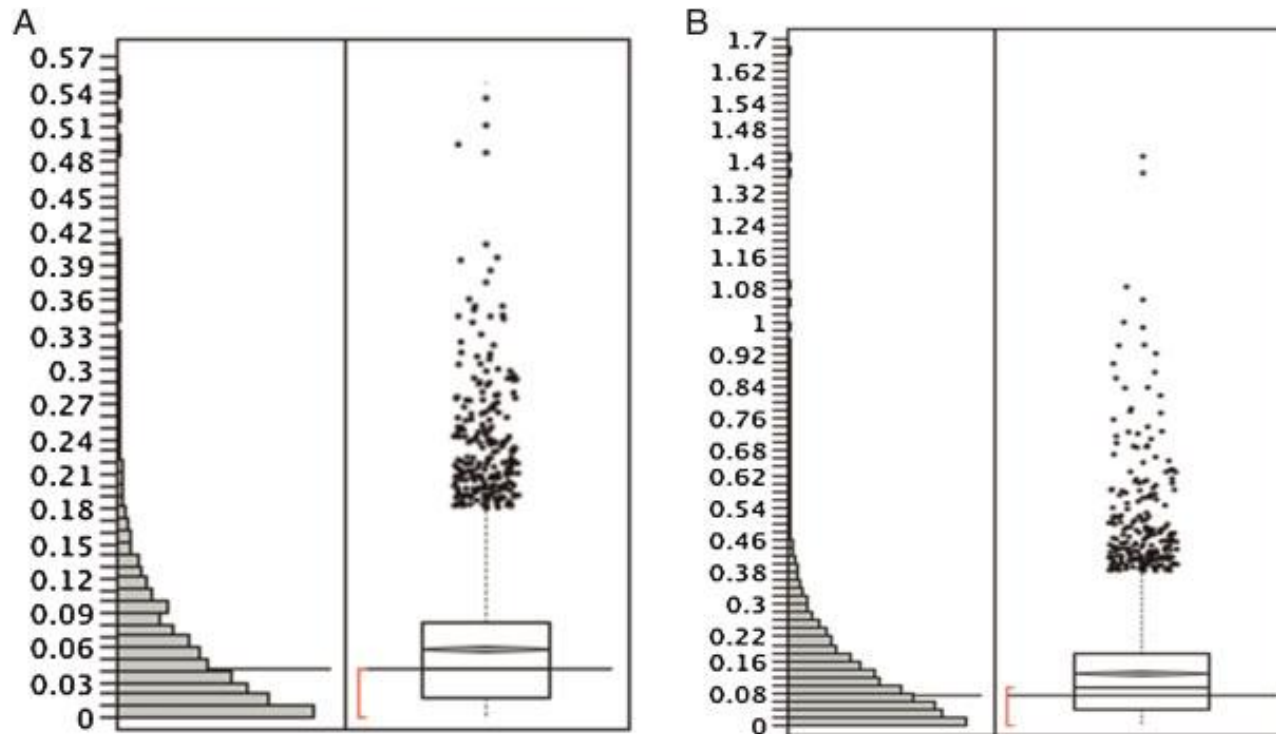


Figure 4.2 Folliculin is a slower than average evolving gene

A: K_a of 5057 mouse-human orthologs. Horizontal line shows the result for folliculin. Median for all orthologs is 0.04115 (quartiles: 0.0168-0.0817). K_a for folliculin = 0.0407. B: K_a/K_4 of 5057 mouse-human orthologs. Line shows the result for folliculin. Median for all is 0.0932 (quartiles: 0.0414-0.1765). K_a/K_4 for folliculin = 0.0724. Li's K_a estimation and Tamura and Nei's K_4 estimation were used in this analysis.

(Analysis was undertaken with thanks to Professor Laurence Hurst, University of Bath)

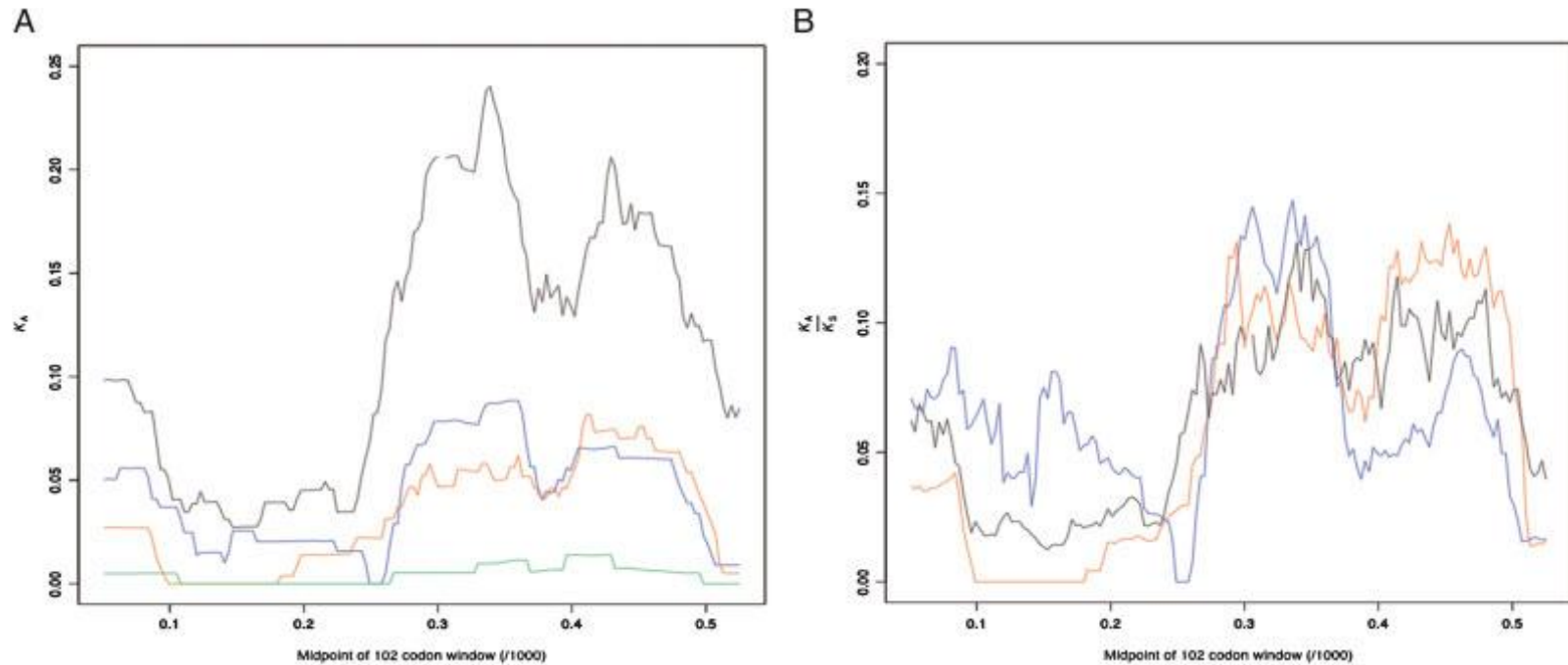


Figure 4.3 Folliculin while under purifying selection is less constrained 3' than 5'

Across four species comparisons, (chicken – Xenopus: black, human – rat: blue, cow – dog: red and human – chimp: green), there is a zone (approximately codon 100 to codon 230) with low rates of protein evolution (A) and K_a/K_s (B). Human chimp comparison K_s is generally zero for most windows hence K_a/K_s has no meaning and is omitted.

(Analysis was undertaken with thanks to Professor Laurence Hurst, University of Bath)

4.4.2 Pathogenic missense and inframe deletion mutations significantly affect the stability of the folliculin protein

The folliculin mutation database was reviewed and 6 previously reported non-truncating *FLCN* mutations as well as 1 unreported missense change identified. In agreement with the evolutionary conservation results that suggested deleterious mutations could be expected anywhere within the coding sequence, the missense and IFD mutations that have been reported in *FLCN* are relatively well spread out throughout the *FLCN* coding regions (see Figure 4.1).

To investigate whether the selected missense/IFD *FLCN* variants were likely to be pathogenic and the likely mechanism of pathogenicity, 10 candidate missense/IFD mutations were studied *in vitro* (see Table 4.1). The mutations were introduced into the *FLCN* sequence using a site-directed mutagenesis method, and the mutants and control sequences were cloned into the pIRES2-AcGFP1 vector (Clontech) (Figure 4.4). These constructs were then transiently expressed in the FTC-133 cell line (folliculin deficient) (Lu, et al., 2011).

A common mechanism of pathogenicity for non-truncating mutations is to disrupt stability of the encoded protein. The p.His429ProfsX27 frameshift mutation, the pAla204X nonsense mutation, and six of the eight missense/IFD mutations impaired stability of the folliculin proteins, significantly reducing protein steady state levels. This is consistent with the hypothesis that most of the reported *FLCN* missense/IFD mutations

are pathogenic by significantly disrupting the stability of the folliculin protein (Figure 4.5).

Amino acid change	Nucleotide change	Normal Sequence	Mutant sequence
p.Phe157del	c.469_471delTTC	C C T T C T T C A T C 	C C T T C A T C
p.Ala204X	c.610delGCinsTA	C A A G G C G C T C A 	C A A G T A G C T C A
p.Arg239Cys	c.715C>T	C C G C C C G C T C G 	C C G C C T G C T C G
p.His255Pro	c.764A>C	C C T G C A C A C C T 	C C T G C C C A C C T
p.Arg362Cys	c.1084C>T	C T T T C C G C A T G 	C T T T C T G C A T G
p.Val400Ile	c.1198G>A	G C T G C G T C C G C 	G C T G C A T C C G C
p.His429ProfsX27	c.1285dupC	T C C C C C C C C A 	T C C C C C C C C A
p.Lys508del	c.1522_1524delAAG	C C T C A A G G A G G 	C C T C G A G G
p.Lys508Arg	c.1523A>G	C C T C A A G G A G G 	C C T C A G G G A G G
p.Glu510del	c.1528_1530delGAG	G G A G G A G T G G 	G G A G T G G

Figure 4.4 FLCN mutations introduced using site-directed mutagenesis

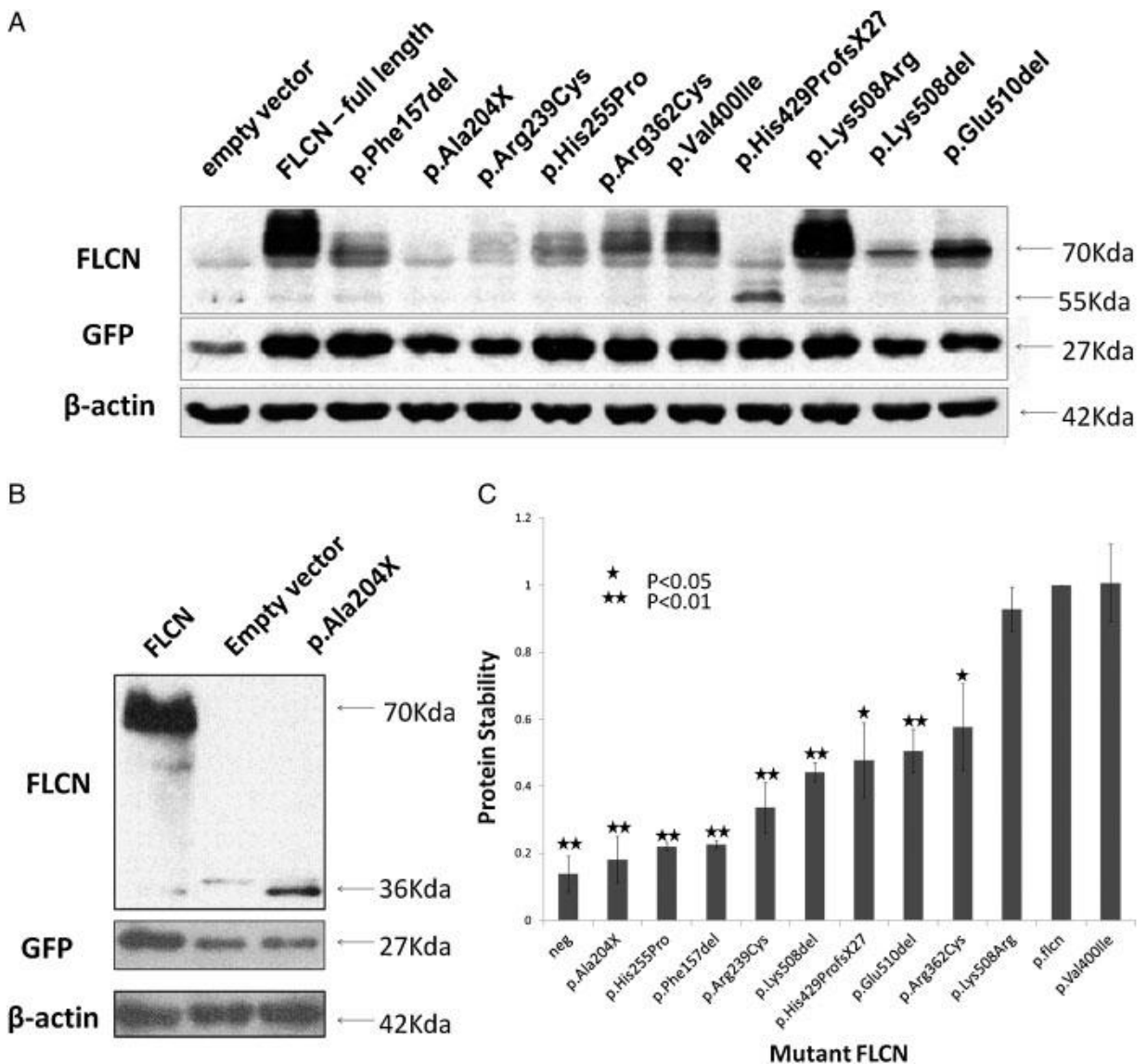


Figure 4.5 Most *FLCN* missense and IFD mutations analysed significantly disrupted stability of the protein

The stability of each mutant construct was determined, relative to wild type *FLCN*, by dividing the level of *FLCN* signal by that of *GFP*, an indicator of the efficiency of transfection. Experiments were carried out in triplicate. **A:** Western blot for *FLCN*, *GFP* and β -actin for each mutation analysed **B:** Western blot for the pAla204X mutation **C:** Graphical representation of the stability of each construct from at least 3 independent repeats. Error bars represent standard deviation. One star indicates significance $p < 0.05$, two stars indicate $p < 0.01$ (Independent T Test).

The putative functional consequences of the *FLCN* non-truncating mutants were evaluated *in silico*, using predictive computational analyses (SIFT software (Ng and Henikoff, 2001) and PolyPhen Web predictive server (Sunyaev, et al., 2001)). Both programmes produced comparable results with four of the proteins that disrupted folliculin stability being predicted to be “probably damaging” the other two “possibly damaging”. Both mutations with no effect of folliculin stability were predicted to be benign (Table 4.2).

Mutation	PolyPhen	SIFT
p.Phe157del	Probably damaging	n/a
p.Arg239Cys	Probably damaging	not tolerated
p.His255Pro	Probably damaging	not tolerated
p.Arg362Cys	Probably damaging	not tolerated
p.Val400Ile	Benign	Tolerated
p.Lys508Arg	Benign	Tolerated
p.Lys508del	Possibly damaging	n/a
p.Glu510del	Possibly damaging	n/a

Table 4.2 In silico analysis predicting the possible functional consequences of missense and IFD mutations

4.4.3 Analysis of BHD tumour in patient with p.Arg239Cys

The *FLCN* mutation p.Arg239Cys was originally identified in a patient presenting with inherited susceptibility to RCC but no known causative syndrome (Woodward, et al., 2008). In the studies presented in this chapter, the p.Arg239Cys mutation disrupted stability of the folliculin protein and was predicted to be “probably damaging” and “not tolerated” by PolyPhen and SIFT programs respectively. In the time since the publication of this mutation by Woodward *et al.* (2008), another patient was identified with the same heterozygous p.Arg239Cys mutation. This patient had developed 3 separate primary tumours at a young age (chromophobe RCC, adenocarcinoma of the oesophagus and rectal adenocarcinoma). The patient was confirmed to have fibrofolliculomas and was diagnosed with BHD syndrome. The RCC and a section of normal kidney tissue were surgically removed and the DNA and protein extracted from each sample. Loss of heterozygosity was observed in the tumour sample and this correlated with greatly reduced folliculin protein levels in the tumour tissue (Figure 4.6).

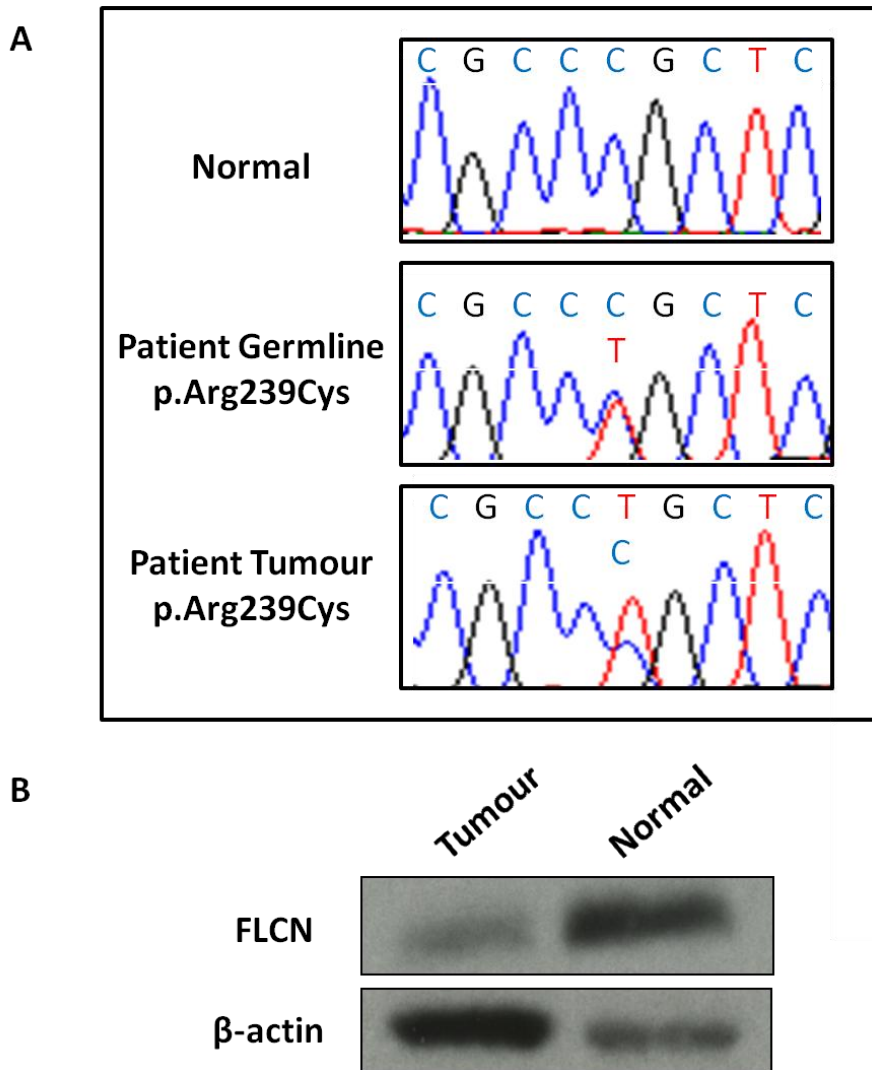


Figure 4.6 Loss of heterozygosity and reduced folliculin expression in p.Arg239Cys RCC

A: There is a loss of heterozygosity of the wild type allele in the renal tumour of a BHD patient with a germline p.Arg239Cys mutation. **B:** Reduced folliculin expression in the tumour tissue

4.4.4 p.Val400Ile and p.Lys508Arg constructs retain anchor independent growth suppression

Two putative *FLCN* missense mutations, p.Val400Ile and p.Lys508Arg did not seem to disrupt the stability of the folliculin protein. It was postulated that they may be pathogenic via an alternative mechanism, or that they might represent non-pathogenic polymorphisms. To determine the likely pathogenicity of these two variants, their impact on the ability of folliculin to suppress growth of cells unadhered to a surface, suspended in soft agar (*in vitro* tumour suppressor assay) was investigated. These mutant proteins were also analysed by fluorescence microscopy to investigate any potential alterations to folliculin distribution within the cell.

Stable, mutant folliculin constructs, pVal400Ile and p.Lys508Arg and two further mutations (p.His255Pro and p.His429ProfsX27) which were expected pathogenic, were transfected into FTC-133 cells as stable mixed populations. The cell populations were grown in soft agar and the number of colonies compared with introducing wild type folliculin or empty vector. Compared to wild type expressing cells, FTC-133 cells expressing p.His255Pro and p.His429ProfsX27 produced a significantly larger number of colonies (similar to empty vector expressing cells). However stable mutants, p.Val400Ile and p.Lys508Arg exerted a significant suppressive activity on colony formation, behaving like wild type folliculin. It was concluded that neither mutation impaired the growth suppressive activity of the folliculin protein (Figure 4.7).

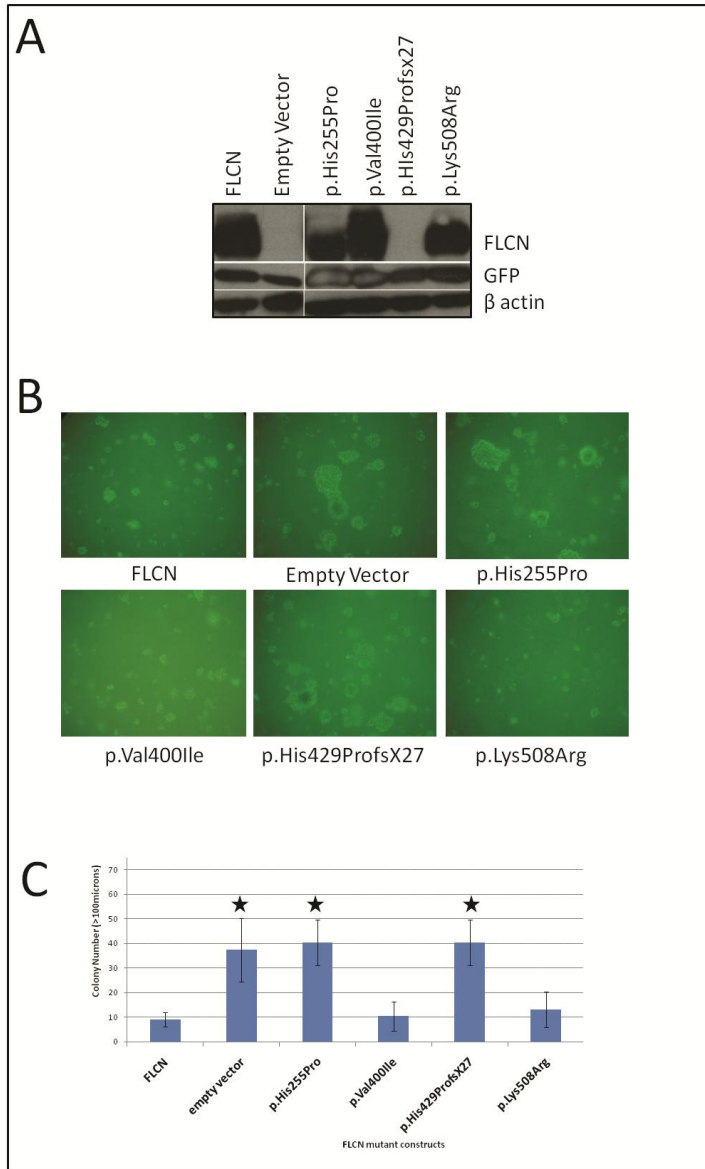


Figure 4.7 Assessment of the tumour suppressive activity of FLCN mutant proteins.

p.Val400Ile and p.Lys508Arg variants retain folliculin tumour suppressor activity, and, when grown in soft agar, produced a significantly lower number of colonies compared with cells transfected with empty vector. The p.His255Pro and p.His429ProfsX27 variants have lost this function, and produced a significantly larger number of colonies than cells transfected with wild type FLCN, indicating they are pathogenic mutations. **A:** confirmation of stable transfection by western blot, **B:** representative picture of soft agar plates transfected with each construct, **C:** Graph of the colony counts for each population of cells, from three independent experiments. Error bars represent standard deviation.

One star indicates significance $p < 0.05$ (Independent T Test).

4.4.5 p.Val400Ile and p.Lys508Arg constructs do not affect protein intracellular distribution

To investigate if the p.Val400Ile or p.Lys508Arg mutants might be affecting the intracellular distribution of folliculin, FTC-133 cells were transfected with these constructs, wild type folliculin and empty vector. These cells were then stained for FLCN and GFP (for identification of successfully transfected cells). Wild-type folliculin is distributed throughout the cytoplasm, and is also present at lower levels in the nucleus. Neither p.Val400Ile nor p.Ly508Arg expressing cells displayed any discernible difference in localisation pattern compared to wild type folliculin (Figure 4.8

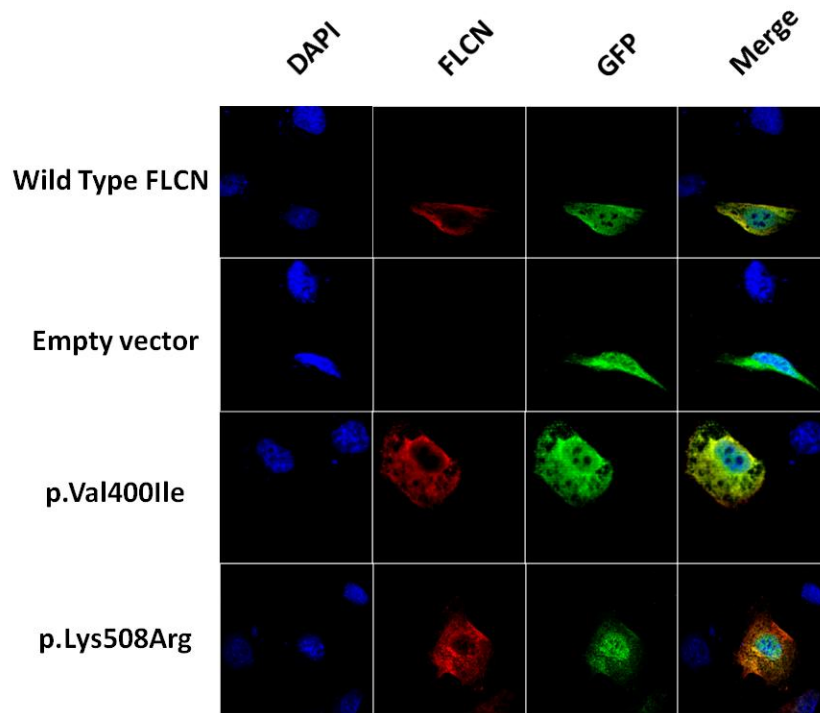


Figure 4.8 The cellular localisation of the p.Val400Ile and p.Lys508Arg FLCN variants is similar to that of wild type FLCN.

Transiently transfected cells were co-stained for FLCN and GFP. The nuclei were stained with 4',6-diamidino-2-phenylindole (DAPI). In wild type folliculin, pVal400Ile and p.Lys508Arg expressing cells, folliculin is distributed throughout the cytoplasm and at a reduced level in the nucleus (17.4%, 23.3% and 17.5% compared to the cytoplasm level respectively, $p=0.53$, $p=0.97$). Results pooled from three independent experiments and tested for significance using independent Student's T test. GFP signal indicates transfected cells.

4.4.6 No evidence for a dominant negative effect for pHis429ProfsX27 mutation

Chapter 3 described that in our cohort, BHD patients harbouring a germline p.His429ProfsX27 frameshift mutation were at significantly higher risk of colorectal neoplasia than those with a p.Ala204X nonsense mutation. This could potentially be explained if the mutant folliculin protein resulting from the pHis429ProfsX27 frameshift is stable and might exert a dominant negative effect, disrupting the function of wild type folliculin. When these mutants were transiently transfected into FTC-133 cells, both mutants produced a translated, truncated product, displaying reduced protein stability.

To further investigate if there was evidence of a dominant negative effect, the pHis429ProfsX27 construct was introduced into the DLD-1 colorectal cancer cell line (which expresses endogenous levels of folliculin), and the cells grown in soft agar. However the number of colonies produced by the empty vector transfected DLD-1 cells was not significantly different to those produced in the cells expressing the truncated p.His429ProfsX27 mutant construct ($p=0.22$). Overexpressing folliculin exerted a significant growth suppressive effect compared to empty vector and p.His429ProfsX27 expressing cells ($p=0.0002$) (Figure 4.9).

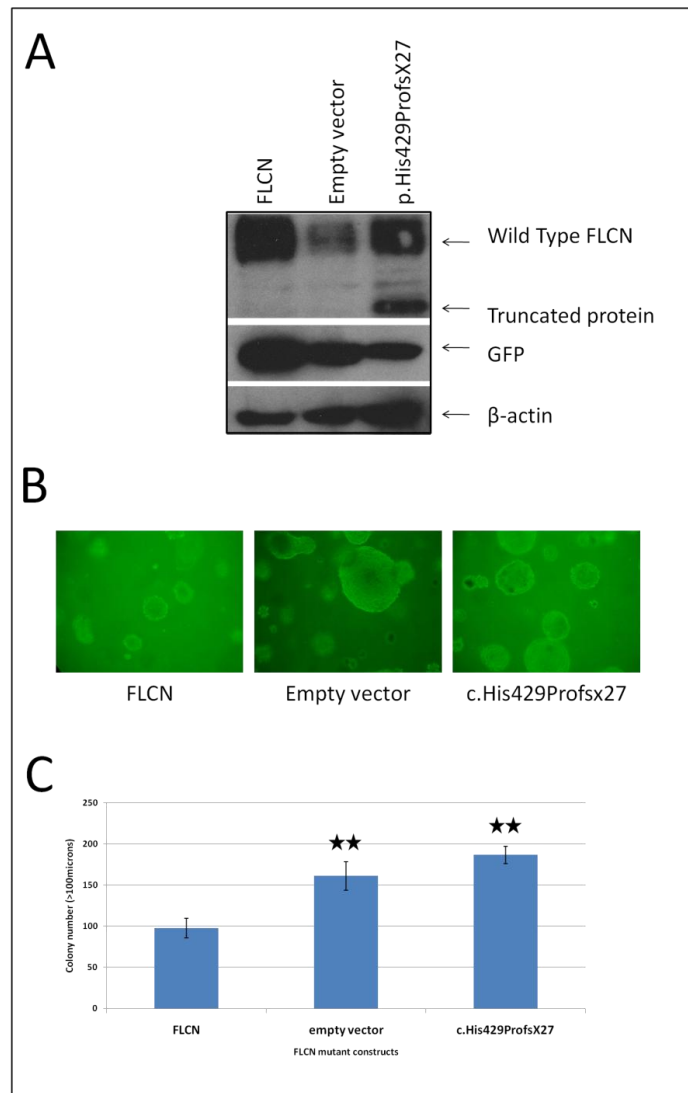


Figure 4.9 No evidence of a dominant negative effect associated with the p.His429ProfsX27 mutation when introduced into DLD-1 cells

Wild type folliculin, empty vector and the p.His429ProfsX27 construct were introduced into the DLD-1 colorectal cell line. There was no significant difference in the growth suppressor activity of the truncated folliculin protein compared with transfection of empty vector providing no evidence of a dominant negative effect in this cell background ($p=0.23$). **A:** Confirmation of stable transfection by western blot, **B:** Representative picture of soft agar plates transfected with each construct, **C:** Graph of the colony counts for each population of cells, the average of 6 experiments. Two stars indicate $p<0.01$. Error bars represent standard deviation. Comparison of colonies between empty vector and p.His429Profsx27, ($p = 0.23$)

Folliculin has been reported to impact upon the mTOR signalling pathway (Baba, et al., 2008), with folliculin loss resulting in increased signalling through both mTORC1 and mTORC2 (Baba, et al., 2008; Hasumi, et al., 2009). In order to gain insights into the effects of the *FLCN* mutants on mTOR signalling, the *FLCN* mutants were transiently and (a subset) stably transfected into FTC-133 cells. Lysates from these experiments were immuno-blotted for phosphorylation of ribosomal protein S6 (indicative of mTORC1 activation) and phosphorylation of Akt (indicative of mTORC2 activation). However, under neither normal serum conditions, nor in controlled serum free or amino acid free media, could robust, repeatable effects on the phosphorylation status of S6 or Akt be determined.

4.5 DISCUSSION

This chapter aimed to gain further insights into the way *FLCN* mutations affect folliculin function, and into a potential genotype-phenotype correlation previously identified. The patterns of evolutionary conservation of the *FLCN* gene investigated *in silico* by Professor Hurst were consistent with the folliculin protein evolving more slowly and being under stronger purifying selection compared with the average gene. Within the *FLCN* gene, the slower evolution and purifying selection was most apparent within the first half of the protein, approximately between codons 100 and 230.

Determining the rate of protein evolution is a powerful tool for quantifying the relative importance of a gene and it is a long held view that proteins with a high density of important sites are likely to evolve more slowly (Zuckerandl, 1976). See review by (Pal, et al., 2006).

Our analysis suggested that such is the conservation across the whole gene, that nonsynonymous mutations might be pathogenic throughout the *FLCN* sequence. Close to 90 % of mutations described in *FLCN* to date prematurely truncate the encoded protein (Lim, et al., 2010). The small number of non-truncating *FLCN* mutants identified, are not constrained to any particular domains and are relatively well spread out throughout the sequence, consistent with the *in silico* analysis. There is, however, a cluster of three putative mutations at amino acid positions 508, 508 and 510 respectively, which were of particular interest due to their close proximity.

When experimentally modelled *in vitro*, the majority of missense/IFD mutations analysed had a significant impact upon the stability of the folliculin proteins. This suggests they are acting in a similar manner to the effects of truncating mutants (also significantly destabilised in this study) by causing a deficiency of the full length *FLCN* gene product. It appears probable that folliculin has multiple functions and that in causing BHD syndrome, *FLCN* mutations compromise multiple aspects of folliculin function. The functions of folliculin are not well characterised, however the insights to date suggest a role for folliculin in mTOR signalling through its interactions with FNIP1 and FNIP2/FNIPL and indirectly AMPK (Baba, et al., 2006; Hasumi, et al., 2008; Takagi, et al., 2008). Folliculin binds to FNIP1 and FNIP2 at regions beyond codons 516 and 362 respectively and therefore these interactions appear unrelated to the domain of strong evolutionary selection and strong purifying selection we have identified between codons 100 and 230. This region could be particularly crucial for maintaining folliculin structural integrity (the only IFD mutation described within this regions p.Phe157del significantly alters protein stability), or could represent the binding site for another, yet unidentified, folliculin binding partner.

In collaboration with Dr Ravi Nookala (University of Cambridge), a bioinformatic analysis of the structural homologues of the codon 100 to 230 domain of folliculin was carried out. The N-terminus of folliculin carries a KOG3715 domain which spans the region of interest identified. This is not assigned to any domain super family and hence the structure of such a domain is yet to be determined. The only homologous sequence for the region which has been annotated is that encoding the *Saccharomyces cerevisiae*

protein LST7 (Lethal with Sec 13 protein 7). LST7 is only 242 amino acids in size and is hence far smaller than the human folliculin, representing the smallest evolutionarily functional folliculin protein. This protein is required for the nitrogen-regulated transport of two amino acid permeases (GAP1 and PUT4) from the Golgi to the cell surface (Roberg, et al., 1997).

A range of the missense/IFD mutations that were modelled (p.Phe157del, p.Arg239Cys, p.His255Pro, p.Arg362Cys, p.Lys508del and Glu510del) distributed across the folliculin protein impaired protein stability. As aforementioned, this was not necessarily predictable despite being consistent with the evolutionary analysis, as we had hypothesised that the three putative mutations at codons 508 and 510 may have disrupted an interaction with a critical folliculin binding partner (hence maintaining a stable structure in this assay). The ability to determine the pathogenicity of rare polymorphic variants is of crucial importance in diagnosing BHD syndrome and the clinical outcomes associated with this. Most of the mutations modelled caused impaired protein stability consistent with the interpretation that they are pathogenic.

However, the assays undertaken only represent one way to identify possible impairment of protein stability, by testing effects on steady state levels of folliculin. To confirm that the reduction in folliculin levels caused by introducing the missense mutations is at the protein level, it would be important to use real-time quantitative PCR to determine if there is any reduction in stability of *FLCN* mutant constructs at the mRNA level. It would also be interesting to further investigate the mechanism of reduced stability by

treating the cells with a proteasome inhibitor such as MG132, to determine if this would return the levels of folliculin back to wild-type levels, thus suggesting the mutations are causing folliculin to be degraded more quickly. Finally, the cells could be treated with a protein synthesis inhibitor such as cyclohexamide and cells lysed as a time course, to determine if the mutant proteins have a reduced half life, which might be responsible for the reduced steady-state levels observed.

The p.Arg239Cys mutation was previously detected in a patient who presented with multicentric clear cell RCC but no other BHD syndrome manifestations (Woodward, et al., 2008). The mutation was predicted to be pathogenic, and the functional analysis undertaken in this project confirms this previous interpretation that the p.Arg239Cys mutation is responsible for the patient's condition. The same mutation has subsequently been described in another unrelated BHD patient, presenting with fibrofolliculoma's and three primary tumours. Analysis of the BHD renal tumour derived from the affected patient showed loss of heterozygosity for the second copy of *FLCN* in the tumour and reduced levels of folliculin in the tumour tissue.

The p.His255Pro mutation is of interest as it is the human equivalent of the mutation found in the naturally occurring canine model of BHD syndrome (see section 1.3.5.3 for full description) (Lingaas, et al., 2003). This can also be confirmed as pathogenic.

Of the other mutations that impaired folliculin stability, the p.Arg362Cys variant was identified in the colorectal cell line LoVo (see section 3.4.1). The p.Lys508del IFD was described in a patient with fibrofolliculomas and features of spontaneous pneumothorax

(So, 2009). The p.Glu510del IFD has been described in a number of BHD patients presenting with at least one of the classical BHD manifestations, although none were reported to have renal tumours (Toro, et al., 2008).

Two of the variants modelled, p.Val400Ile and p.Lys508Arg, produced stable folliculin proteins. These were therefore of interest as they could potentially represent stable but non-functional folliculin proteins and thus provide insights into important folliculin functions. Folliculin is a tumour suppressor and reintroduction of the protein into null cell is able to inhibit tumour growth in nude mice xenografts (Hong, et al., 2010; Vocke, et al., 2005). To test the pathogenicity of these two stable variants, the growth suppressive effects of the variant proteins were tested by soft agar colony formation assay. Both of the variants produced a strong growth suppressive effect when introduced into FTC-133 cells, behaving similarly to wildtype folliculin. In contrast, the p.His255Pro unstable missense mutant and the p.His429ProfsX27 frameshift mutation displayed a loss of growth suppressive function. The possibility that the mutations might be having effects on the intracellular distribution of folliculin, was also tested. Neither of the variants were mislocalised compared with wildtype folliculin expressing FTC-133 cells. A pathogenic control construct was not included in this assay as all have been shown to reduced protein stability, however if a mutation within *FLCN* were to be identified which resulted in a stable protein, this would represent an important control for further experiments regarding protein localisation.

Both the p.Lys508Arg and the p.Val400Ile mutations were described in a single BHD patient. Since the completion of this chapter, the p.Val400Ile variant was found not to segregate with disease status in the affected family and another pathogenic folliculin mutation was detected in this family. This therefore represents a useful control for indentifying the pathogenicity of non-truncating *FLCN* variants. The BHD family with the p.Lys508Arg mutation is still under investigation. It is unclear whether the mutation may affect splicing, which is not tested in the assays reported here, or if the family may also harbour another *FLCN* variant, for example a large deletion or duplication, where detection is currently in its infancy (Benhammou, et al., 2011).

Interestingly, both the *in silico* methods used to predict pathogenicity using computational modelling alone (SIFT and POLYPHEN) predicted both the pLys508Arg and p.Val400Ile variants to be benign, consistent with the experimental data. These programs are predicted to be 65% and 70% accurate respectively (Thusberg and Vihinen, 2009), so while it is can be interpreted that when both programs predict the same outcome, they are likely to be correct, the accuracy of these programs is not yet sufficient to reliably replace the experimental tests conducted in this chapter. Studies have shown that the performance of variant prediction software can be increased by combining MSA information with three-dimensional protein structure (Bromberg and Rost, 2007), highlighting that efforts to determine the crystal structure of folliculin may be crucial in reliably predicting pathogenic *FLCN* variants without the need for experimental analysis.

Mutations in *FLCN* are responsible for a range of phenotypes, including those associated with BHD syndrome and familial primary spontaneous pneumothorax (Menko, et al., 2009). Only few genotype-phenotype correlations have been described to date, and the molecular pathogenesis responsible for the variability of BHD phenotype is unclear. The association between BHD syndrome and colorectal cancer is currently unconfirmed. Chapter 3 reported a heterozygous, missense variant in the LoVo colorectal cell line (c.1084C>T, pArg362Cys). Although the pathogenicity of this variant was uncertain, the evidence presented in this chapter suggests that it is likely to be pathogenic, due to a reduction in folliculin stability. However further investigation is required to identify whether the effects of this mutation as a heterozygote in the LoVo cell line are sufficient to affect folliculin associated signalling pathways, perhaps as a result of reduced folliculin dosage.

Chapter 3 reported that pHis429ProfsX27 mutation carriers are at significantly increased risk of colorectal neoplasia compared with p.Ala204X mutation carriers. We hypothesised that this may be as a result of a dominant negative effect associated with the p.His429ProfsX27 truncated protein. This chapter demonstrates that both mutations result in a translated, truncated protein, although presents no evidence for a dominant negative effect when DLD-1 colorectal cells were transfected with p.His429ProfsX27 mutant expressing vector. Previous studies had demonstrated the efficacy of using soft agar studies to investigate potential dominant negative effects (Kim, et al., 2003), however as DLD-1 cells were developed from a late stage colorectal cancer, the

possibility that a dominant negative effect may only be exerted by the p.His429ProfsX27 mutant as an initiating/early stage of colorectal tumourigenesis, cannot be excluded.

Folliculin is known to bind to two proteins FNIP1 and FNIP2, which interact with 5'AMP-activated protein kinase (AMPK) an important energy sensor for the cell. These interactions are reported to negatively regulate mTOR, a signalling hub for growth and cell proliferation. At the time that this project was undertaken, folliculin loss has been reported to upregulate mTOR signalling through both mTORC1 and mTORC2 activation in a number of studies (Baba, et al., 2006; Hasumi, et al., 2008; Hasumi, et al., 2009). Thus we hypothesised that the effects of expressing the *FLCN* mutants in our cell lines may also lead to an upregulation of mTOR signalling. However, after many months work, investigating a range of cell culture conditions and cell lines, we were unable to identify robust, repeatable effects on mTOR signalling associated with each of our *FLCN* mutants. Subsequent publications reveal the effects of *FLCN* loss on mTOR signalling to be more complicated than initially suggested, appearing to be complex and context-dependent with both abnormally high and abnormally low levels of mTOR signalling reported when functional *FLCN* is absent (Hartman, et al., 2009; Hudon, et al., 2010). This may go some way to explaining the inconsistencies we observed when investigating the effects of *FLCN* mutations on mTOR signalling.

In summary, the findings reported in this chapter are consistent with the hypothesis that the vast majority of *FLCN* mutations are pathogenic by impairing stability and/or causing deficiency of the full length folliculin protein. Hence it is likely that multiple aspects of

folliculin function must be disrupted to cause the associated phenotypes. Further elucidation of folliculin function and description of the protein structure might provide novel insights into the significance of the strongly conserved domain (codons 100-230) identified. In addition this chapter demonstrates a practical strategy for establishing the likely pathogenicity of putative *FLCN* variants as they are discovered.

However, no data was generated from our studies into of the effects of these mutations on previously reported *FLCN* signalling pathways. It is likely folliculin plays multiple molecular roles within the cell which may be more robustly affected by *FLCN* inactivation. A yeast-2-hybrid screen was undertaken to identify previously unknown folliculin binding partners and potential novel functions. Investigations into a novel folliculin binding partner and the associated functional relevance of this interaction are discussed in the next chapter.

Chapter 5 Investigation of the molecular and cellular impact of the folliculin/plakophilin-4 interaction

5.1 Introduction

Identification of the molecular functions of folliculin within the cell is crucial for understanding the role of its inactivation in renal neoplasia as well as providing clues for developing therapeutic agents for the BHD syndrome. It is anticipated that once the major aspects of folliculin function (which drive BHD phenotype when disrupted) are well elucidated, targeted therapies may be developed as reported for VHL disease. Currently the functions of folliculin are poorly understood; folliculin loss being linked to mTOR signalling deregulation through the interaction between folliculin and FNIP1 and FNIP2 (discussed in detail in section 1.3.6.1). However, in the experiments described in the previous chapter, I was unable to reliably define the impact of *FLCN* inactivation on the regulation of mTOR signalling and others have also suggested that folliculin regulation of the mTOR pathway appears to be variable and context dependent. It is likely that the functions of folliculin are multi-faceted, and identification of novel folliculin binding partners might provide further insights into the mechanisms of folliculin tumour suppressor function. A yeast-2-hybrid screen was performed for folliculin, with plakophilin-4 (p0071, pkp4) identified as a candidate interacting protein. This chapter investigates the interaction between folliculin and p0071 and the potential associated relevance for folliculin function.

5.1.1 Plakophilin 4 (p0071/pkp4)

Plakophilin 4 (p0071) is a member of the armadillo-repeat family of cell-adhesion proteins of which p120^{ctn} is the prototype. Members of the p120 family co-localise with classical cadherins at adherens junctions, mediated by a direct interaction of classical cadherins with the armadillo repeat domain (Hatzfeld, 2005). Interaction of p0071 with E-cadherin results in increased E-cadherin stabilisation at cell-cell junctions. p0071 is also able to bind desmosomal proteins through its N-terminal head domain (Hatzfeld, et al., 2003; Hatzfeld and Nachtsheim, 1996). p0071 has been reported to function in the cross talk between adherens junctions and desmosomes (Hatzfeld, 2005). A brief introduction to the reported functions of p0071 is described below.

5.1.2 Cell-cell adhesion

In a multicellular organism, cell junctions are required for the adhesion of cells to each other and the extracellular matrix in order to maintain tissue form and structure. Intercellular junctions also maintain cell and tissue polarity. The three types of cell junction crucial for forming and maintaining barriers are adherens junctions, tight junctions and desmosomes (Niessen, 2007).

5.1.2.1 Adherens junctions, Tight junctions and Desmosomes

Tight junctions are the most apical structure of cell-cell contacts, marking the border between apical and basolateral membrane domains. They are comprised of two types of

transmembrane proteins, claudins and occludins and also the cytoplasmic scaffolding proteins ZO-1, ZO-2 and ZO-3. Tight junctions control ion selectivity and permeability of the paracellular pathway between adhering cells (Hartsock and Nelson, 2008).

Adherens junctions are positioned directly below tight junctions (Niessen, 2007). They are made up of proteins of the cadherin superfamily, such as E-cadherin, and catenin family members including p120-catenin, β -catenin and α -catenin. Adherens junctions function in initiating and stabilising cell-cell adhesion, regulating the actin cytoskeleton, transcriptional regulation and intracellular signalling (Hartsock and Nelson, 2008). Junction formation is induced by E-cadherin initiating intercellular contacts through trans-pairing with cadherin molecules on adjacent cells, a process which is dependent on the presence of calcium ions (Gumbiner, 2005). It has been reported that the formation of the adherens junction leads to the formation of tight junctions, but is not required for tight junctional maintenance (Capaldo and Macara, 2007). Together adherens junctions and tight junctions make up the apical junction complex (AJC) complex widely believed to be the driving process for the generation of apical basolateral polarity (Nelson, 2003).

Desmosomes are intercellular junctions that connect intermediate filaments to the plasma membrane, and are crucial in tissues which experience mechanical stress such as the bladder, gastrointestinal mucosa and the skin (Delva, et al., 2009). Desmosomes consist of transmembrane glycoproteins desmogleins and desmocollins, which are members of the cadherin superfamily. Cytoplasmic associations with desmosomal cadherins are

mediated by the armadillo family proteins plakoglobin and plakophilins (Delva, et al., 2009).

Plakophilin-4 has been reported to be both present in both desmosomes and adherens junctions (Hatzfeld, et al., 2003), and can bind to both classical and desmosomal cadherins via its armadillo repeats or N-terminal head domain respectively (Keil, et al., 2007).

A schematic of cell-cell contacts and the localisation of p0071 is displayed in Figure 5.1.

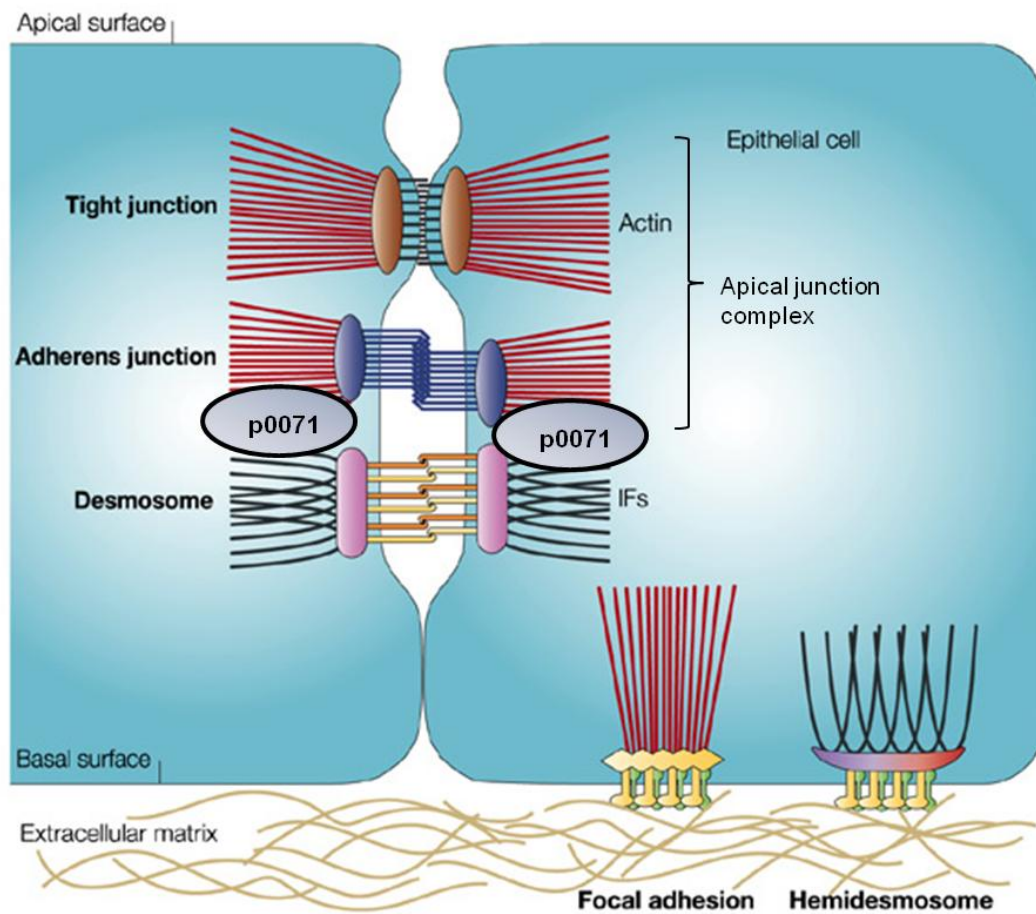


Figure 5.1 Schematic diagram of the location of p0071 in epithelial cell contacts
 p0071 is localised at both adherens junctions and desmosomes, by binding to classical and desmosomal cadherins through its armadillo and head domain respectively

Figure adapted from (Jefferson, et al., 2004)

5.1.2.2 Polarity and the apical junction complex

The apical-basal polarity of epithelial cells within multicellular organisms is characterised by the generation of functionally distinct membrane domains. The basolateral membrane contacts other cells and the underlying connective tissue while the apical surface faces the organ lumen. Polarised cells display an asymmetrical distribution of lipids and proteins between both domains, the result of polarised trafficking and the presence of the physical barrier of the apical junction complex (Moreno-Bueno, et al., 2008).

5.1.2.3 Loss of cell polarity and cell junction down regulation lead to cancer

Metastasis is the most important cause of mortality in human cancers (Moreno-Bueno, et al., 2008). Loss of cell polarity and cell-cell adhesion is a frequent feature of epithelial cancers which is strongly linked to tissue invasion and metastasis and can also occur early in tumourigenesis (Tervonen, et al., 2011). The ability of cells to escape the primary tumour and migrate to distant sites of metastasis is crucial to cancer progression. The epithelial to mesenchymal transition (EMT) is an epithelial process during embryogenesis and can be hijacked by a tumour, inducing loss of cell-cell adhesion and apical basal cell polarity as well as increasing cell motility (Thiery, 2003). One of the earliest steps in EMT is loss of E-cadherin, through modulation of transcription factors that repress E-cadherin and other similar proteins (Moreno-Bueno, et al., 2008). A full

description of EMT is beyond the scope of this thesis, however for excellent review of EMT in the context of all steps of tumour metastasis see (Valastyan and Weinberg, 2011).

Understanding of the role of desmosomes in cancer is still in its infancy, however *in vivo* genetic loss of function studies in the mouse, have revealed a causal relationship between the downregulation of certain desmosomal genes (*Dsp*, *Dsg2*, *Dsc2* and *Pkp2*) and the development of cancer (Chun and Hanahan, 2010; Dusek and Attardi, 2011).

5.1.3 RhoA signalling and cancer

5.1.3.1 Rho GTPases

P120 protein family members, including p0071, have been previously implicated in the regulation of Rho signalling (see section 5.1.3.5). This is particularly interesting in light of the results reported in the chapter, identifying p0071 as a potential folliculin interacting protein. Malignant tumour cells display uncontrolled proliferation, loss of epithelial polarity, enhanced cell migration and altered interaction with neighbouring cells and the extracellular matrix (Karlsson, et al., 2009). Rho GTPase family members regulate all these processes in cell culture and more recent evidence shows that increased Rho signalling correlates with tumour progression *in vivo*, suggesting the potential efficacy of using Rho inhibitors as a feasible new avenue in tumour treatment (Karlsson, et al., 2009). Rho is a member of the Ras superfamily of small GTPase binding proteins. The mammalian Rho GTPase family consists of five subfamilies, Rho-like, Rac-like,

CDC42-like, Rnd and RhoBTB (Burrige and Wennerberg, 2004). This chapter focuses on RhoA, the best characterised of three members of the Rho-like GTPase family (also including RhoB and RhoC) which share the same group of effectors and have similar modes of action (Narumiya, et al., 2009).

5.1.3.2 RhoA

RhoA is a small GTPase which functions as a molecular switch in a wide range of cellular processes including cell adhesion, migration and cell cycle progression at cytokinesis (Burrige and Wennerberg, 2004; Jaffe and Hall, 2005). Conversion from the GDP-bound inactive form to the GTP-bound active form of Rho is catalysed by specific guanine nucleotide exchange factors (Rho GEFs) of the Dbl family (Zheng, 2001). Conversion back to the inactive GDP-bound form is due to the intrinsic GTPase activity of Rho, stimulated by GTPase activating proteins (Rho GAPs) (Moon and Zheng, 2003). An additional level of control is provided by Rho-GDP dissociation inhibitors (Rho GDI's) which bind to inactive Rho and holding it in a complex in the cytoplasm away from the site of GTP/GDP exchange at the cell membrane (Garcia-Mata, et al., 2011) (see Figure 5.2).

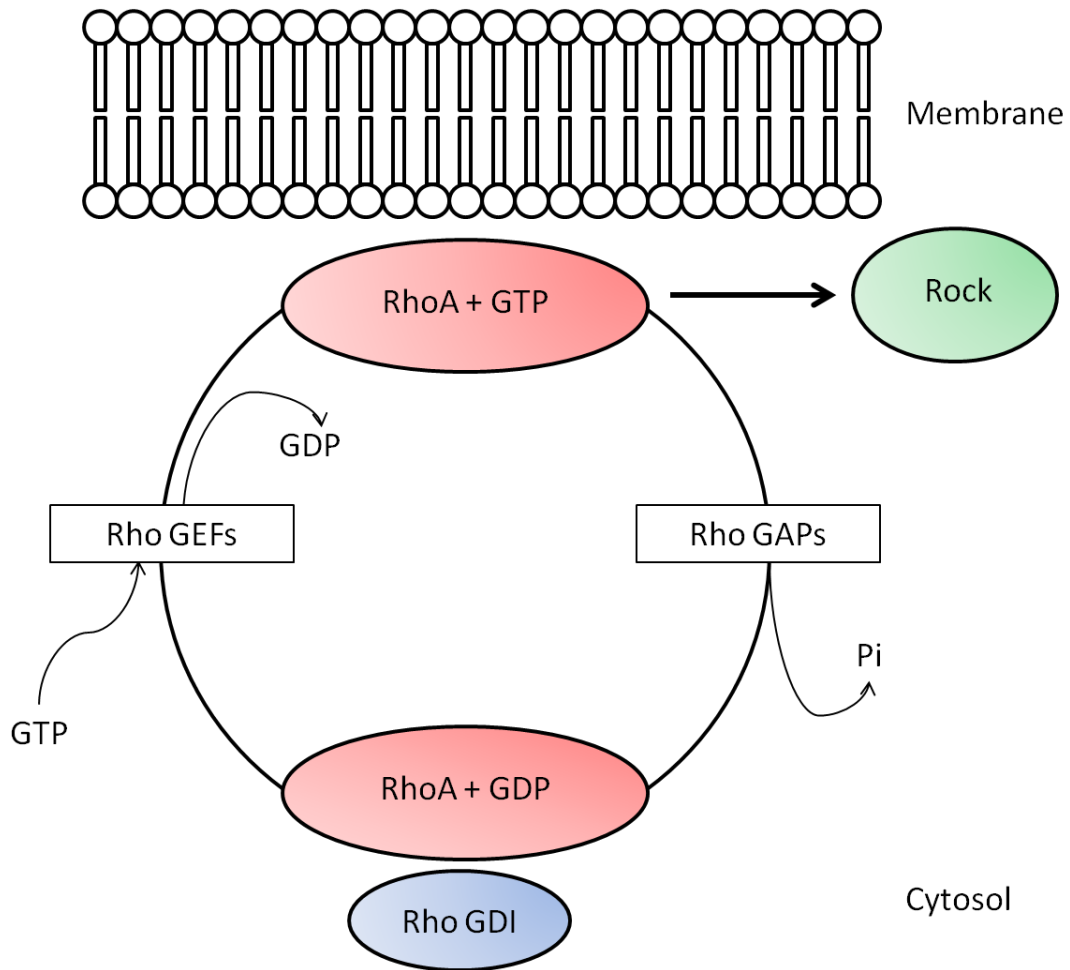


Figure 5.2 The RhoA GTPase cycle

The Rho GTPase switches between GDP (inactive) and GTP (active) forms. Rho guanine exchange factors (GEFs) catalyse the conversion from GDP to GTP bound RhoA (at the membrane). Conversion back to GDP bound RhoA occurs by GTP hydrolysis, stimulated by Rho GTPase activating proteins (GAPs). GTP bound RhoA activates downstream targets such as ROCK (Rho-dependent kinase), whereas the GDP bound form binds Rho GDP dissociation inhibitor (GDI) which maintain an inactive state in the cytosol. Pi represents phosphate.

RhoA signalling is responsible for the induction of a specific type of actin cytoskeleton in the cell and also modulates local dynamics of microtubules (Narumiya, et al., 2009). RhoA induces actin stress fibres and focal adhesions in the interphase cell, and is required for contractile ring formation in the mitotic cell (see Figure 5.3). These actions of RhoA are carried out by the effectors activated downstream of Rho; ROCK (Rho-associated coiled-coil forming kinase) and mDia (mammalian homolog of *Drosophila* diaphanous) (Matsui, et al., 1996; Watanabe, et al., 1997).

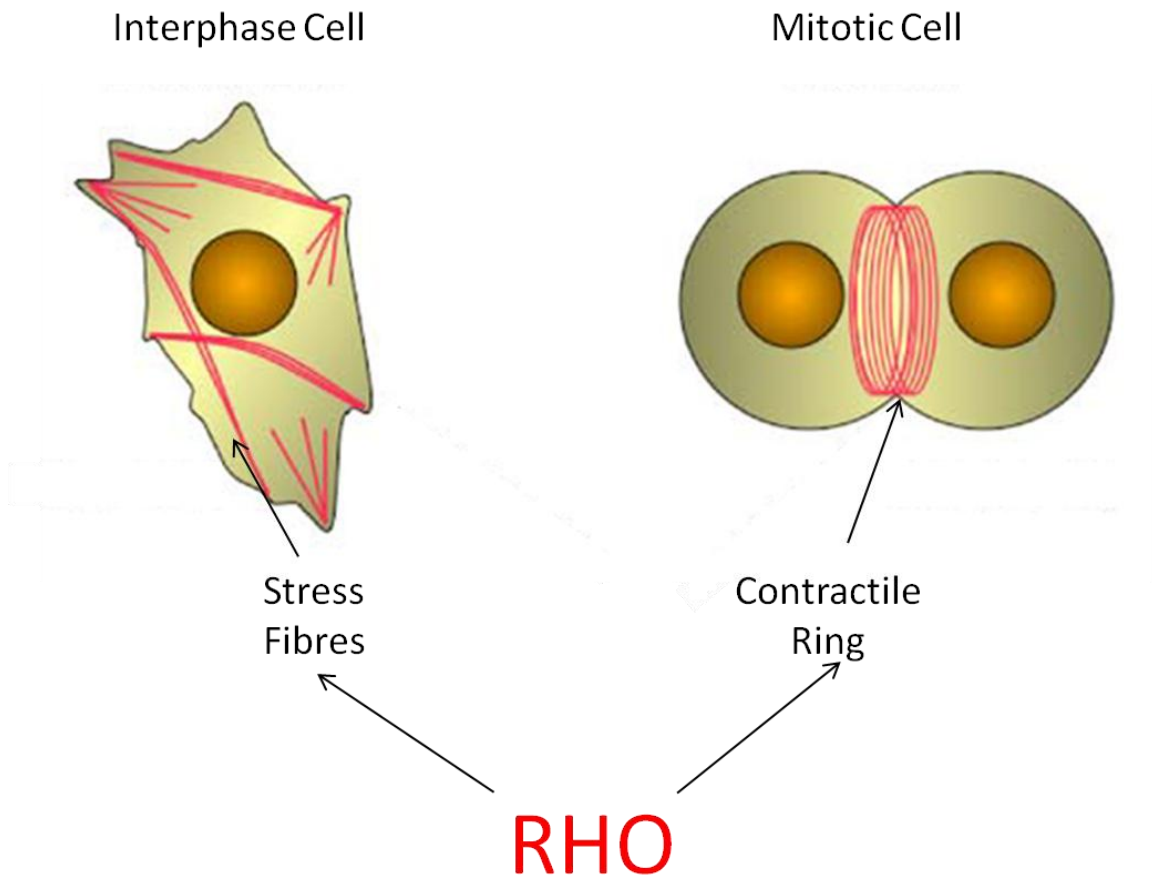


Figure 5.3 The role of Rho in the interphase and mitotic cell

Stress fibres and the contractile ring are two actin cytoskeletons induced by Rho, and are composed of anti-parallel actin filaments cross linked by myosin II. Figure adapted from (Narumiya, et al., 2009)

5.1.3.3 The role of RhoA in invasion and metastasis

Invasion of malignant tumour cells and formation of metastasis is critically dependent on the migratory properties of the cancer cell (Karlsson, et al., 2009). Cells undergo migration by polarising to the direction of migration with extending protrusions at the front edge and tail retraction at the rear. Microtubules and the actin cytoskeleton are crucial for this function (Narumiya, et al., 2009). It is well established that in the interphase cell, RhoA activation mediates cell migration through retraction at the rear of cells, but recent evidence suggests it also actively functions at the protruding edge, with a role in the initial events of protrusion (Machacek, et al., 2009; Spiering and Hodgson, 2011). As previously mentioned, an early step in the metastatic cascade involves loss of cell polarity and disruption of cell-cell contacts (for example during EMT). Interestingly, Rho activation has also been implicated in AJC disassembly, by triggering the formation of acto-myosin rings required for disruption of the AJC (Samarin, et al., 2007).

5.1.3.4 The role of RhoA in cytokinesis

Cytokinesis requires the spatio and temporal control of actin and myosin to cause contractile ring assembly and contraction. In eukaryotes, activation of RhoA is the critical step in orchestrating cytokinesis, functioning by binding and regulating specific protein effectors which manipulate the actomyosin contractile network (Piekny, et al., 2005). Furrow formation is controlled downstream of RhoA, by formin-mediated actin polymerisation. Ingression of the furrow is mediated by ROCK (Rho dependent kinase)

activation of myosin II, another downstream target of RhoA. Completion of furrow ingression and the final stages of cytokinesis are reliant on citron kinase, also activated by RhoA (Piekny, et al., 2005). Cytokinesis is a complex process and requires tight spatiotemporal regulation of RhoA activation, for which the Rho GEF, ECT2 is an important player (Glotzer, 2005). Deregulation of RhoA induces cytokinetic defects, which can result in polyploidy and increased genome instability, features characteristic of the cancer cell (Li, et al., 2010). Given the important roles of RhoA in cell migration and mitosis it is unsurprising that over expression of RhoA has been described in a wide variety of human tumours (Karlsson, et al., 2009).

5.1.3.5 P0071 regulates RhoA activity

P120 family proteins are considered multifunctional and have a signalling role beyond their structural role in cell contacts, reflected in their cytoplasmic and nuclear localisation (Keil, et al., 2007). A number of studies have demonstrated a role for p120^{ctn} in regulating Rho GTPases, with p120^{ctn} overexpression resulting in a branching phenotype and providing evidence for inhibition of RhoA activity by p120^{ctn} (Anastasiadis, et al., 2000; Reynolds, et al., 1996). Currently little is known about the role of p0071 in Rho signalling in the interphase cell, although it is believed regulation of small GTPases might be a common function of all p120 family proteins. Thus p0071 can induce a similar “branching phenotype” albeit to a reduced extent (Hatzfeld, 2005). However insights have been made into the role of p0071 in regulating RhoA in the dividing cell, an

important study by Wolf *et al.* demonstrating that p0071 plays an essential role in controlling Rho signalling during mitosis (Wolf, et al., 2006).

The authors investigated the subcellular localisation of p0071 in the mitotic cell, and demonstrated that in the course of mitosis, p0071 was associated with centrosomes, but became focussed at the midbody during cytokinesis (see Figure 5.4) (Keil, et al., 2007; Wolf, et al., 2006).

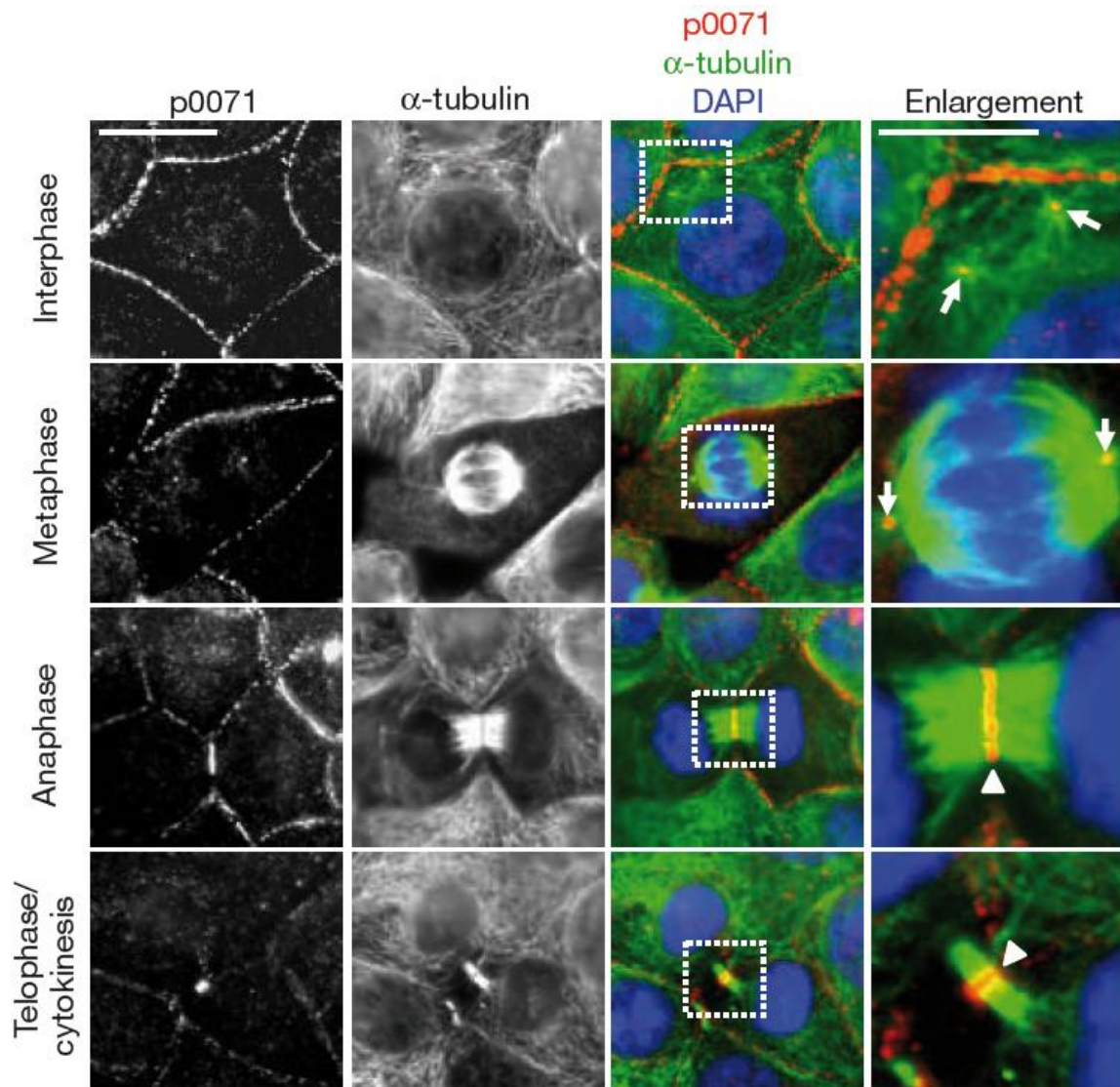


Figure 5.4 Localisation of p0071 in the mitotic cell

During interphase, p0071 is localised at the plasma membrane and centrosomes. In metaphase, it becomes enriched at the spindle poles and retains its membrane localisation. p0071 becomes focused at the midbody region during late anaphase through to cytokinesis (Wolf, et al., 2006).

The authors demonstrated a functional role for p0071 in cell division with treatment of cells with a p0071 siRNA inducing multinucleation due to defects in cytokinesis. Overexpression of p0071 produced similar effects. p0071 knockdown caused a downregulation of RhoA, and reduced accumulation of filamental actin at the contractile ring. P0071 was shown to bind RhoA, preferentially to the active GTP-bound form, and to modulate the spatio-temporal activity of RhoA by binding to and enhancing the activity of the Rho guanine exchange factor Ect2 (Keil, et al., 2007; Wolf, et al., 2006). Further light was shed on the subject of p0071-mediated, spatio-temporal control of Rho signalling with the motor protein KIF3b being identified as a p0071 binding partner, and functioning in targeting p0071 to the midbody at cytokinesis (Keil, et al., 2009).

5.2 Aims

Yeast-2-hybrid analysis identified p0071 as a potential folliculin interacting protein. This chapter aimed to confirm and define the intracellular context of the p0071/folliculin interaction, and also the functional effects of cell folliculin status on p0071 associated functions.

5.3 Methods

5.3.1 Co-immunoprecipitation

Co-immunoprecipitation experiments were undertaken as described in Methods 2.4.3 to confirm the interaction between p0071 and folliculin *in vitro*. Co-immunoprecipitation of folliculin and p0071 was confirmed with pull down of both proteins separately, and western blotting for the other protein. Experiments were carried out with over expression of flag-tagged folliculin and also at endogenous levels in Hek293 cells.

5.3.2 Immunofluorescence analysis

Immunofluorescence analysis was carried out to define the intracellular context of the folliculin and p0071 interaction. A number of cell lines were fixed and stained for folliculin and p0071, both at over-expressed and endogenous levels. Cell lines investigated were HeLa, HaCat, MCF-7, ACHN, ACHN Kd1 (FLCN stable knockdown), FTC -133 (stable vector control), FTC-133 (Flag tagged folliculin stable expressor).

5.3.2.1 Bimolecular fluorescence complementation analysis

Bimolecular fluorescence complementation analysis enabled the direct visualization of the interaction between folliculin and p0071 in living cells. The assay is based on the association of two non-fluorescent proteins (folliculin and p0071 in this case) fused to separate halves of YFP (empty Venus constructs kindly provided by Prof M Hatzfeld), which when co-expressed, result in the re-formation of the fluorescent protein. This allows the identification of the subcellular localisation the interaction between the two proteins. The principle of the assay is displayed in Figure 5.5.

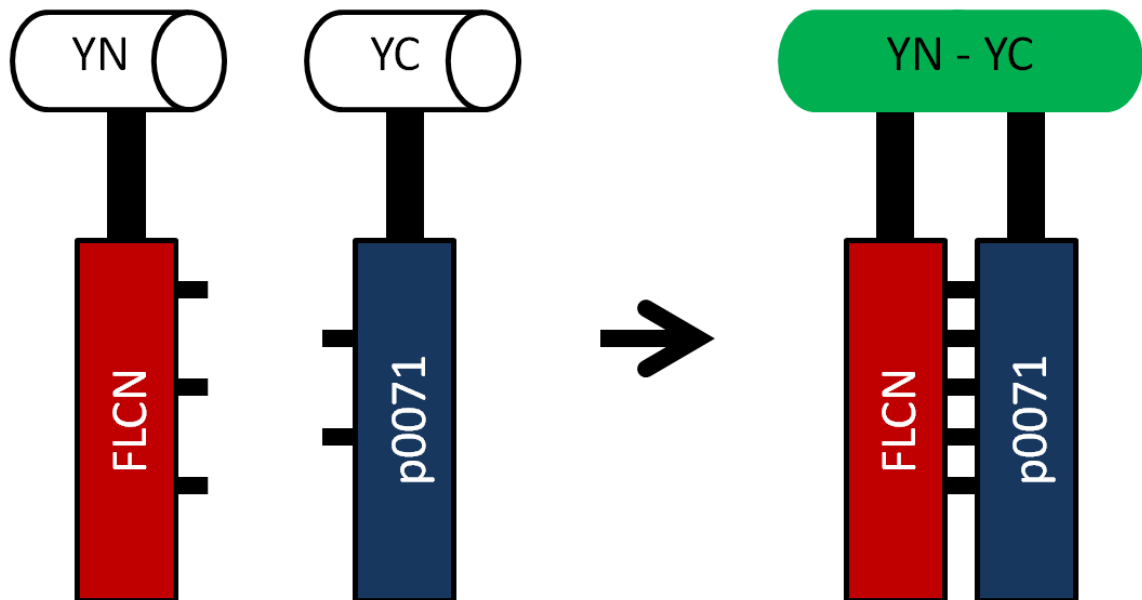


Figure 5.5 Principle of BiFC analysis

YN = N terminus of YFP, YC = C terminus of YFP

Venus constructs expressing p0071 fused to both the N terminal half (Venus 1 - amino acids 1-115) and C terminal half (Venus 2 - amino acids 115-238) of YFP respectively, were kindly donated by Prof Mechthild Hatzfeld. Truncation of YFP at amino acid 115 has been previously shown to produce relatively bright fluorescent signal when two proteins are genuine interactors, but produce only nominal fluorescence when fused to proteins which do not interact (Kerppola, 2008). Full length *FLCN* was amplified from human cDNA by PCR, and cloned into both Venus 1 and Venus 2 BiFC vectors (Using *EcoR*I and *Bam*H1 restriction enzyme site containing primers given in Table 2.14), in both N-terminal fusion and C-terminal fusion orientation respectively. All four combinations of *FLCN*-Venus fusions are displayed in Figure 5.6. This was to overcome any steric constraints that might result from the YFP fusions not being able to collide sufficiently frequently with each other to facilitate BiFC complex formation, as a result of being too distant from each other when the fusion proteins interact.

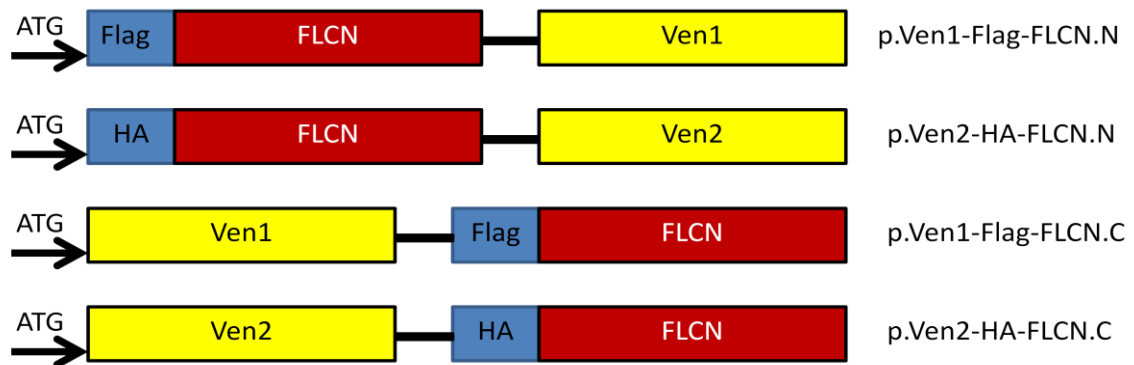


Figure 5.6 FLCN Venus constructs cloned for BiFC analysis

Ven1 = N terminus of YFP, Ven2 = C terminus of YFP. Flag and HA represent protein tags at the N terminus of FLCN

All folliculin and p0071 venus construct combinations were co-transfected into HeLa cells and detection of BiFC signal determined as described in Methods 2.7.1.

5.3.3 Analysis of Rho activity in folliculin isogenic cell lines

The effect of folliculin status on RhoA cellular levels was tested by western blot in Hek293 cells treated with folliculin siRNA compared with control siRNA, in ACHN cells stably expressing folliculin specific shRNA or scrambled control, and in FTC-133 cells (no endogenous folliculin expressed) stably expressing flag tagged folliculin or empty vector.

The effect of folliculin status on RhoA activity was tested using the G-Lisa RhoA activation assay, as described in Methods 2.8. The assay tests the levels of GTP-bound RhoA in each cell lysate and hence the level of RhoA signalling in the presence or absence of folliculin.

5.3.4 Multinucleation analysis

Effects of folliculin absence on defects in cytokinesis were determined in FTC-133 cells grown on poly-L-lysine coated coverslips. Cells were grown to 50% confluence, fixed and stained for α -tubulin. The number of multinucleated cells was counted in the presence or absence of folliculin and the results of three separate experiments collated.

5.3.5 Cell migration analysis

The potential impact of folliculin on the migratory ability of cells was tested using the *in vitro* cell scratch migration assay. FTC-133 cells were plated at full confluency, starved of serum and a scratch introduced into the cell monolayer. The migratory ability of cells was assessed by quantification of percentage scratch healed every 24 hours.

To test whether the differences observed in migratory ability of the cells was due to differences in Rho signalling, the well characterised Y-27632 ROCK inhibitor was added to the cells, at a concentration of 10 μ M. For review of the pharmacological properties of Y-27632, see (Ishizaki, et al., 2000).

5.3.6 Transepithelial electrical resistance assay and effect of folliulin/p0071 knockdown on epithelial cell polarisation

- Cell culture, immunofluorescence in IMCD-3 cells and TEER results calculated by Ania Straatman-Iwanowska

To assess the impact of folliculin loss on cell polarity and cell junction formation, IMCD-3 cells were used. This cell model was used as it is derived from the murine inner medullary collecting duct and thus represents a “normal” kidney cell model, whereas cancer cell lines may harbour multiple genetic and epigenetic events that can disrupt epithelial polarity. IMCD-3 cells have been widely used to investigate the physiology of

epithelial polarisation, and can be induced to polarise in vitro by growth on Transwell permeable supports.

IMCD-3 cells were treated with either p0071, FLCN or Luciferase siRNA and seeded onto Transwell supports. Trans epithelial electrical resistance (TEER) was measured after 8 days using an EVOM AC square wave current resistance meter (World Precision Instruments). TEER measurements were used to assess whether FLCN or p0071 knockdown affected the integrity of the epithelial monolayer.

At day 8, filters were mounted between coverslips and fixed with 4% formaldehyde. Cells were stained for E-Cadherin, Claudin-1 and ZO-1 to assess junctional formation, and were visualised using a Leica SP5 Laser Scanning Confocal Microscope.

5.4 Results

5.4.1 *Yeast-2-hybrid Screen*

Identification of the proteins that bind to a protein of interest can often provide important insights into the functions of that protein, as they are often related. To identify potential novel folliculin binding proteins, a yeast-2-hybrid screen was carried out (DFKZ Cancer Research Centre) using full length folliculin as bait against a human fetal brain cDNA library. The screen yielded 17 candidates which were then assessed for their likelihood of representing genuine interactors by the number of clones identified to interact with folliculin and the promiscuity rating of the protein. They were then categorised into one of three categories; likely interactors, uncertain interactors and likely false positive (see Table 5.1).

<i>Gene symbol</i>	<i>Gene name</i>	<i>Number of times prey isolated</i>	<i>Promiscuity rating</i>	
IK	IK cytokine, down-regulator of HLA II	37	2	Likely interactors
PKP4	plakophilin 4	4	3	
ZNF74	zinc finger protein 74	4	3	
NCOR1	nuclear receptor co-repressor 1	2	3	
ZBTB17	zinc finger and BTB domain containing 17	2	3	
CNRIP1	chromosome 2 open reading frame 32	1	1	
KIAA1450	KIAA1450 protein	1	1	
LOC644456	similar to RED protein	1	1	
HS.706042	N/A	1	1	
OTUD1	OTU domain containing 1	1	1	

SOBP	sine oculis binding protein homolog (Drosophila)	1	1	Uncertain interactors
TRIP4	thyroid hormone receptor interactor 4	1	1	
ZNF251	zinc finger protein 251	1	4	
S100A2	S100 calcium binding protein A2	1	5	Likely false positives
MAP3K7IP2	mitogen- activated protein kinase 7 interacting protein 2	33	6	
MAP1S	microtubule- associated protein 1S	5	11	
PCBP1	poly(rC) binding protein 1	1	39	

Table 5.1Yeast-2-hybrid results for folliculin

5.4.2 Folliculin and p0071 interact in vitro

p0071 was identified as a potential interacting partner of folliculin by a yeast-2-hybrid screen, with four independent clones of p0071 encompassing exons 7-10 detected. This region of p0071 corresponds to a section of the p0071 head domain (amino acids 1 – 509). To investigate the reliability of the yeast-2-hybrid results, co-immunoprecipitation studies were undertaken to confirm the potential interaction *in vitro*. Initially flag tagged folliculin was transfected into Hek293 cells at high levels and immunoprecipitation undertaken for both p0071 and flag. In both cases the respective binding partner was also pulled down as a complex (see Figure 5.7 a and b).

To confirm the interaction at endogenous levels, untransfected Hek293 cells were lysed and immunoprecipitated for folliculin and p0071 respectively. Consistent with the results at over-expressed levels, when p0071 was pulled down folliculin was also detected by immunoblotting, and when folliculin was immunoprecipitated p0071 was also detectable (see Figure 5.7 c).

Immunoprecipitation with control antibody produced no visible folliculin or p0071 signal.

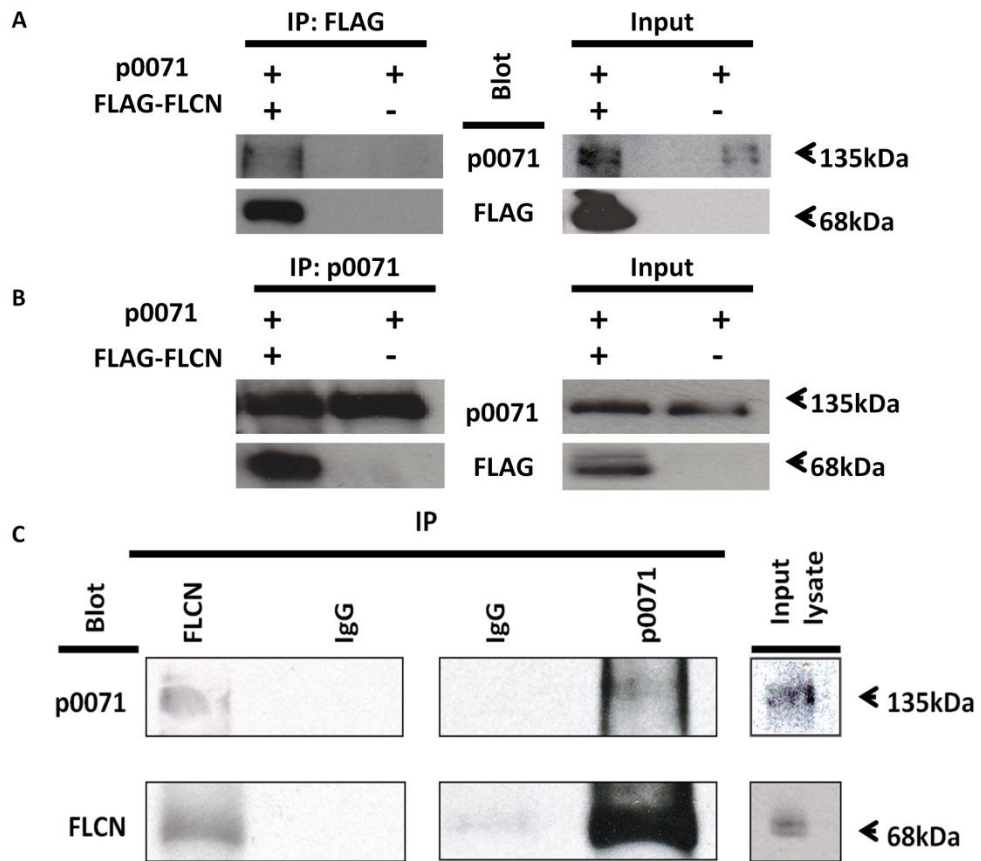


Figure 5.7 P0071 and FLCN interact in vitro

FLCN and p0071 interact *in vitro*: Flag tagged FLCN was stably transfected into Hek293 cells. Cell lysates were immunoprecipitated (IP) with flag (A) or p0071 (B) and blotted with flag and p0071. (C) Endogenous interaction was confirmed in Hek293 parental cells. Lysates were immunoprecipitated with FLCN, p0071 or control IgG and blotted for p0071 and FLCN. In both IP's p0071 and FLCN immunoprecipitated together, there was no pull down with control IgG. Arrows indicated size of bands kDa, + and - represent presence or absence of transfected construct respectively

5.4.3 Folliculin and p0071 colocalise and interact at cell junctions during interphase

To identify the context of the folliculin and p0071 interaction within the cell, comprehensive immunofluorescence microscopic analysis was undertaken. The localisation pattern of p0071 is dependent on cell cycle stage, being located at cell junctions in the interphase cell and at the midzone during late anaphase/cytokinesis in the mitotic cell.

Interphase MCF-7 cells were co-transfected with Flag-tagged folliculin and dsRed tagged p0071 using lipofectamine transfection reagent. The cells were fixed and stained for folliculin and DAPI. Microscopic analysis demonstrated a co-localisation of folliculin and p0071 at cell contacts and also a more disperse co-localisation pattern throughout the cytoplasm (see Figure 5.8a).

The co-localisation at cell junctions was also observed at endogenous levels in untransfected MCF-7 cells in interphase, although the pattern of folliculin signal is more consistent with a transient role for folliculin at cell junctions rather than as a major structural component (see Figure 5.8b). Co-localised pixels were identified using ImageJ software and a Manders overlap co-efficient was 0.599.

To confirm folliculin and p0071 were interacting at these sites of co-localisation, bimolecular fluorescence complementation (BiFC) analysis was undertaken. Microscopic analysis of HeLa cells co-transfected with both p.Ven1-p0071-Flag and p.Ven2-HA-FLCN-N displayed a strong BiFC signal at cell junctions and also at regions within the cytoplasm, indicating interaction *in vivo* (see Figure 5.8c).

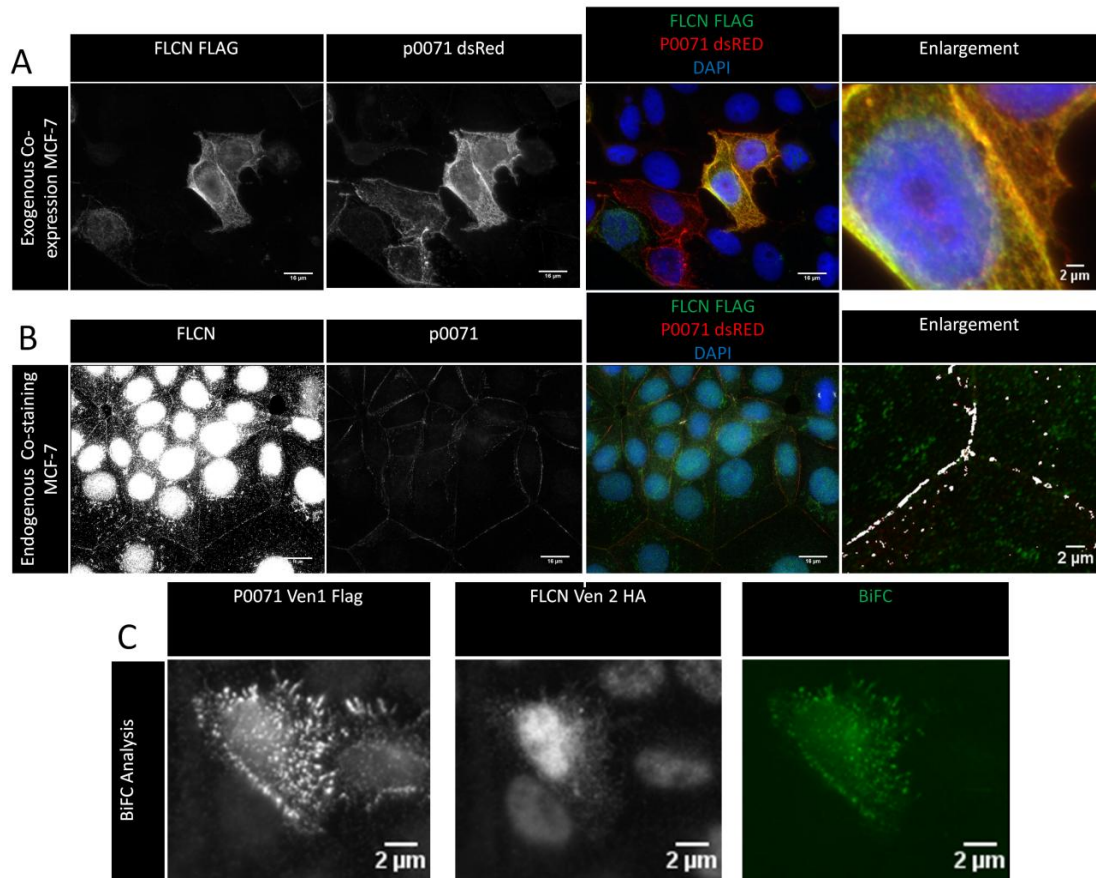


Figure 5.8 Folliculin and p0071 are co-localised and interact at cell junctions

A) MCF-7 cells were co-transfected with Flag tagged FLCN and p0071dsRed, fixed and stained for Flag and DAPI. Folliculin and p0071 co-localise at cell junctions and in a disperse pattern at certain points within the cytoplasm. Manders overlap coefficient = 0.968 (B) Confluent MCF-7 cells were fixed and stained for endogenous folliculin and p0071. Both p0071 and FLCN localised to cell junctions displaying a colocalised pattern. FLCN and p0071 colocalised pixels were identified using ImageJ software, and are displayed in white on the zoomed images. Manders overlap coefficient = 0.599 (C) Bimolecular fluorescence complementation (BiFC) analysis was used to confirm/identify the location of the interaction between FLCN and p0071 in living cells. HeLa cells co-expressed with pVen-1-flag-p0071 and pVen2-HA-FLCN display clear BiFC signal at cell junctions and throughout the cytoplasm. Images displayed are representative of >3 repeats, in a variety of cell lines

5.4.4 Folliculin and p0071 co-localise and interact at the midbody during cytokinesis

P0071 has been previously reported to become localised in the midzone region in anaphase and telophase, then tightly localised at the midbody during cytokinesis (Wolf, et al., 2006). To test whether folliculin also co-localised with p0071 at this region in the mitotic cell, FTC-133 cells stably transfected with flag tagged folliculin were fixed and stained for flag, p0071 and tubulin (to identify cells in the late stages of mitosis). A tight co-localisation of exogenous folliculin and endogenous p0071 was observed at the midbody during cytokinesis (see Figure 5.9a).

This was also investigated at endogenous levels in the HaCat cell line, which displayed a concentrated folliculin and p0071 staining at the midbody with evidence of co-localisation (see Figure 5.9b). Co-localised pixels were again identified using imageJ software (manders overlap coefficient for FTC-133s = 0.625; for HaCat cells = 0.687).

Using BiFC analysis, a direct interaction of folliculin and p0071 was observed in dividing HeLa cells at late telophase/cytokinesis (see Figure 5.9c).

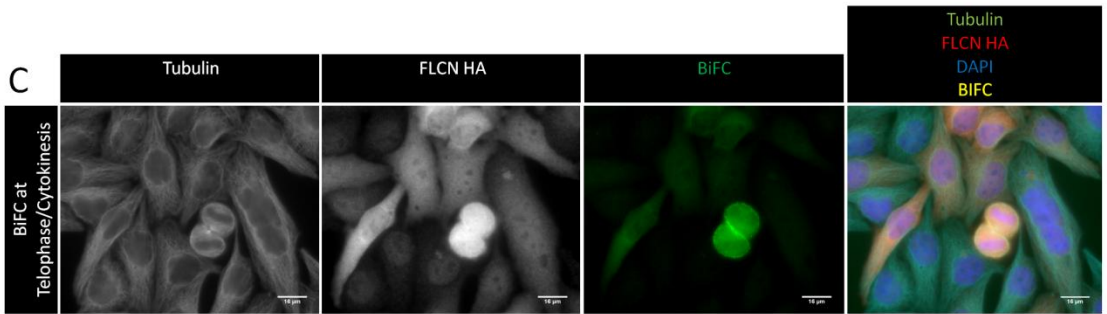
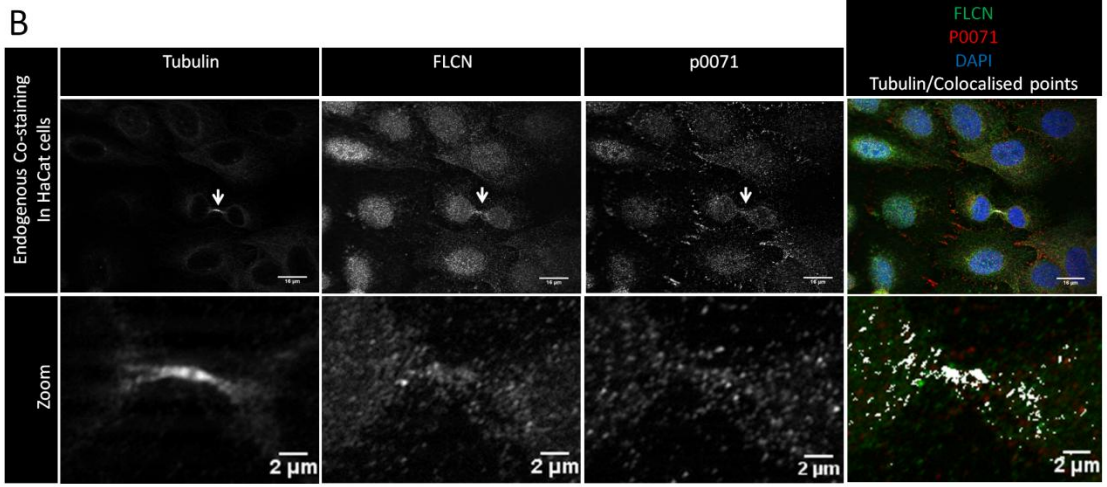
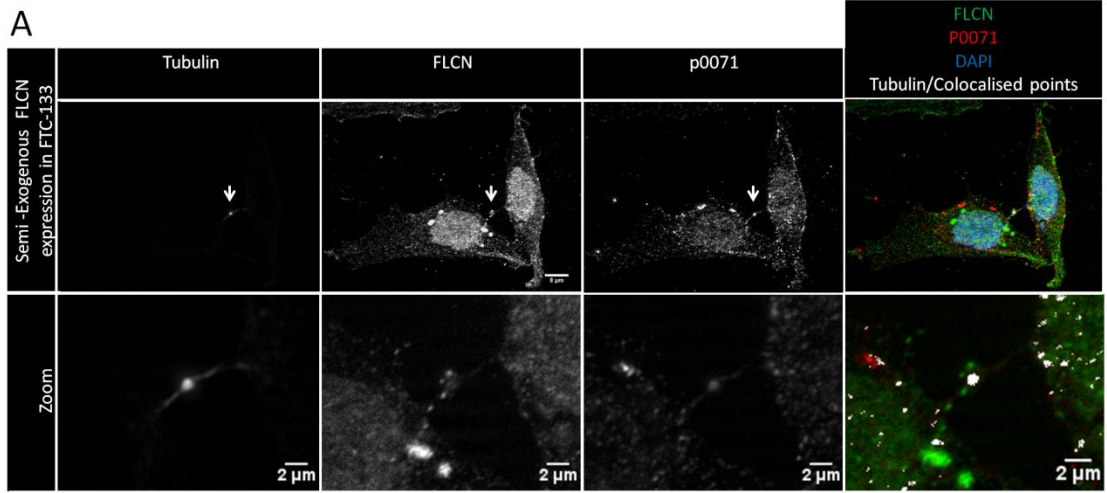


Figure 5.9 FLCN and p0071 colocalise and interact at the midbody during telophase/cytokinesis

(A) FTC-133 cells transfected with FLCN were stained for FLCN, endogenous p0071 and α tubulin. Enlargements of midbodies are displayed below the original images with only FLCN and p0071 channels displayed. P0071 and FLCN are concentrated at the midbody (stained with α tubulin) at cytokinesis. FLCN and p0071 co-localised pixels are displayed in white on the zoomed images. Manders overlap coefficient = 0.625 (B) HaCat cells were fixed and stained for FLCN, p0071 and α tubulin. Both proteins show concentrated localisation at the midbody at endogenous levels. FLCN and p0071 co-localised pixels are displayed in white on the zoomed images. Manders overlap coefficient = 0.687. (C) Hela cells were co-expressed with pVen-1-flag-p0071 and pVen2-HA-FLCN and fixed after 24 hours. Cells were stained for HA (to identify transfected cells) and α -tubulin (to identify cells in the late stages of cytokinesis). Association was detected by BiFC, displaying a focussed signal at the midzone of a telophase cell.

5.4.5 Loss of folliculin deregulates RhoA signalling/activity

As described previously, p0071 has been reported to regulate RhoA signalling, a common feature of p120 family proteins. As p0071 was required for correct RhoA signalling during cytokinesis and folliculin interacts with p0071 at cell junctions and at the midzone during cytokinesis, it was hypothesised that folliculin might also impinge upon RhoA signalling.

The levels of RhoA protein were tested in three different isogenic cell models. RhoA levels were significantly upregulated in FTC-133 cells expressing vector only compared to those where folliculin had been stably re-expressed. Similarly, in the renal cancer cell model ACHN, stable knockdown of folliculin also resulted in increased levels of RhoA protein. Furthermore, level of folliculin knockdown by stable shRNA was inversely correlated with RhoA levels in a dose-dependent manner. The same effect was observed in HEK293 cells treated with folliculin transient siRNA (see Figure 5.10).

RhoA is a small GTPase which functions as a molecular switch which is inactive when bound to GDP and active when bound to GTP. This switch is controlled by Rho GEFs, GAPs and GDIs as described in Figure 5.2. It was important to confirm if folliculin status influenced cellular RhoA activity as well as cellular levels. To investigate this hypothesis, the G-LISA RhoA activation assay was used, which can be used to determine only the levels of RhoA which are GTP-bound.

In the FTC-133 cell line, the levels of active RhoA were significantly higher (greater than 2 fold increase) in folliculin deficient cells than in those in which folliculin have been re-

expressed (see Figure 5.10). Stable knockdown of folliculin in ACHN cells also caused a significant increase in RhoA activation (~30%) (see Figure 5.10). Results displayed are collated from at least three independent repeats.

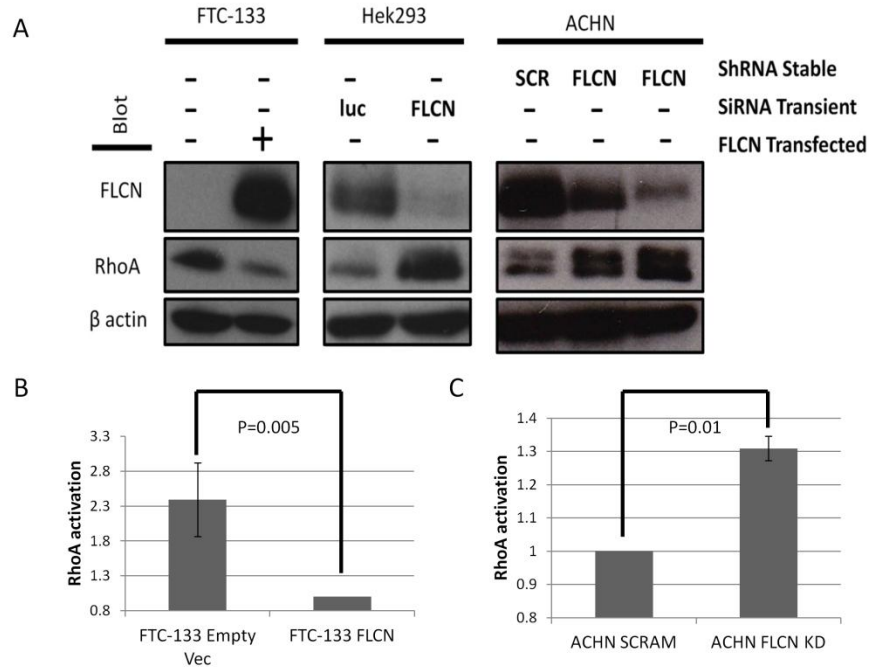


Figure 5.10 Loss of folliculin induces deregulation of RhoA signaling

(A) 3 BHD cell models were tested for levels of RhoA. RhoA levels significantly increased in FTC133 cells (FLCN negative) compared with FLCN re-expressing clone. In both renal cell models Hek293 and ACHN, transient and stable FLCN knockdown respectively, caused an increase in RhoA levels. (B) GTP bound (active) RhoA is increased in FLCN null cells (FTC-133) compared with FLCN re-expressing cells (~2 fold). Results normalised to FLCN expressing FTC-133 cells (C) Active RhoA is increased in ACHN cells with stable FLCN knock down (~30% increase). Repeats normalised to activation of ACHN scrambled control. Error bars represent standard deviation of at least 3 independent repeats. Significance tested with independent Student's T test.

5.4.6 Loss of FLCN causes cytokinesis defects resulting in multinucleation

Wolf *et al.* reported that depletion or overexpression of p0071 resulted in severe cytokinesis defects, inducing a multinucleation phenotype correlated with deregulation of RhoA signalling (Wolf, et al., 2006). As folliculin was located at the midbody during cytokinesis interacting with p0071 and loss of folliculin increased flux through RhoA signalling, it was investigated if folliculin loss might also influence levels of multinucleation. By fixing FTC-133 cells at 50% confluence and staining them with tubulin, the numbers of multinucleated cells were counted in cells deficient for and re-expressing folliculin. In the folliculin deficient FTC-133 cell line, >16% of cells were found to be multinucleated, but reintroduction of folliculin in the FTC-133 cell line significantly reduced this number to ~2% multinucleated cells ($p < 0.005$, T test calculated from three independent repeats) indicating folliculin is required for cells to complete cytokinesis correctly (see Figure 5.11).

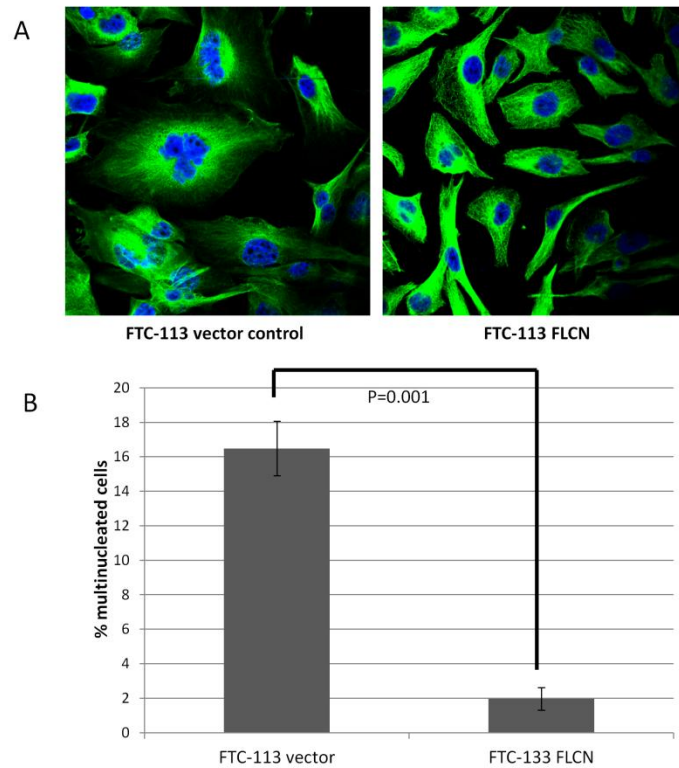


Figure 5.11 Reintroduction of folliculin rescues multinucleation phenotype in FTC-133 cells

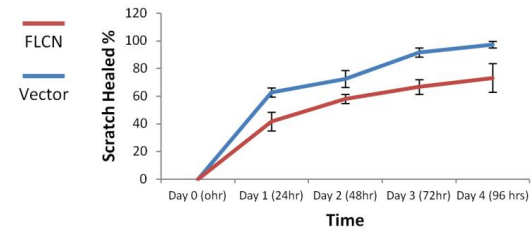
- A) Representative images of FLCN^{+/-} FTC-133 cells stained with tubulin and DAPI.
 (B) Graph of percentage of multinucleated cells in FTC-133 vector expressing and FLCN expressing cells ($p < 0.01$) (at least 400 cells counted from at least 3 independent experiments, tested for significance by independent Student's T test). Error bars represent standard deviation

5.4.7 Re-introduction of FLCN into null metastatic cells ameliorates migratory phenotype

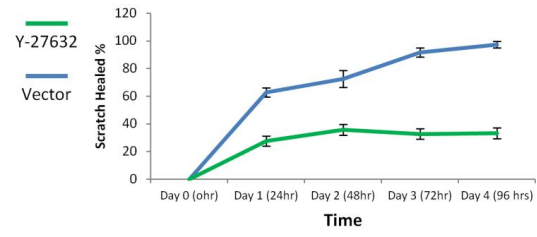
As mentioned in the introduction to this chapter, altered expression and activity of RhoA has been shown to correlate with a number of metastatic diseases. The FTC-133 cell model used in this project is derived from a metastatic thyroid carcinoma and thus provides an interesting model to test whether the dysregulation of RhoA induced by loss of folliculin might be associated with a more migratory phenotype. The *in vitro* scratch assay is a well-developed method for measuring cell migration in culture (Liang, et al., 2007). Cells were grown to full confluence and serum starved (to stop the cells proliferating, so that only migration of cells was tested). A scratch was introduced into the monolayer of cells and the scratch photographed at time point 0 and again every 24 hours until the scratch had healed completely. Folliculin expressing FTC-133 cells migrated significantly more slowly than folliculin deficient (empty vector expressing) cells ($p < 0.05$) (see Figure 5.12 a and c).

The Rho associated kinases ROCK1 and ROCK2 function downstream of RhoA and can be specifically targeted by the compound Y-27632, a well characterised ROCK inhibitor (Liu, et al., 2009). To test if inhibiting signalling downstream of RhoA in folliculin deficient FTC-133 cells might ameliorate the migratory phenotype and phenocopy re-expression of folliculin, FTC cells were treated with 10 μ M Y-27632 every 12 hours. Addition of the ROCK inhibitor to folliculin null cells significantly reduced the migratory ability of the cells ($p < 0.005$) (see Figure 5.12 b and c).

A



B



C

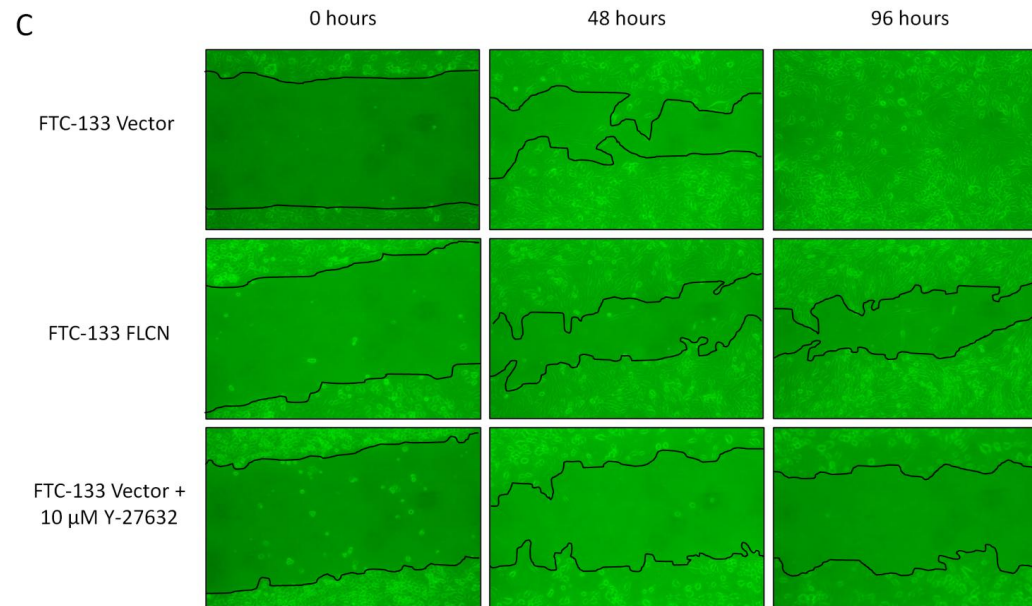


Figure 5.12 FTC-133 cells lacking folliculin are more migratory due to increased RhoA signaling.

A serum starved monolayer of confluent FTC-133 cells was scratched with a sterile pipette and left to migrate for 96 hours. (A) Graph displaying % of scratch healed every 24 hours for FLCN re-expressing FTC-133 cells (Red line) and FTC-133 empty vector expressing cells (Blue line). (B) Graph displaying % of scratch healed for FTC-133 empty vector expressing cells treated with a 12 hourly, 10 uM dose of Y27632 (Rock inhibitor) (Green line) compared with the same cells treated with water control (Blue line). Error bars represent standard deviation calculated from 3 independent experiments.

(C) Representative pictures of migrations at 0, 48 and 96 hours after scratching.

5.4.8 Both knockdown of folliculin and p0071 disrupts cell junctional formation

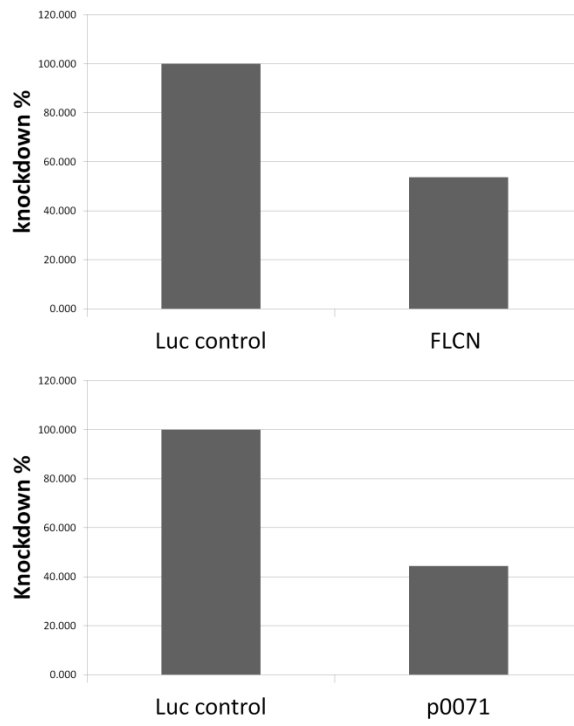
TEER experiments and staining carried out by Ania Straatman-Iwanowska, University College, London

As shown previously, folliculin and p0071 co-localise and interact at cell junctions. To investigate the functional impact of this interaction, the polarised epithelial cell line mIMCD-3 was cultured on Transwell permeable supports. siRNA oligonucleotides designed for *FLCN* and *p0071* produced 46% and 55% transient knockdown respectively at day 4, tested by quantitative real-time PCR (Figure 5.13a). The transepithelial electrical resistance of the cell monolayer (TEER), which tests monolayer integrity, was taken on day 8 once the control cells had become polarised. Cells treated with either *FLCN* or *p0071* siRNA showed significantly reduced TEER at day 8 (*FLCN* knockdown, 52.5% residual TEER $p=0.004$; *p0071* knockdown, 72.1% residual TEER, $p=0.005$) (see Figure 5.13b). As the correct formation of tight junctions is required to cause a trans-epithelial resistance, the results suggested a defect in tight junctional formation when *FLCN* or *p0071* is knocked down.

To test the possible cause of the TEER results, the cells were stained for Claudin-1 (an inter-cellular tight junction component) and ZO-1 (a tight junctional component located on the cytoplasmic surface of intercellular tight junctions). Claudin-1 staining was reduced and disordered in both *FLCN* and *p0071* knockdown cells, however no abnormality was detected for either knockdown in the staining pattern of ZO-1 (see Figure 5.14). It is known that the formation of tight junctions is dependent on the correct formation of adherens junctions, located just below the tight junctions in cell-cell

contacts, so we proceeded to test whether the adherens junction protein E Cadherin was located correctly in the *FLCN* and *p0071* knockdowns. E-Cadherin staining was similarly reduced and disordered in both FLCN and p0071 knockdown cells (see Figure 5.14).

A



B

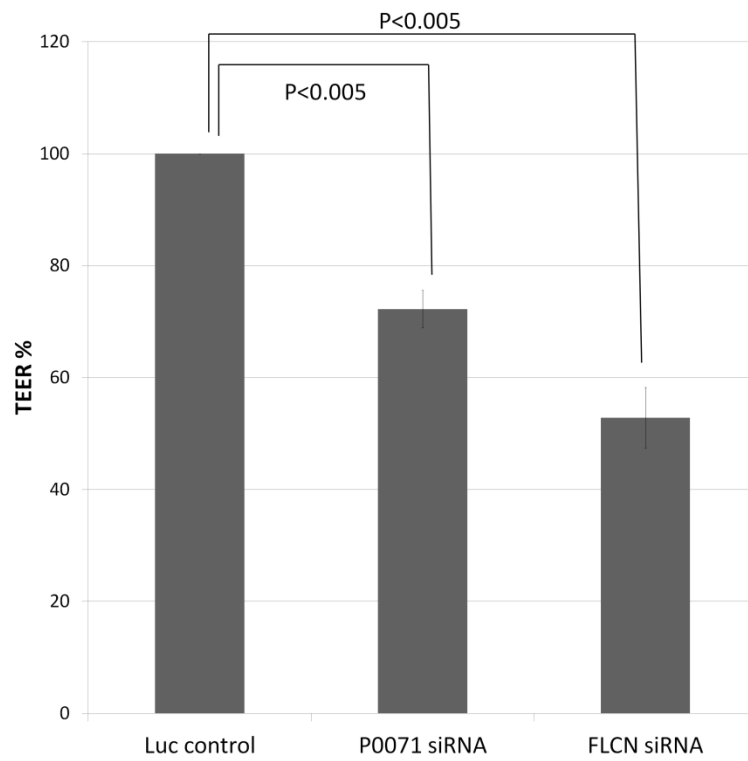


Figure 5.13 TEER of cells with FLCN and p0071

C

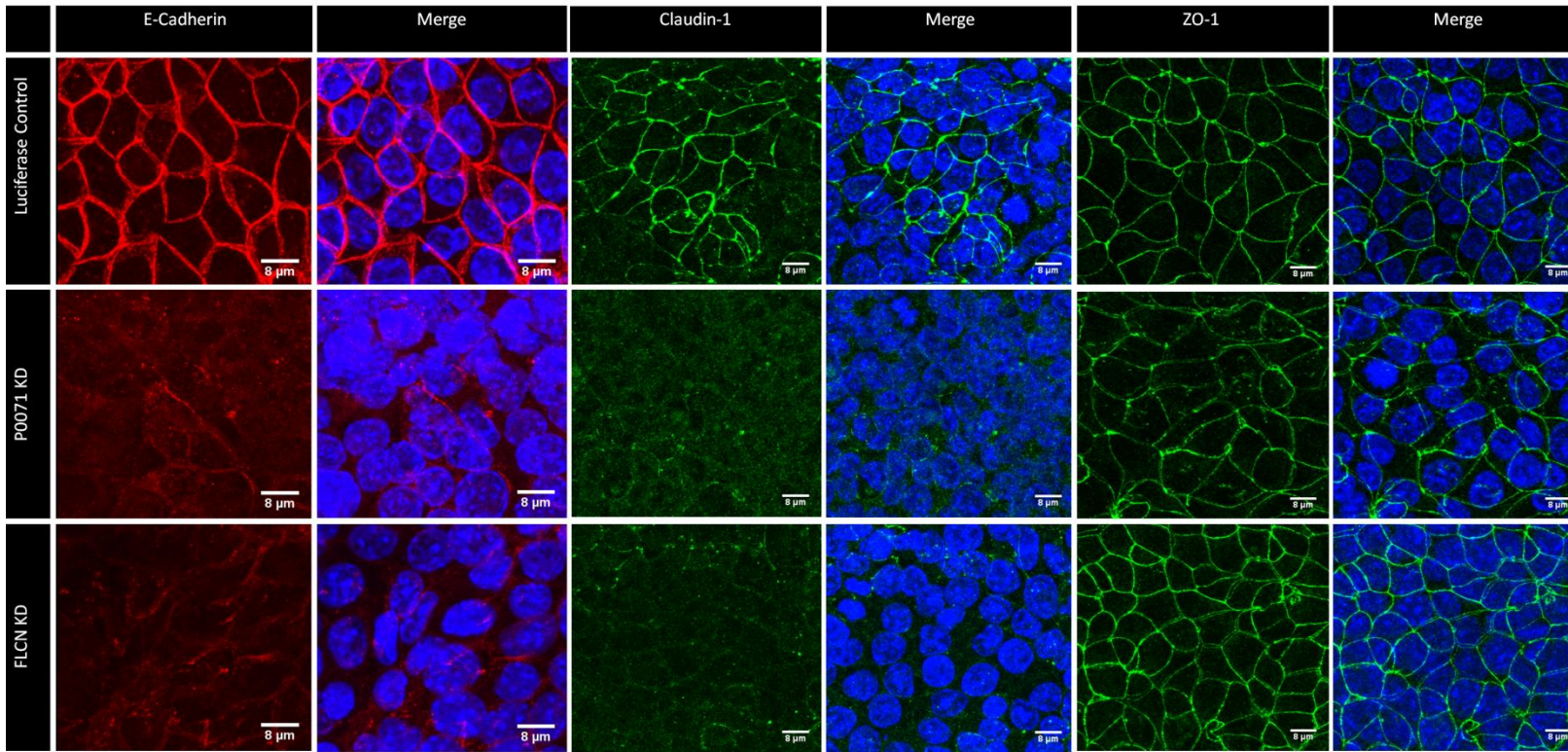


Figure 5.14 Staining for junctional proteins in IMCD-3 cells treated with *FLCN* and *p0071* siRNA

Cell junctional defects in mIMCD-3 cells with reduced FLCN or p0071. Cells were seeded onto transwell supports to induce cell polarisation.

(Figure 5.13) (A) Knockdown of FLCN and p0071 was confirmed by quantitative real-time PCR. (B) There is a significantly reduced trans-epithelial electrical resistance in cells depleted of FLCN or p0071 at day 8 ($p < 0.005$). Experiments were carried out in triplicate and significance tested by independent Student's T test. Error bars represent standard deviation

(Figure 5.14) There is a reduced expression of both E-Cadherin and Claudin-1 at cell junctions in cells treated with FLCN or p0071 siRNA, however ZO-1 staining appears normal.

5.5 Discussion

In order to reveal novel insights into the tumour suppressive mechanisms of folliculin, a yeast-2-hybrid screen was undertaken, and plakophilin 4 (p0071) identified as a potential folliculin interacting protein. Given the reported functions of p0071 in cancer related functions such as cell junctional maintenance and regulation of RhoA signalling, this appeared an interesting interaction to investigate further.

After confirming the interaction between p0071 and folliculin by co-immunoprecipitation analyses, the cellular context of the interaction was defined by immunofluorescence analysis. When both proteins were overexpressed, a co-localisation was clearly observed at cell-cell contacts and at the midbody of cells undergoing late mitosis. The same pattern was observed by staining the endogenous proteins in a number of cell types.

To determine if folliculin and p0071 were indeed interacting at these regions of co-localisation, bimolecular fluorescence complementation analysis (BiFC) was undertaken. BiFC analysis enables direct visualisation of the interaction between folliculin and p0071 in living cells. Both folliculin and p0071 were fused to separate halves of yellow fluorescent protein (YFP) and co-expressed in HeLa cells. BiFC analysis displayed concentrated signal at cell junctions in the interphase cell and at the midbody between dividing cells in late telophase/cytokinesis. BiFC also appeared to show interaction (albeit less strong) at certain points within the cytoplasm. Co-localisation was also observed in the cytoplasm in cells in which both p0071 and folliculin had been overexpressed. The cytoplasmic function of p0071 is yet to be elucidated, and thus this

represents a potentially significant finding. However, due to the lack of obvious co-localisation observed at endogenous levels, it is currently unclear whether these regions of interaction may be only apparent when both proteins are overexpressed and thus requires further investigation.

Previous to this study, few studies had investigated the intracellular localisation of folliculin. While folliculin had not previously been linked to the cell junctions, p0071 and folliculin were found to co-localise and interact at cell-cell contacts. Loss of cell polarity and cell-cell adhesion is a frequent feature of epithelial cancers, linked to both tissue invasion and metastasis and also can occur early in tumourigenesis (Tervonen, et al., 2011). Cancer cell lines often harbour mutations and epigenetic changes which can disrupt epithelial polarity, thus the IMCD-3 mouse normal kidney cell line was used in this study. These cells are widely used to investigate the physiology of epithelial polarisation and are easily polarised by culture on transwell supports.

Knockdown of *FLCN* expression in IMCD-3 cells was associated with a significant reduction in trans-epithelial electrical resistance (TEER) at day 8, indicating the incorrect formation of tight junctions. This effect was phenocopied by knockdown of p0071, suggesting a function role for the interaction between folliculin and p0071 at cell junctions. Consistent with these results, both *FLCN* and *p0071* depleted cells displayed reduced expression and disordered patterns of Claudin-1 tight junction staining. p0071 binds classical cadherins through its armadillo repeat region, and is known to regulate cadherin stability (Hatzfeld, 2005). As the adhesive activity of E-cadherin is required for

the assembly of tight junctions, it was possible that the disruption of Claudin-1 staining might be a result of abnormal E-cadherin localisation. Both *FLCN* and *p0071* depleted cells also showed a reduced and abnormal pattern of E-cadherin staining, thus suggesting both folliculin and p0071 together are required for the maintenance of adherens junctions. This could be an important finding as loss of E-cadherin is frequently observed in epithelial cancers and is part of the epithelial to mesenchymal transition cascade which is a crucial process in a tumours progression to metastasis in certain cancers (Moreno-Bueno, et al., 2008). Moreover, the major clear cell RCC tumour suppressor gene, *VHL*, is associated with downregulation of E-cadherin expression (Evans, et al., 2007).

The maintenance of epithelial polarity requires the specific targeting of proteins to the apical and basolateral membrane domains (Nelson, 2003). p0071 contains a PDZ domain, placing it in a family of proteins which are implicated in establishing epithelial cell polarity (Hatzfeld, 2005). It is therefore not entirely unexpected that knockdown of p0071 induced cell polarity defects. Folliculin deficiency causes similar defects in cell polarity, even in the presence of p0071, thus suggesting the functional importance of the folliculin/p0071 interaction in establishing cell polarity.

As well as interacting at cell-cell contacts, folliculin and p0071 were also found to interact at the midzone of mitotic cells. Disordered cytokinesis is a frequent feature of human cancers and RhoA and its regulators have been demonstrated to be critical for normal cytokinesis (Piekny, et al., 2005). The small GTPase RhoA functions as a molecular switch in a diverse range of cellular processes including cell adhesion, cell

cycle progression and migration (see section 5.1.3). p0071 has been previously shown to regulate RhoA at the midzone, through a direct association with Ect2 (a Rho guanine-nucleotide exchange factor essential for cytokinesis) (Wolf, et al., 2006). The results presented in this chapter show that, in addition to folliculin co-localising with p0071 at the midzone, folliculin deficiency was associated with deregulation of Rho signalling and cytokinesis defects with significantly increased numbers of multinucleated cells. However, the effects of folliculin status on RhoA activation were studied in cells of mixed cell cycle stage. This therefore suggests the possibility that folliculin impinges upon RhoA signalling also in the interphase cell. Efforts to determine the effect of folliculin deficiency on RhoA specifically in mitotic cells was unsuccessful due to difficulties in synchronising the isogenic cell models used in this study. Thus dissection of the exact mechanism of folliculin impact on RhoA signalling in both interphase and dividing cells represents a potentially interesting area for future research.

The role of RhoA in the interphase cell is to induce actin cytoskeletal stress fibres and facilitate cell migration at both the front edge of cells and inducing retraction at the rear edge (Machacek, et al., 2009; Timpson, et al., 2011). RhoA has thus been found to be over-expressed in clinical cancers, being implicated in invasion and metastasis through its role in cell adhesion and migration (Narumiya, et al., 2009). BHD-associated tumours have been previously reported to metastasise (Pavlovich, et al., 2005; Toro, et al., 2008), and therefore the effects of RhoA deregulation on cell migration was investigated in the FTC-133 isogenic *FLCN* cell model described previously in (Lu, et al., 2011). Cells not expressing folliculin migrated significantly more quickly than those expressing folliculin.

To confirm this effect was due to increased RhoA signalling, folliculin null cells were also treated with Y-27632 to inhibit ROCK, a downstream effector of RhoA. Treatment with Y-27632 significantly reduced the migratory phenotype of folliculin null cells. Inhibition of ROCK has been previously shown to reduce cancer cell motility *in vivo* (Wyckoff, et al., 2006) and such, these findings suggest a novel potential therapeutic strategy for treating metastatic BHD renal tumours with deregulated Rho signalling.

In summary, work presented in this chapter has identified a novel folliculin binding partner, plakophilin 4 (p0071), and through investigation of the effects of folliculin loss on previously reported p0071 functions, folliculin inactivation has been linked to loss of epithelial polarity and normal intercellular junction formation, disordered cytokinesis and deregulated RhoA signalling. It is tempting to suggest that these novel folliculin-related cellular pathways are directly implicated in the mechanisms of folliculin tumour suppressor function. These findings also suggest novel potential therapeutic approaches for the treatment of cancer in BHD patients and, in view of the frequent overlap between the pathways implicated in familial and sporadic forms of cancer, provide new avenues of research for both BHD-related and sporadic kidney cancers.

Chapter 6 Discussion

6.1 Summary of thesis

Mutations in the *FLCN* gene are responsible for the Birt Hogg Dubé syndrome of fibrofolliculomas, increased susceptibility to lung cysts, pneumothorax and RCC. Since discovery of the causative gene in 2002, research has focused on elucidation of how mutations in *FLCN* compromise aspects of folliculin function and give rise to these manifestations. While mutations in *FLCN* have now been identified in the vast majority of BHD kindreds, links between genotype and BHD syndrome phenotype have proved harder to identify. Similarly, efforts to uncover the role of folliculin in the cell and the effects of folliculin loss/mutation on intracellular signaling have arguably not yet identified the complete spectrum of folliculin functions.

Identification of genotype-phenotype correlations is very important in aiding the clinical management of “at risk” subgroups of BHD patients. The findings in Chapter 3 of this thesis indicate that patients with a mutation in the mononucleotide tract in *FLCN* exon 11 are at increased risk of colorectal neoplasia. The identification of *FLCN* mutations at this region in sporadic colon cancers adds weight to the argument of an association between BHD syndrome and increased risk of colorectal neoplasia. Further work is required to identify a functional explanation for the apparent relationship between *FLCN* mutations at this region and colorectal cancer risk.

Investigation of the small number of non-truncating *FLCN* mutations which have been reported, aimed to provide insights into functionally important domains of folliculin. Results in Chapter 4 of this thesis indicate there is an evolutionarily important region

within folliculin, spanning codons 100-230, but that pathogenic, non-truncating *FLCN* mutations spread throughout the gene act by destabilising the protein product. This is consistent with the hypothesis that pathogenic mutations in *FLCN* result in deficiency of the entire folliculin protein and that it is likely multiple facets of folliculin function must be compromised to result in BHD syndrome.

0 detailed the identification of a novel folliculin interacting partner (p0071/plakophilin4) and the functional consequences of this interaction. It is my opinion that it is only through unravelling the molecular functions of folliculin within the cell, that the potential for targeted therapeutics for BHD syndrome can be realised. At the start of this project, the first insights into potential folliculin functions were provided by the identification of the association between folliculin and mTOR signalling (Baba, et al., 2006). In more recent years, a number of other signalling pathways have been described which are affected when folliculin is inactivated. These are described below, in the context of the work presented in this thesis.

6.2 Recent breakthroughs in elucidating folliculin function (2008-2012)

6.2.1 Folliculin and HIF signaling

Hypoxia inducible factor (HIF) is a transcription factor which controls many cellular pathways, including energy metabolism, angiogenesis, cell survival and proliferation, and metastasis (Semenza, 2004). Under normal conditions, HIF only becomes functional when tissues become starved of oxygen. However, HIF is also central to the tumour

formation of renal cancers with tumours from patients with *VHL* and *FH* mutations displaying higher levels HIF-mediated signaling (see introduction 1.2.2.3) (Isaacs, et al., 2005; Kaelin, 2005). Folliculin has also been implicated in regulating HIF signaling in a study by (Preston, et al., 2011). Absence of folliculin in UOK257 cells caused upregulation of HIF activity, and increased transcription of HIF target genes. The authors demonstrated that due to the high levels of HIF-mediated gene expression in folliculin null cells, the cells display an altered metabolic phenotype, reflecting a “Warburg effect”, in which the cells favour glycolytic rather than lipid metabolism (Preston, et al., 2011). This is an interesting finding as there has been some success previously in developing targeted therapeutics against HIF targets in VHL disease (see introduction), and provides evidence that altered metabolic function may be driving BHD tumours. However the molecular mechanisms by which folliculin influences HIF activity are yet to be elucidated. In agreement with this hypothesis, (Klomp, et al., 2010) found BHD tumours to show high expression of mitochondria and oxidative phosphorylation associated genes, indicative of mitochondrial dysfunction.

6.2.2 Folliculin and TGF- β signaling

Transforming growth factor- β (TGF- β) is a cytokine which inhibits cell growth and displays apoptotic functions, and thus loss of these effects is often observed in clinical cancers. Interestingly, tumour cells that have lost the growth constraints applied by TGF- β can then later over-produce it to drive metastatic behavior (Siegel and Massague,

2003). The TGF- β signalling pathway functions by TGF- β binding to its receptors on the cell surface and inducing a phosphorylation cascade resulting in the modulation of transcription of TGF- β target genes in the nucleus. Using gene expression microarrays on UOK239 (folliculin null) and folliculin re-expressing cells, (Hong, et al., 2010) identified several critical genes involved in TGF- β signalling to be differentially expressed in the two cell types and also in BHD-associated renal tumours. The link between folliculin and TGF- β was extended by experiments from Cash *et al.*, who demonstrated that folliculin deficient cells exhibit defects in apoptosis correlating with loss of the pro-apoptotic protein Bim. This resulted from reduced Bim transcription associated with the general loss of TGF- β mediated transcription (Cash, et al., 2011).

Thus it appears folliculin is also impinging upon TGF- β signalling, however just as with the folliculin/HIF relationship, the molecular mechanisms of this impact are unclear.

6.2.3 Further investigations of folliculin and mTOR

As described in the introduction to this thesis, folliculin has been previously reported to interact with AMPK, mediated by interaction with FNIP1 and FNIP2 and is thus involved in mTOR signaling (Baba, et al., 2006; Hasumi, et al., 2008). However in the four years since starting the research presented in this thesis, a number of studies have reported contradictory impacts of folliculin on mTOR signaling. In agreement with the research of Takagi *et al.* (which identified FNIP2 as a folliculin interacting protein), a study by Hartman *et al.* showed knockdown of *FLCN* by siRNA in a human cancer cell line to

downregulate signalling through mTORC1 (Hartman, et al., 2009)(Takagi, et al., 2008). This is in direct contrast to the earlier publications which reported the binding of folliculin to FNIP1, that suggested folliculin loss induced mTORC1 upregulation (Baba, et al., 2008; Baba, et al., 2006). Hartman *et al.* also observed reduction of p-S6R (indicating a reduction in mTORC1 signaling) in the renal cysts of mice that were bred as heterozygous knockouts for *FLCN*. These findings were in direct contrast to the homozygous knockout mice developed by Baba *et al.* and Chen *et al.* who reported mTOR upregulation in their mouse models. However another heterozygous knockout mouse for folliculin was reported by Hasumi *et al.* which similarly displayed activation of mTOR signaling in its kidney tumours (Hasumi, et al., 2009)(Baba, et al.,2008; Chen, et al., 2008).

The reasons for these discrepancies are unclear, but a number of explanations have been put forward. It is possible that, *in vivo*, mTOR activation is not a primary consequence of folliculin inactivation, but rather due to activation of kinases upstream of mTOR, for example ERK, Akt and Rsk1 (all reported as upregulated in the kidneys of KSP-Cre driven inactivation of folliculin by Baba *et al.* (2008)). This might also go some way to explaining why mTOR signaling appeared lowered in the tumours of the heterozygote *FLCN* mice described by Hartman *et al.*, which represented early lesions, as such kinases might only be activated later in tumorigenesis.

In possible agreement with this hypothesis, a recent study by Hudon *et al.*, demonstrated that loss of folliculin expression in their heterozygote *FLCN* knockout mouse resulted in

both upregulation and down regulation of mTORC1 signaling in large polycystic renal cysts and smaller single cysts respectively (Hudon, et al., 2010).

It appears clear that that the impact of loss of folliculin in renal cysts/tumours is more complex than affecting the mTORC1 pathway alone, and is likely to be context dependent. In agreement with the findings of Hudon *et al*, I also found no repeatable effects of folliculin re-expression in cell culture (using folliculin null FTC-133 cells) on either mTORC1 or mTORC2 signaling. Neither were there effects associated with the expression of a range of pathogenic mutant folliculin proteins (Chapter 4).

6.2.4 Folliculin interacts with p0071 – implications for further research

In light of these findings, and the failure to identify reliable effects of *FLCN* mutation on the mTOR signaling pathway, further possible folliculin functions were investigated by identification of a novel folliculin binding partner plakophilin 4 (p0071). Folliculin and p0071 interact at both cell junctions and at the midzone during late mitosis, and deficiency of folliculin impacts upon a number of previously reported functions of p0071. Folliculin loss, across a number of cell lines, resulted in dysregulation of RhoA signaling, disordered mitosis, cell polarization and junctional formation. This represents a potentially important finding for the field as p0071 is only the third folliculin binding partner identified. Furthermore, these novel, folliculin-related cellular pathways have the potential to be directly implicated in the mechanisms of folliculin tumour suppressor function.

The molecular link for the phenotypes observed through the interaction of folliculin with p0071, opens up a new avenue of research for the BHD field. It is clear that folliculin is required for p0071 to carry out its normal functions, however the mechanism by which folliculin affects p0071 function is less clear. Folliculin deficiency induced no reliable impact on the cellular levels of p0071, but it remains possible that folliculin is somehow working synergistically with p0071. The molecular basis of this potential synergy remains unknown.

It is currently unclear how folliculin is affecting RhoA signalling, although it appears to be at both the level of transcription and activation. p0071 was reported to affect RhoA signalling at the midbody by binding to, and influencing the activity of the Rho guanine exchange factor (GEF) Ect2 (Wolf, et al., 2006). However, the RhoA activation assays and cell migration assays presented in this thesis suggest folliculin is affecting RhoA activity also in the interphase cell. In the first instance, it is important to dissect the effects of folliculin knockdown on RhoA activity at each stage of the cell cycle, and then investigate how folliculin may be affecting RhoA (by influencing a Rho GEF, GAP or GDI perhaps). It is becoming increasingly clear that the dynamics of RhoA activities are tightly regulated and highly complex, and that the traditional methods of observing activation of Rho GTPases observe only a snap shot of GTP-loading states, while missing the dynamic changes in activation which occur in the time-scale of seconds (Spiering and Hodgson, 2011). It is now becoming possible to detect the activity of Rho GTPases in living cells using fluorescent biosensors (for review see (Spiering and Hodgson, 2011)).

It is possible that by utilising new technologies such as these, the control of RhoA activity by folliculin can be more comprehensively dissected.

The stable knockdown of folliculin in the ACHN line is far from optimal, and such induces only a 30% increase in RhoA signalling (compared to ~130% increase in the FTC-133 null cells compared with folliculin re-expressers). The ACHN cells (kindly donated by Professor Arnim Pause, McGill University, Montreal) are derived from a cancer cell and display multinucleation even in the scrambled control. To determine whether the induction of multinucleation that was observed in the FTC-133 cell model is reliant on folliculin loss alone or if the phenotype requires the background of other alterations present in a cancer cell, it is crucial to develop optimal folliculin knockdowns in normal cells.

The data presented in this thesis shows folliculin to localise to cell contacts and that both folliculin and p0071 together are required for the correct induction of cell junctions in polarised IMCD3 cells. The reduced levels and disordered pattern of E-cadherin and Claudin-1 staining in both p0071 and folliculin deficient cells demonstrate a functional role for folliculin at the cell junction. It is tempting to suggest that disruption of E-Cadherin when folliculin is deficient might relate to the increased metastatic potential of BHD tumour cells described in previous reports (Claessens, et al., 2010a; Pavlovich, et al., 2005; Toro, et al., 2008). VHL loss has been previously linked to epithelial to mesenchymal transition (EMT), largely dependent on HIF- α induced NF-kappaB (Pantuck, et al., 2010), and it thus should be investigated whether folliculin loss also

affects other proteins involved in EMT, and through which pathways it might be exerting its effect. Such pathways would represent novel therapeutic targets for BHD renal tumours.

Folliculin null FTC-133 cells display a more migratory phenotype compared to those re-expressing folliculin. I have demonstrated a potential therapeutic impact of treating folliculin null cells with a ROCK inhibitor, rescuing this phenotype. It would be intriguing to investigate the effects of folliculin and/or p0071 loss in an *in vivo* mouse model, testing Rho pathway inhibition on the metastatic potential of tumour cells which develop. However there is currently no reported evidence of metastasis in any of the BHD mouse models described to date. Rho inhibitors are not currently in clinical trials for treating cancer; however they are currently being researched in mouse models as a proof-of-principle (For Example the Rho inhibitor RhostatinTM and ROCK inhibitor BA-1049 (BioAxone)). In addition, Fasudil (the only clinically available inhibitor of ROCK at present) demonstrates no severe side effects when administered to patients with acute ischemic stroke or stable effort angina, thus highlighting the possibility of safely using ROCK inhibition as a cancer therapy in humans (Kubo, et al., 2008).

6.3 Conclusions

Identifying the molecular mechanisms by which folliculin exerts its tumour suppressor function has proved a challenging task, particularly due to the lack of sequence homology between folliculin and any other known protein. This thesis extends the knowledge of

the functions of folliculin in a number of interesting areas, with the next step for the field being the identification of the precise biochemical functions for this protein, and the mechanisms by which it exerts its reported functions.

In my opinion, these next steps in BHD syndrome research should be to identify and investigate all potential interacting partners and to search for possible patterns in the cellular effects, which might link these interactions. This may provide a clue as to the molecular function of the folliculin protein. Also, it is hoped that ongoing work to identify the crystal structure of folliculin might provide important insights into the biochemical function of this protein within the cell.

Familial cancer syndromes have not provided an attractive target for large-scale drug development programs due to their rare nature; however developments in genomic technologies in the last decade have provided an opportunity for exerting a real impact on the management and treatment of these patients. This can be achieved through a concerted effort of clinicians, geneticists and functional biologists. Clinical studies provide the proper definitions of the syndrome phenotype, which is crucial for informing clinical management and providing better surveillance of affected families. In the case of BHD syndrome where tumours are generally slow developing, this could arguably have singly the greatest impact on reducing BHD mortality. These studies also provide the framework for genetic modelling studies (as described in Chapter 4) by identifying causative mutations, which can provide important insights into how certain genotypes relate to BHD syndrome phenotype, with the potential for the results to directly feed back

into the clinic. Also, the availability of next generation sequencing and whole genome array studies on tumour material has the promise to define the crucial factors driving tumour progression at the genetic level. The extension of genetic studies into molecular biological investigations that provide functional explanations of how the folliculin tumour suppressor exerts its effects and thus how *FLCN* mutations cause increased risk of cancer, make up another crucial facet of BHD syndrome research. It is by understanding the cellular functions of the folliculin protein that a real idea of the factors causing this syndrome can be developed, with the hope that they will provide opportunities for treatment with already available therapeutics. A good example of this is that since the identification of mTOR dysregulation in folliculin deficient cells by Baba *et al.* 2006 and Chen *et al.* 2008, a clinical trial is currently underway investigating the possible effects of rapamycin application on fibrofolliculoma development. Over the next decade, it is a realistic hope that information obtained from functional studies will also translate back into the clinic, to the benefit of BHD syndrome patients.

We are currently at a very interesting period of time in the history of research into cancer. With previously unforeseen technologies, now within the financial grasp of the vast majority of laboratories, the data pooled from next generation sequencing projects will give ever increasing insight into the landscape of the cancer genome in the next decade. It is my opinion that despite such technical advance, it is only through identifying and understanding the cellular pathways which are disrupted in the development of cancer that the enormous power of next generation technologies can really impact upon cancer treatment. Once the mutations identified in these deep sequencing studies can be linked

to deregulation of a specific cellular function/s, the potential for true personalised therapy can be realised.

A key component of these investigations will lie in the identification of the driving factors of tumours caused by inherited mutations within the germline. Research into rare syndromes provides us with not only the syndrome-associated factors driving tumourigenesis, but can also inform research into sporadic forms of the disease, as exemplified by the disruption of VHL associated pathways in a large proportion of sporadic kidney cancers. The findings presented in this thesis provide a number of insights into the pathogenesis of the clinical manifestations of Birt Hogg Dubé syndrome, but also contribute a small but novel impact upon the general mechanisms of renal tumourigenesis, which has the potential to prove relevant to the wider cancer field.

Chapter 7 Appendices

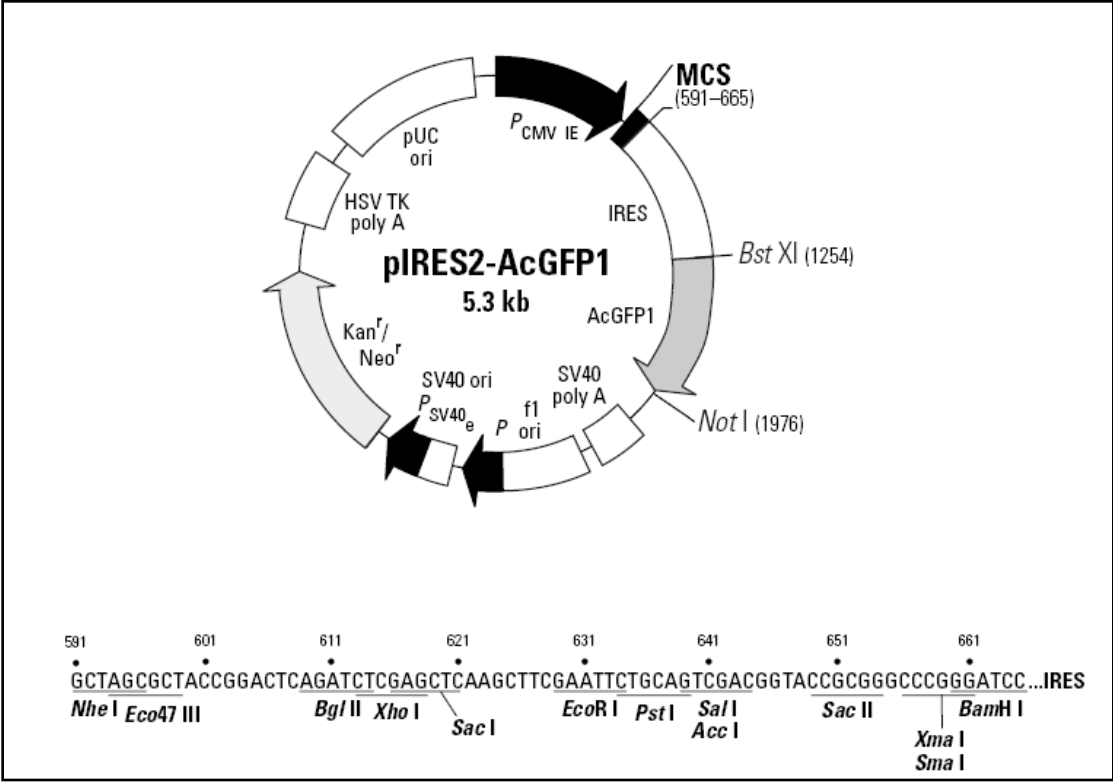
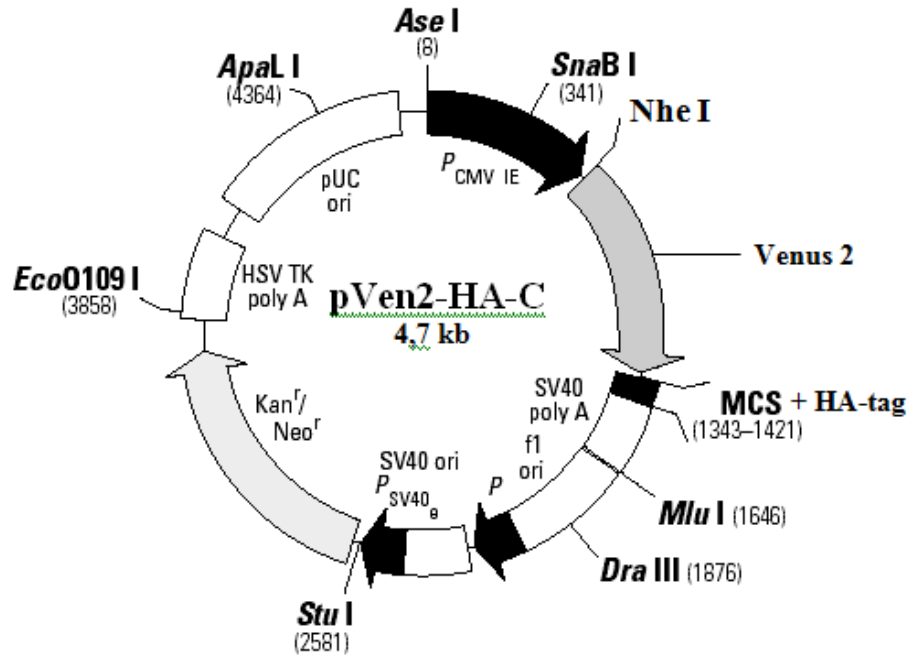


Figure 7.2 p.IRES2-AcGFP1 plasmid map



MCS + HA-tag

AAG AGA TCT ATG GGC TAC CCC TAC GAC GTG CCC GAC TAC GCC
 Bgl II

 Kpn I Apa I BamH I S
 GAA TTC TGC AGT CGA CGG TAC CGC GGG CCC GGG ATC CAC CGG ATC TAG A
 EcoR I Sal I Sac II Xma I Xba I⁺

Figure 7.6 p.Ven2-HA-C plasmid map

7.2 Site-directed mutagenesis primers

<i>Mutation</i>	<i>Primer sequence F</i>	<i>Primer sequence R</i>	<i>T_m</i>
Phe157del	CAGCCACACCTTCATCAAGGACAGCC	GGCTGTCCTTGATGAAGGTGTGGCTG	79.3
Val400Ile	CCCGTGGGCTGCATCCGCATCATCCC	GGGATGATGCGGATGCAGCCCACGGG	80.1
Lys508del	CCTCGTCTGCCTCGAGGAGTGGATG	CATCCACTCCTCGAGGCAGACGAGG	80.9
Glu510del	GTCTGCCTCAAGGAGTGGATGAACAAAGTG	CACTTTGTTCATCCACTCCTTGAGGCAGAC	79.5
His429ProfsX27	CACGTGCAGATCCCCCCCCACGTGCTCTC	GAGAGCACGTGGGGGGGGGATCTGCACGTG	87.0
Ala204X	GATGAGCTCCAGGCAAGTAGCTCAAGTGTTGAGGC	GCCTCAAACACCTTGAGCTACTTGCCCTGGAGTCATC	81.3
Arg362Cys	GGGTGCCCTTCTTTCTGCATGCTGGCCTGGC	GCCAGGCCAGCATGCAGAAAGAAGGGGCACCC	84.5
His255Pro	GTGGGCGTGCCTGCCACCTCCTTTGCC	GGCAAAGGAGGTGGGCAGGCACGCCAC	82.5

Table 7.1 Site-directed mutagenesis primers

Chapter 8 References

1993. Identification and characterization of the tuberous sclerosis gene on chromosome 16. *Cell* 75:1305-15.
- Al-Tassan N, Chmiel NH, Maynard J, Fleming N, Livingston AL, Williams GT, Hodges AK, Davies DR, David SS, Sampson JR and others. 2002. Inherited variants of MYH associated with somatic G:C-->T:A mutations in colorectal tumors. *Nature genetics* 30:227-32.
- Alberici P, Fodde R. 2006. The role of the APC tumor suppressor in chromosomal instability. *Genome dynamics* 1:149-70.
- Anastasiadis PZ, Moon SY, Thoreson MA, Mariner DJ, Crawford HC, Zheng Y, Reynolds AB. 2000. Inhibition of RhoA by p120 catenin. *Nature cell biology* 2:637-44.
- Baba M, Furihata M, Hong SB, Tessarollo L, Haines DC, Southon E, Patel V, Igarashi P, Alvord WG, Leighty R and others. 2008. Kidney-targeted Birt-Hogg-Dube gene inactivation in a mouse model: Erk1/2 and Akt-mTOR activation, cell hyperproliferation, and polycystic kidneys. *Journal of the National Cancer Institute* 100:140-54.
- Baba M, Hong SB, Sharma N, Warren MB, Nickerson ML, Iwamatsu A, Esposito D, Gillette WK, Hopkins RF, 3rd, Hartley JL and others. 2006. Folliculin encoded by the BHD gene interacts with a binding protein, FNIP1, and AMPK, and is involved in AMPK and mTOR signaling. *Proceedings of the National Academy of Sciences of the United States of America* 103:15552-7.
- Bazensky I, Shoobridge-Moran C, Yoder LH. 2007. Colorectal cancer: an overview of the epidemiology, risk factors, symptoms, and screening guidelines. *Medsurg Nurs* 16:46-51; quiz 52.
- Benhammou JN, Vocke CD, Santani A, Schmidt LS, Baba M, Seyama K, Wu X, Korolevich S, Nathanson KL, Stolle CA and others. 2011. Identification of intragenic deletions and duplication in the FLCN gene in Birt-Hogg-Dube syndrome. *Genes Chromosomes Cancer* 50:466-77.
- Bessis D, Giraud S, Richard S. 2006. A novel familial germline mutation in the initiator codon of the BHD gene in a patient with Birt-Hogg-Dube syndrome. *Br J Dermatol* 155:1067-9.
- Birt AR, Hogg GR, Dube WJ. 1977. Hereditary multiple fibrofolliculomas with trichodiscomas and acrochordons. *Archives of dermatology* 113:1674-7.

- Boland CR, Thibodeau SN, Hamilton SR, Sidransky D, Eshleman JR, Burt RW, Meltzer SJ, Rodriguez-Bigas MA, Fodde R, Ranzani GN and others. 1998. A National Cancer Institute Workshop on Microsatellite Instability for cancer detection and familial predisposition: development of international criteria for the determination of microsatellite instability in colorectal cancer. *Cancer research* 58:5248-57.
- Bonsdorff TB, Jansen JH, Lingaas F. 2008. Second hits in the FLCN gene in a hereditary renal cancer syndrome in dogs. *Mamm Genome* 19:121-6.
- Bonsdorff TB, Jansen JH, Thomassen RF, Lingaas F. 2009. Loss of heterozygosity at the FLCN locus in early renal cystic lesions in dogs with renal cystadenocarcinoma and nodular dermatofibrosis. *Mamm Genome* 20:315-20.
- Borkowska J, Schwartz RA, Kotulska K, Jozwiak S. 2011. Tuberous sclerosis complex: tumors and tumorigenesis. *International journal of dermatology* 50:13-20.
- Bottaro DP, Rubin JS, Faletto DL, Chan AM, Kmieciak TE, Vande Woude GF, Aaronson SA. 1991. Identification of the hepatocyte growth factor receptor as the c-met proto-oncogene product. *Science (New York, N.Y)* 251:802-4.
- Bromberg Y, Rost B. 2007. SNAP: predict effect of non-synonymous polymorphisms on function. *Nucleic acids research* 35:3823-35.
- Burridge K, Wennerberg K. 2004. Rho and Rac take center stage. *Cell* 116:167-79.
- Cahill DP, Lengauer C, Yu J, Riggins GJ, Willson JK, Markowitz SD, Kinzler KW, Vogelstein B. 1998. Mutations of mitotic checkpoint genes in human cancers. *Nature* 392:300-3.
- Capaldo CT, Macara IG. 2007. Depletion of E-cadherin disrupts establishment but not maintenance of cell junctions in Madin-Darby canine kidney epithelial cells. *Mol Biol Cell* 18:189-200.
- Cargill M, Altshuler D, Ireland J, Sklar P, Ardlie K, Patil N, Shaw N, Lane CR, Lim EP, Kalyanaraman N and others. 1999. Characterization of single-nucleotide polymorphisms in coding regions of human genes. *Nature genetics* 22:231-8.

- Cash TP, Gruber JJ, Hartman TR, Henske EP, Simon MC. 2011. Loss of the Birt-Hogg-Dube tumor suppressor results in apoptotic resistance due to aberrant TGFbeta-mediated transcription. *Oncogene* 30:2534-46.
- Chen J, Futami K, Petillo D, Peng J, Wang P, Knol J, Li Y, Khoo SK, Huang D, Qian CN and others. 2008. Deficiency of FLCN in mouse kidney led to development of polycystic kidneys and renal neoplasia. *PloS one* 3:e3581.
- Chen J, Lui WO, Vos MD, Clark GJ, Takahashi M, Schoumans J, Khoo SK, Petillo D, Lavery T, Sugimura J and others. 2003. The t(1;3) breakpoint-spanning genes LSAMP and NORE1 are involved in clear cell renal cell carcinomas. *Cancer Cell* 4:405-13.
- Cheng L, Zhang S, MacLennan GT, Lopez-Beltran A, Montironi R. 2009. Molecular and cytogenetic insights into the pathogenesis, classification, differential diagnosis, and prognosis of renal epithelial neoplasms. *Hum Pathol* 40:10-29.
- Chun MG, Hanahan D. 2010. Genetic deletion of the desmosomal component desmoplakin promotes tumor microinvasion in a mouse model of pancreatic neuroendocrine carcinogenesis. *PLoS Genet* 6:
- Chung JY, Ramos-Caro FA, Beers B, Ford MJ, Flowers F. 1996. Multiple lipomas, angioliipomas, and parathyroid adenomas in a patient with Birt-Hogg-Dube syndrome. *International journal of dermatology* 35:365-7.
- Claessens T, Weppler SA, van Geel M, Creytens D, Vreeburg M, Wouters B, van Steensel MA. 2010a. Neuroendocrine carcinoma in a patient with Birt-Hogg-Dube syndrome. *Nat Rev Urol* 7:583-7.
- Claessens T, Weppler SA, van Geel M, Creytens D, Vreeburg M, Wouters B, van Steensel MAM. 2010b. Neuroendocrine carcinoma in a patient with Birt-Hogg-Dube syndrome. *Nat Rev Urol* 7:583-587.
- Clevers H. 2006. Wnt/beta-catenin signaling in development and disease. *Cell* 127:469-80.
- Costa LJ, Drabkin HA. 2007. Renal cell carcinoma: new developments in molecular biology and potential for targeted therapies. *Oncologist* 12:1404-15.
- da Silva NF, Gentle D, Hesson LB, Morton DG, Latif F, Maher ER. 2003. Analysis of the Birt-Hogg-Dube (BHD) tumour suppressor gene in sporadic renal cell carcinoma and colorectal cancer. *J Med Genet* 40:820-4.

- de la Chapelle A. 2004. Genetic predisposition to colorectal cancer. *Nat Rev Cancer* 4:769-80.
- Delva E, Tucker DK, Kowalczyk AP. 2009. The desmosome. *Cold Spring Harb Perspect Biol* 1:a002543.
- Dusek RL, Attardi LD. 2011. Desmosomes: new perpetrators in tumour suppression. *Nat Rev Cancer* 11:317-23.
- Edgar RC. 2004. MUSCLE: a multiple sequence alignment method with reduced time and space complexity. *BMC Bioinformatics* 5:113.
- Escudier B, Eisen T, Stadler WM, Szczylik C, Oudard S, Siebels M, Negrier S, Chevreau C, Solska E, Desai AA and others. 2007a. Sorafenib in advanced clear-cell renal-cell carcinoma. *The New England journal of medicine* 356:125-34.
- Escudier B, Pluzanska A, Koralewski P, Ravaud A, Bracarda S, Szczylik C, Chevreau C, Filipek M, Melichar B, Bajetta E and others. 2007b. Bevacizumab plus interferon alfa-2a for treatment of metastatic renal cell carcinoma: a randomised, double-blind phase III trial. *Lancet* 370:2103-11.
- Evans AJ, Russell RC, Roche O, Burry TN, Fish JE, Chow VW, Kim WY, Saravanan A, Maynard MA, Gervais ML and others. 2007. VHL promotes E2 box-dependent E-cadherin transcription by HIF-mediated regulation of SIP1 and snail. *Mol Cell Biol* 27:157-69.
- Fearon ER, Vogelstein B. 1990. A genetic model for colorectal tumorigenesis. *Cell* 61:759-67.
- Fodde R, Kuipers J, Rosenberg C, Smits R, Kielman M, Gaspar C, van Es JH, Breukel C, Wiegant J, Giles RH and others. 2001. Mutations in the APC tumour suppressor gene cause chromosomal instability. *Nature cell biology* 3:433-8.
- Franke G, Bausch B, Hoffmann MM, Cybulla M, Wilhelm C, Kohlhase J, Scherer G, Neumann HP. 2009. Alu-Alu recombination underlies the vast majority of large VHL germline deletions: Molecular characterization and genotype-phenotype correlations in VHL patients. *Human mutation* 30:776-86.
- Frohlich BA, Zeitz C, Matyas G, Alkadhi H, Tuor C, Berger W, Russi EW. 2008. Novel mutations in the folliculin gene associated with spontaneous pneumothorax. *Eur Respir J* 32:1316-20.
- Fujishita T, Aoki K, Lane HA, Aoki M, Taketo MM. 2008. Inhibition of the mTORC1 pathway suppresses intestinal polyp formation and reduces

- mortality in ApcDelta716 mice. *Proceedings of the National Academy of Sciences of the United States of America* 105:13544-9.
- Gad S, Lefevre SH, Khoo SK, Giraud S, Vieillefond A, Vasiliu V, Ferlicot S, Molinie V, Denoux Y, Thiounn N and others. 2007. Mutations in BHD and TP53 genes, but not in HNF1beta gene, in a large series of sporadic chromophobe renal cell carcinoma. *Br J Cancer* 96:336-40.
- Gallou C, Joly D, Mejean A, Staroz F, Martin N, Tarlet G, Orfanelli MT, Bouvier R, Droz D, Chretien Y and others. 1999. Mutations of the VHL gene in sporadic renal cell carcinoma: definition of a risk factor for VHL patients to develop an RCC. *Human mutation* 13:464-75.
- Gao X, Zhang Y, Arrazola P, Hino O, Kobayashi T, Yeung RS, Ru B, Pan D. 2002. Tsc tumour suppressor proteins antagonize amino-acid-TOR signalling. *Nature cell biology* 4:699-704.
- Garami A, Zwartkruis FJ, Nobukuni T, Joaquin M, Roccio M, Stocker H, Kozma SC, Hafen E, Bos JL, Thomas G. 2003. Insulin activation of Rheb, a mediator of mTOR/S6K/4E-BP signaling, is inhibited by TSC1 and 2. *Mol Cell* 11:1457-66.
- Garcia-Mata R, Boulter E, Burridge K. 2011. The 'invisible hand': regulation of RHO GTPases by RHOGDIs. *Nat Rev Mol Cell Biol* 12:493-504.
- Gatalica Z, Torlakovic E. 2008. Pathology of the hereditary colorectal carcinoma. *Familial cancer* 7:15-26.
- Gemmill RM, Bemis LT, Lee JP, Sozen MA, Baron A, Zeng C, Erickson PF, Hooper JE, Drabkin HA. 2002. The TRC8 hereditary kidney cancer gene suppresses growth and functions with VHL in a common pathway. *Oncogene* 21:3507-16.
- Gemmill RM, West JD, Boldog F, Tanaka N, Robinson LJ, Smith DI, Li F, Drabkin HA. 1998. The hereditary renal cell carcinoma 3;8 translocation fuses FHIT to a patched-related gene, TRC8. *Proceedings of the National Academy of Sciences of the United States of America* 95:9572-7.
- Glotzer M. 2005. The molecular requirements for cytokinesis. *Science (New York, N.Y)* 307:1735-9.
- Graham RB, Nolasco M, Peterlin B, Garcia CK. 2005. Nonsense mutations in folliculin presenting as isolated familial spontaneous pneumothorax in adults. *American journal of respiratory and critical care medicine* 172:39-44.

- Gryfe R. 2009. Inherited colorectal cancer syndromes. *Clin Colon Rectal Surg* 22:198-208.
- Guertin DA, Sabatini DM. 2005. An expanding role for mTOR in cancer. *Trends Mol Med* 11:353-61.
- Gumbiner BM. 2005. Regulation of cadherin-mediated adhesion in morphogenesis. *Nat Rev Mol Cell Biol* 6:622-34.
- Gunji Y, Akiyoshi T, Sato T, Kurihara M, Tominaga S, Takahashi K, Seyama K. 2007. Mutations of the Birt Hogg Dube gene in patients with multiple lung cysts and recurrent pneumothorax. *J Med Genet* 44:588-93.
- Hagenkord JM, Gatalica Z, Jonasch E, Monzon FA. 2011. Clinical genomics of renal epithelial tumors. *Cancer Genet* 204:285-97.
- Hanahan D, Weinberg RA. 2011. Hallmarks of cancer: the next generation. *Cell* 144:646-74.
- Hartman TR, Nicolas E, Klein-Szanto A, Al-Saleem T, Cash TP, Simon MC, Henske EP. 2009. The role of the Birt-Hogg-Dube protein in mTOR activation and renal tumorigenesis. *Oncogene* 28:1594-604.
- Hartsock A, Nelson WJ. 2008. Adherens and tight junctions: structure, function and connections to the actin cytoskeleton. *Biochim Biophys Acta* 1778:660-9.
- Hasumi H, Baba M, Hong SB, Hasumi Y, Huang Y, Yao M, Valera VA, Linehan WM, Schmidt LS. 2008. Identification and characterization of a novel folliculin-interacting protein FNIP2. *Gene* 415:60-7.
- Hasumi Y, Baba M, Ajima R, Hasumi H, Valera VA, Klein ME, Haines DC, Merino MJ, Hong SB, Yamaguchi TP and others. 2009. Homozygous loss of BHD causes early embryonic lethality and kidney tumor development with activation of mTORC1 and mTORC2. *Proceedings of the National Academy of Sciences of the United States of America* 106:18722-7.
- Hatzfeld M. 2005. The p120 family of cell adhesion molecules. *Eur J Cell Biol* 84:205-14.
- Hatzfeld M, Green KJ, Sauter H. 2003. Targeting of p0071 to desmosomes and adherens junctions is mediated by different protein domains. *J Cell Sci* 116:1219-33.
- Hatzfeld M, Nachtsheim C. 1996. Cloning and characterization of a new armadillo family member, p0071, associated with the junctional

- plaque: evidence for a subfamily of closely related proteins. *J Cell Sci* 109 (Pt 11):2767-78.
- Hay N, Sonenberg N. 2004. Upstream and downstream of mTOR. *Genes Dev* 18:1926-45.
- Hong SB, Oh H, Valera VA, Stull J, Ngo DT, Baba M, Merino MJ, Linehan WM, Schmidt LS. 2010. Tumor suppressor FLCN inhibits tumorigenesis of a FLCN-null renal cancer cell line and regulates expression of key molecules in TGF-beta signaling. *Mol Cancer* 9:160.
- Hornstein OP. 1976. Generalized dermal perifollicular fibromas with polyps of the colon. *Hum Genet* 33:193-7.
- Hudon V, Sabourin S, Dydensborg AB, Kottis V, Ghazi A, Paquet M, Crosby K, Pomerleau V, Uetani N, Pause A. 2010. Renal tumour suppressor function of the Birt-Hogg-Dube syndrome gene product folliculin. *J Med Genet* 47:182-9.
- Iliopoulos O, Kibel A, Gray S, Kaelin WG, Jr. 1995. Tumour suppression by the human von Hippel-Lindau gene product. *Nat Med* 1:822-6.
- Iliopoulos O, Ohh M, Kaelin WG, Jr. 1998. pVHL19 is a biologically active product of the von Hippel-Lindau gene arising from internal translation initiation. *Proceedings of the National Academy of Sciences of the United States of America* 95:11661-6.
- Imai K, Yamamoto H. 2008. Carcinogenesis and microsatellite instability: the interrelationship between genetics and epigenetics. *Carcinogenesis* 29:673-80.
- Inoki K, Zhu T, Guan KL. 2003. TSC2 mediates cellular energy response to control cell growth and survival. *Cell* 115:577-90.
- Isaacs JS, Jung YJ, Mole DR, Lee S, Torres-Cabala C, Chung YL, Merino M, Trepel J, Zbar B, Toro J and others. 2005. HIF overexpression correlates with biallelic loss of fumarate hydratase in renal cancer: novel role of fumarate in regulation of HIF stability. *Cancer Cell* 8:143-53.
- Ishizaki T, Uehata M, Tamechika I, Keel J, Nonomura K, Maekawa M, Narumiya S. 2000. Pharmacological properties of Y-27632, a specific inhibitor of rho-associated kinases. *Mol Pharmacol* 57:976-83.
- Jaffe AB, Hall A. 2005. Rho GTPases: biochemistry and biology. *Annu Rev Cell Dev Biol* 21:247-69.

- Jefferson JJ, Leung CL, Liem RK. 2004. Plakins: goliaths that link cell junctions and the cytoskeleton. *Nat Rev Mol Cell Biol* 5:542-53.
- Jemal A, Thomas A, Murray T, Thun M. 2002. Cancer statistics, 2002. *CA Cancer J Clin* 52:23-47.
- Kaelin WG, Jr. 2005. The von Hippel-Lindau protein, HIF hydroxylation, and oxygen sensing. *Biochem Biophys Res Commun* 338:627-38.
- Kaelin WG, Jr. 2009. Treatment of kidney cancer: insights provided by the VHL tumor-suppressor protein. *Cancer* 115:2262-72.
- Kahnoski K, Khoo SK, Nassif NT, Chen J, Lobo GP, Segelov E, Teh BT. 2003. Alterations of the Birt-Hogg-Dube gene (BHD) in sporadic colorectal tumours. *J Med Genet* 40:511-5.
- Karlsson R, Pedersen ED, Wang Z, Brakebusch C. 2009. Rho GTPase function in tumorigenesis. *Biochim Biophys Acta* 1796:91-8.
- Keil R, Kiessling C, Hatzfeld M. 2009. Targeting of p0071 to the midbody depends on KIF3. *J Cell Sci* 122:1174-83.
- Keil R, Wolf A, Huttelmaier S, Hatzfeld M. 2007. Beyond regulation of cell adhesion: local control of RhoA at the cleavage furrow by the p0071 catenin. *Cell Cycle* 6:122-7.
- Kerppola TK. 2008. Bimolecular fluorescence complementation (BiFC) analysis as a probe of protein interactions in living cells. *Annu Rev Biophys* 37:465-87.
- Khoo SK, Bradley M, Wong FK, Hedblad MA, Nordenskjold M, Teh BT. 2001. Birt-Hogg-Dube syndrome: mapping of a novel hereditary neoplasia gene to chromosome 17p12-q11.2. *Oncogene* 20:5239-42.
- Khoo SK, Giraud S, Kahnoski K, Chen J, Motorna O, Nickolov R, Binet O, Lambert D, Friedel J, Levy R and others. 2002. Clinical and genetic studies of Birt-Hogg-Dube syndrome. *J Med Genet* 39:906-12.
- Khoo SK, Kahnoski K, Sugimura J, Petillo D, Chen J, Shockley K, Ludlow J, Knapp R, Giraud S, Richard S and others. 2003. Inactivation of BHD in sporadic renal tumors. *Cancer research* 63:4583-7.
- Kim HJ, Shen SS, Ayala AG, Ro JY, Truong LD, Alvarez K, Bridge JA, Gatalica Z, Hagenkord JM, Gonzalez-Berjon JM and others. 2009. Virtual-karyotyping with SNP microarrays in morphologically challenging renal cell neoplasms: a practical and useful diagnostic modality. *The American journal of surgical pathology* 33:1276-86.

- Kim TY, Lee KH, Chang S, Chung C, Lee HW, Yim J, Kim TK. 2003. Oncogenic potential of a dominant negative mutant of interferon regulatory factor 3. *The Journal of biological chemistry* 278:15272-8.
- Kinzler KW, Nilbert MC, Vogelstein B, Bryan TM, Levy DB, Smith KJ, Preisinger AC, Hamilton SR, Hedge P, Markham A and others. 1991. Identification of a gene located at chromosome 5q21 that is mutated in colorectal cancers. *Science (New York, N.Y)* 251:1366-70.
- Klomp JA, Petillo D, Niemi NM, Dykema KJ, Chen J, Yang XJ, Saaf A, Zickert P, Aly M, Bergerheim U and others. 2010. Birt-Hogg-Dube renal tumors are genetically distinct from other renal neoplasias and are associated with up-regulation of mitochondrial gene expression. *BMC Med Genomics* 3:59.
- Knudson AG, Jr. 1971. Mutation and cancer: statistical study of retinoblastoma. *Proceedings of the National Academy of Sciences of the United States of America* 68:820-3.
- Kovacs G, Akhtar M, Beckwith BJ, Bugert P, Cooper CS, Delahunt B, Eble JN, Fleming S, Ljungberg B, Medeiros LJ and others. 1997. The Heidelberg classification of renal cell tumours. *The Journal of pathology* 183:131-3.
- Kovacs G, Fuzesi L, Emanuel A, Kung HF. 1991. Cytogenetics of papillary renal cell tumors. *Genes Chromosomes Cancer* 3:249-55.
- Kubo T, Yamaguchi A, Iwata N, Yamashita T. 2008. The therapeutic effects of Rho-ROCK inhibitors on CNS disorders. *Ther Clin Risk Manag* 4:605-15.
- Latif F, Tory K, Gnarr J, Yao M, Duh FM, Orcutt ML, Stackhouse T, Kuzmin I, Modi W, Geil L and others. 1993. Identification of the von Hippel-Lindau disease tumor suppressor gene. *Science (New York, N.Y)* 260:1317-20.
- Laurila K, Vihinen M. 2009. Prediction of disease-related mutations affecting protein localization. *BMC Genomics* 10:122.
- Li FY, Lai MD. 2009. Colorectal cancer, one entity or three. *J Zhejiang Univ Sci B* 10:219-29.
- Li J, Wang J, Jiao H, Liao J, Xu X. 2010. Cytokinesis and cancer: Polo loves ROCK'n' Rho(A). *J Genet Genomics* 37:159-72.
- Li WH. 1993. Unbiased estimation of the rates of synonymous and nonsynonymous substitution. *J Mol Evol* 36:96-9.

- Liang CC, Park AY, Guan JL. 2007. In vitro scratch assay: a convenient and inexpensive method for analysis of cell migration in vitro. *Nat Protoc* 2:329-33.
- Lim DH, Rehal PK, Nahorski MS, Macdonald F, Claessens T, Van Geel M, Gijezen L, Gille JJ, Giraud S, Richard S and others. 2010. A new locus-specific database (LSDB) for mutations in the folliculin (FLCN) gene. *Human mutation* 31:E1043-51.
- Linehan WM, Pinto PA, Bratslavsky G, Pfaffenroth E, Merino M, Vocke CD, Toro JR, Bottaro D, Neckers L, Schmidt LS and others. 2009. Hereditary kidney cancer: unique opportunity for disease-based therapy. *Cancer* 115:2252-61.
- Lingaas F, Comstock KE, Kirkness EF, Sorensen A, Aarskaug T, Hitte C, Nickerson ML, Moe L, Schmidt LS, Thomas R and others. 2003. A mutation in the canine BHD gene is associated with hereditary multifocal renal cystadenocarcinoma and nodular dermatofibrosis in the German Shepherd dog. *Human molecular genetics* 12:3043-53.
- Liu S, Goldstein RH, Scepansky EM, Rosenblatt M. 2009. Inhibition of rho-associated kinase signaling prevents breast cancer metastasis to human bone. *Cancer research* 69:8742-51.
- Lium B, Moe L. 1985. Hereditary multifocal renal cystadenocarcinomas and nodular dermatofibrosis in the German shepherd dog: macroscopic and histopathologic changes. *Vet Pathol* 22:447-55.
- Livingston RJ, von Niederhausern A, Jegga AG, Crawford DC, Carlson CS, Rieder MJ, Gowrisankar S, Aronow BJ, Weiss RB, Nickerson DA. 2004. Pattern of sequence variation across 213 environmental response genes. *Genome Res* 14:1821-31.
- Logan CY, Nusse R. 2004. The Wnt signaling pathway in development and disease. *Annu Rev Cell Dev Biol* 20:781-810.
- Lu X, Wei W, Fenton J, Nahorski MS, Rabai E, Reiman A, Seabra L, Nagy Z, Latif F, Maher ER. 2011. Therapeutic targeting the loss of the birt-hogg-dube suppressor gene. *Mol Cancer Ther* 10:80-9.
- Lynch HT, de la Chapelle A. 2003. Hereditary colorectal cancer. *The New England journal of medicine* 348:919-32.
- Machacek M, Hodgson L, Welch C, Elliott H, Pertz O, Nalbant P, Abell A, Johnson GL, Hahn KM, Danuser G. 2009. Coordination of Rho GTPase activities during cell protrusion. *Nature* 461:99-103.

- Maher ER. 2004. Von Hippel-Lindau disease. *Current molecular medicine* 4:833-42.
- Maher ER. 2011. Genetics of familial renal cancers. *Nephron Exp Nephrol* 118:e21-6.
- Maher ER, Iselius L, Yates JR, Littler M, Benjamin C, Harris R, Sampson J, Williams A, Ferguson-Smith MA, Morton N. 1991. Von Hippel-Lindau disease: a genetic study. *J Med Genet* 28:443-7.
- Maher ER, Neumann HP, Richard S. 2011. von Hippel-Lindau disease: a clinical and scientific review. *Eur J Hum Genet* 19:617-23.
- Malkhosyan S, Rampino N, Yamamoto H, Perucho M. 1996. Frameshift mutator mutations. *Nature* 382:499-500.
- Matsui T, Amano M, Yamamoto T, Chihara K, Nakafuku M, Ito M, Nakano T, Okawa K, Iwamatsu A, Kaibuchi K. 1996. Rho-associated kinase, a novel serine/threonine kinase, as a putative target for small GTP binding protein Rho. *EMBO J* 15:2208-16.
- Maxwell PH, Wiesener MS, Chang GW, Clifford SC, Vaux EC, Cockman ME, Wykoff CC, Pugh CW, Maher ER, Ratcliffe PJ. 1999. The tumour suppressor protein VHL targets hypoxia-inducible factors for oxygen-dependent proteolysis. *Nature* 399:271-5.
- McCubrey JA, Steelman LS, Chappell WH, Abrams SL, Wong EW, Chang F, Lehmann B, Terrian DM, Milella M, Tafuri A and others. 2007. Roles of the Raf/MEK/ERK pathway in cell growth, malignant transformation and drug resistance. *Biochim Biophys Acta* 1773:1263-84.
- Menko FH, van Steensel MA, Giraud S, Friis-Hansen L, Richard S, Ungari S, Nordenskjold M, Hansen TV, Solly J, Maher ER. 2009. Birt-Hogg-Dube syndrome: diagnosis and management. *The lancet oncology* 10:1199-206.
- Miyoshi Y, Nagase H, Ando H, Horii A, Ichii S, Nakatsuru S, Aoki T, Miki Y, Mori T, Nakamura Y. 1992. Somatic mutations of the APC gene in colorectal tumors: mutation cluster region in the APC gene. *Human molecular genetics* 1:229-33.
- Moon SY, Zheng Y. 2003. Rho GTPase-activating proteins in cell regulation. *Trends Cell Biol* 13:13-22.
- Moreno-Bueno G, Portillo F, Cano A. 2008. Transcriptional regulation of cell polarity in EMT and cancer. *Oncogene* 27:6958-69.

- Morrison PJ, Donnelly DE, Atkinson AB, Maxwell AP. 2010. Advances in the genetics of familial renal cancer. *Oncologist* 15:532-8.
- Motzer RJ, Bander NH, Nanus DM. 1996. Renal-cell carcinoma. *The New England journal of medicine* 335:865-75.
- Nahorski MS, Reiman A, Lim DH, Nookala RK, Seabra L, Lu X, Fenton J, Boora U, Nordenskjold M, Latif F and others. 2011. Birt Hogg-Dube syndrome associated FLCN mutations disrupt protein stability. *Human mutation*
- Narumiya S, Tanji M, Ishizaki T. 2009. Rho signaling, ROCK and mDia1, in transformation, metastasis and invasion. *Cancer Metastasis Rev* 28:65-76.
- Nelson WJ. 2003. Adaptation of core mechanisms to generate cell polarity. *Nature* 422:766-74.
- Neuman NA, Henske EP. 2011. Non-canonical functions of the tuberous sclerosis complex-Rheb signalling axis. *EMBO Mol Med* 3:189-200.
- Ng PC, Henikoff S. 2001. Predicting deleterious amino acid substitutions. *Genome Res* 11:863-74.
- Nickerson ML, Warren MB, Toro JR, Matrosova V, Glenn G, Turner ML, Duray P, Merino M, Choyke P, Pavlovich CP and others. 2002. Mutations in a novel gene lead to kidney tumors, lung wall defects, and benign tumors of the hair follicle in patients with the Birt-Hogg-Dube syndrome. *Cancer Cell* 2:157-64.
- Niessen CM. 2007. Tight junctions/adherens junctions: basic structure and function. *J Invest Dermatol* 127:2525-32.
- Nordstrom-O'Brien M, van der Luijt RB, van Rooijen E, van den Ouweland AM, Majoor-Krakauer DF, Lolkema MP, van Brussel A, Voest EE, Giles RH. 2010. Genetic analysis of von Hippel-Lindau disease. *Human mutation* 31:521-37.
- O'Connell JB, Maggard MA, Ko CY. 2004. Colon cancer survival rates with the new American Joint Committee on Cancer sixth edition staging. *Journal of the National Cancer Institute* 96:1420-5.
- Ohta M, Inoue H, Cotticelli MG, Kastury K, Baffa R, Palazzo J, Siprashvili Z, Mori M, McCue P, Druck T and others. 1996. The FHIT gene, spanning the chromosome 3p14.2 fragile site and renal carcinoma-associated t(3;8) breakpoint, is abnormal in digestive tract cancers. *Cell* 84:587-97.

- Okimoto K, Kouchi M, Matsumoto I, Sakurai J, Kobayashi T, Hino O. 2004a. Natural history of the Nihon rat model of BHD. *Current molecular medicine* 4:887-93.
- Okimoto K, Sakurai J, Kobayashi T, Mitani H, Hirayama Y, Nickerson ML, Warren MB, Zbar B, Schmidt LS, Hino O. 2004b. A germ-line insertion in the Birt-Hogg-Dube (BHD) gene gives rise to the Nihon rat model of inherited renal cancer. *Proceedings of the National Academy of Sciences of the United States of America* 101:2023-7.
- Ong KR, Woodward ER, Killick P, Lim C, Macdonald F, Maher ER. 2007. Genotype-phenotype correlations in von Hippel-Lindau disease. *Human mutation* 28:143-9.
- Painter JN, Tapanainen H, Somer M, Tukiainen P, Aittomaki K. 2005. A 4-bp deletion in the Birt-Hogg-Dube gene (FLCN) causes dominantly inherited spontaneous pneumothorax. *American journal of human genetics* 76:522-7.
- Pal C, Papp B, Lercher MJ. 2006. An integrated view of protein evolution. *Nat Rev Genet* 7:337-48.
- Pantuck AJ, An J, Liu H, Rettig MB. 2010. NF-kappaB-dependent plasticity of the epithelial to mesenchymal transition induced by Von Hippel-Lindau inactivation in renal cell carcinomas. *Cancer research* 70:752-61.
- Parmley JL, Urrutia AO, Potrzebowski L, Kaessmann H, Hurst LD. 2007. Splicing and the evolution of proteins in mammals. *PLoS Biol* 5:e14.
- Pavlovich CP, Grubb RL, Hurley K, Glenn GM, Toro J, Schmidt LS, Torres-Cabala C, Merino MJ, Zbar B, Choyke P and others. 2005. Evaluation and management of renal tumors in the Birt-Hogg-Dube syndrome. *J Urology* 173:1482-1486.
- Pavlovich CP, Walther MM, Eyler RA, Hewitt SM, Zbar B, Linehan WM, Merino MJ. 2002. Renal tumors in the Birt-Hogg-Dube syndrome. *The American journal of surgical pathology* 26:1542-52.
- Perucho M. 1999. Correspondence re: C.R. Boland et al., A National Cancer Institute workshop on microsatellite instability for cancer detection and familial predisposition: development of international criteria for the determination of microsatellite instability in colorectal cancer. *Cancer Res.*, 58: 5248-5257, 1998. *Cancer research* 59:249-56.
- Piekny A, Werner M, Glotzer M. 2005. Cytokinesis: welcome to the Rho zone. *Trends Cell Biol* 15:651-658.

- Polakis P. 2007. The many ways of Wnt in cancer. *Current opinion in genetics & development* 17:45-51.
- Presta LG, Chen H, O'Connor SJ, Chisholm V, Meng YG, Krummen L, Winkler M, Ferrara N. 1997. Humanization of an anti-vascular endothelial growth factor monoclonal antibody for the therapy of solid tumors and other disorders. *Cancer research* 57:4593-9.
- Preston RS, Philp A, Claessens T, Gijezen L, Dydensborg AB, Dunlop EA, Harper KT, Brinkhuizen T, Menko FH, Davies DM and others. 2011. Absence of the Birt-Hogg-Dube gene product is associated with increased hypoxia-inducible factor transcriptional activity and a loss of metabolic flexibility. *Oncogene* 30:1159-73.
- Rawlings JS, Rosler KM, Harrison DA. 2004. The JAK/STAT signaling pathway. *J Cell Sci* 117:1281-3.
- Receveur AO, Couturier J, Molinie V, Vieillefond A, Desangles F, Guillaud-Bataille M, Danglot G, Coullin P, Bernheim A. 2005. Characterization of quantitative chromosomal abnormalities in renal cell carcinomas by interphase four-color fluorescence in situ hybridization. *Cancer Genet Cytogenet* 158:110-8.
- Ren HZ, Zhu CC, Yang C, Chen SL, Xie J, Hou YY, Xu ZF, Wang DJ, Mu DK, Ma DH and others. 2008. Mutation analysis of the FLCN gene in Chinese patients with sporadic and familial isolated primary spontaneous pneumothorax. *Clin Genet* 74:178-83.
- Reynolds AB, Daniel JM, Mo YY, Wu J, Zhang Z. 1996. The novel catenin p120cas binds classical cadherins and induces an unusual morphological phenotype in NIH3T3 fibroblasts. *Exp Cell Res* 225:328-37.
- Ricketts C, Woodward ER, Killick P, Morris MR, Astuti D, Latif F, Maher ER. 2008. Germline SDHB mutations and familial renal cell carcinoma. *Journal of the National Cancer Institute* 100:1260-2.
- Ricketts CJ, Forman JR, Rattenberry E, Bradshaw N, Laloo F, Izatt L, Cole TR, Armstrong R, Kumar VK, Morrison PJ and others. 2010. Tumor risks and genotype-phenotype-proteotype analysis in 358 patients with germline mutations in SDHB and SDHD. *Human mutation* 31:41-51.
- Roberg KJ, Bickel S, Rowley N, Kaiser CA. 1997. Control of amino acid permease sorting in the late secretory pathway of *Saccharomyces cerevisiae* by SEC13, LST4, LST7 and LST8. *Genetics* 147:1569-84.

- Roberts PJ, Der CJ. 2007. Targeting the Raf-MEK-ERK mitogen-activated protein kinase cascade for the treatment of cancer. *Oncogene* 26:3291-310.
- Rongioletti F, Hazini R, Gianotti G, Rebora A. 1989. Fibrofolliculomas, trichodiscomas and acrochordons (Birt-Hogg-Dube) associated with intestinal polyposis. *Clin Exp Dermatol* 14:72-4.
- Rosner I, Bratslavsky G, Pinto PA, Linehan WM. 2009. The clinical implications of the genetics of renal cell carcinoma. *Urol Oncol* 27:131-6.
- Rozen S, Skaletsky H. 2000. Primer3 on the WWW for general users and for biologist programmers. *Methods Mol Biol* 132:365-86.
- Sabatini DM. 2006. mTOR and cancer: insights into a complex relationship. *Nat Rev Cancer* 6:729-34.
- Sadler GJ, Anderson MR, Moss MS, Wilson PG. 2007. Metastases from renal cell carcinoma presenting as gastrointestinal bleeding: two case reports and a review of the literature. *BMC Gastroenterol* 7:4.
- Samarin SN, Ivanov AI, Flatau G, Parkos CA, Nusrat A. 2007. Rho/Rho-associated kinase-II signaling mediates disassembly of epithelial apical junctions. *Mol Biol Cell* 18:3429-39.
- Sarbassov DD, Guertin DA, Ali SM, Sabatini DM. 2005. Phosphorylation and regulation of Akt/PKB by the rictor-mTOR complex. *Science (New York, N.Y)* 307:1098-101.
- Schachtschabel AA, Kuster W, Happle R. 1996. [Perifollicular fibroma of the skin and colonic polyps: Hornstein-Knickenberg syndrome]. *Der Hautarzt; Zeitschrift für Dermatologie, Venerologie, und verwandte Gebiete* 47:304-6.
- Schmidt L, Duh FM, Chen F, Kishida T, Glenn G, Choyke P, Scherer SW, Zhuang Z, Lubensky I, Dean M and others. 1997. Germline and somatic mutations in the tyrosine kinase domain of the MET proto-oncogene in papillary renal carcinomas. *Nature genetics* 16:68-73.
- Schmidt L, Li F, Brown RS, Berg S, Chen F, Wei MH, Tory K, Lerman I, Zbar B. 1995. Mechanism of tumorigenesis of renal carcinomas associated with the constitutional chromosome 3;8 translocation. *Cancer J Sci Am* 1:191-5.
- Schmidt LS, Nickerson ML, Warren MB, Glenn GM, Toro JR, Merino MJ, Turner ML, Choyke PL, Sharma N, Peterson J and others. 2005. Germline BHD-mutation spectrum and phenotype analysis of a large

- cohort of families with Birt-Hogg-Dube syndrome. *American journal of human genetics* 76:1023-33.
- Schmidt LS, Warren MB, Nickerson ML, Weirich G, Matrosova V, Toro JR, Turner ML, Duray P, Merino M, Hewitt S and others. 2001. Birt-Hogg-Dube syndrome, a genodermatosis associated with spontaneous pneumothorax and kidney neoplasia, maps to chromosome 17p11.2. *American journal of human genetics* 69:876-82.
- Schubbert S, Shannon K, Bollag G. 2007. Hyperactive Ras in developmental disorders and cancer. *Nat Rev Cancer* 7:295-308.
- Schulz T, Hartschuh W. 1999. Birt-Hogg-Dube syndrome and Hornstein-Knickenberg syndrome are the same. Different sectioning technique as the cause of different histology. *Journal of cutaneous pathology* 26:55-61.
- Selak MA, Armour SM, MacKenzie ED, Boulahbel H, Watson DG, Mansfield KD, Pan Y, Simon MC, Thompson CB, Gottlieb E. 2005. Succinate links TCA cycle dysfunction to oncogenesis by inhibiting HIF-alpha prolyl hydroxylase. *Cancer Cell* 7:77-85.
- Semenza GL. 2004. Hydroxylation of HIF-1: oxygen sensing at the molecular level. *Physiology (Bethesda)* 19:176-82.
- Shah OJ, Wang Z, Hunter T. 2004. Inappropriate activation of the TSC/Rheb/mTOR/S6K cassette induces IRS1/2 depletion, insulin resistance, and cell survival deficiencies. *Curr Biol* 14:1650-6.
- Shin JH, Shin YK, Ku JL, Jeong SY, Hong SH, Park SY, Kim WH, Park JG. 2003. Mutations of the Birt-Hogg-Dube (BHD) gene in sporadic colorectal carcinomas and colorectal carcinoma cell lines with microsatellite instability. *J Med Genet* 40:364-7.
- Siegel PM, Massague J. 2003. Cytostatic and apoptotic actions of TGF-beta in homeostasis and cancer. *Nat Rev Cancer* 3:807-21.
- Singh SR, Zhen W, Zheng Z, Wang H, Oh SW, Liu W, Zbar B, Schmidt LS, Hou SX. 2006. The Drosophila homolog of the human tumor suppressor gene BHD interacts with the JAK-STAT and Dpp signaling pathways in regulating male germline stem cell maintenance. *Oncogene* 25:5933-41.
- So SY. 2009. Spontaneous pneumothorax due to Birt-Hogg-Dube syndrome in a Chinese family. *Respirology* 14:775-6.
- Souza RF, Appel R, Yin J, Wang S, Smolinski KN, Abraham JM, Zou TT, Shi YQ, Lei J, Cottrell J and others. 1996. Microsatellite instability in

- the insulin-like growth factor II receptor gene in gastrointestinal tumours. *Nature genetics* 14:255-7.
- Sparks AB, Morin PJ, Vogelstein B, Kinzler KW. 1998. Mutational analysis of the APC/beta-catenin/Tcf pathway in colorectal cancer. *Cancer research* 58:1130-4.
- Spiering D, Hodgson L. 2011. Dynamics of the Rho-family small GTPases in actin regulation and motility. *Cell Adh Migr* 5:170-80.
- Stec R, Grala B, Maczewski M, Bodnar L, Szczylik C. 2009. Chromophobe renal cell cancer--review of the literature and potential methods of treating metastatic disease. *J Exp Clin Cancer Res* 28:134.
- Sternberg CN, Davis ID, Mardiak J, Szczylik C, Lee E, Wagstaff J, Barrios CH, Salman P, Gladkov OA, Kavina A and others. 2010. Pazopanib in locally advanced or metastatic renal cell carcinoma: results of a randomized phase III trial. *J Clin Oncol* 28:1061-8.
- Su LK, Vogelstein B, Kinzler KW. 1993. Association of the APC tumor suppressor protein with catenins. *Science (New York, N.Y)* 262:1734-7.
- Sunyaev S, Ramensky V, Koch I, Lathe W, 3rd, Kondrashov AS, Bork P. 2001. Prediction of deleterious human alleles. *Human molecular genetics* 10:591-7.
- Takagi Y, Kobayashi T, Shiono M, Wang L, Piao X, Sun G, Zhang D, Abe M, Hagiwara Y, Takahashi K and others. 2008. Interaction of folliculin (Birt-Hogg-Dube gene product) with a novel Fnip1-like (FnipL/Fnip2) protein. *Oncogene* 27:5339-47.
- Tamura K, Nei M. 1993. Estimation of the number of nucleotide substitutions in the control region of mitochondrial DNA in humans and chimpanzees. *Mol Biol Evol* 10:512-26.
- Tapon N, Ito N, Dickson BJ, Treisman JE, Hariharan IK. 2001. The *Drosophila* tuberous sclerosis complex gene homologs restrict cell growth and cell proliferation. *Cell* 105:345-55.
- Tee AR, Manning BD, Roux PP, Cantley LC, Blenis J. 2003. Tuberous sclerosis complex gene products, Tuberin and Hamartin, control mTOR signaling by acting as a GTPase-activating protein complex toward Rheb. *Curr Biol* 13:1259-68.
- Tejpar S, Van Cutsem E. 2002. Molecular and genetic defects in colorectal tumorigenesis. *Best practice & research* 16:171-85.

- Tervonen TA, Partanen JI, Saarikoski ST, Myllynen M, Marques E, Paasonen K, Moilanen A, Wohlfahrt G, Kovanen PE, Klefstrom J. 2011. Faulty epithelial polarity genes and cancer. *Adv Cancer Res* 111:97-161.
- Thiery JP. 2003. Epithelial-mesenchymal transitions in development and pathologies. *Current opinion in cell biology* 15:740-6.
- Thusberg J, Vihinen M. 2009. Pathogenic or not? And if so, then how? Studying the effects of missense mutations using bioinformatics methods. *Human mutation* 30:703-14.
- Timpson P, McGhee EJ, Morton JP, von Kriegsheim A, Schwarz JP, Karim SA, Doyle B, Quinn JA, Carragher NO, Edward M and others. 2011. Spatial regulation of RhoA activity during pancreatic cancer cell invasion driven by mutant p53. *Cancer research* 71:747-57.
- Togashi Y, Kobayashi T, Momose S, Ueda M, Okimoto K, Hino O. 2006. Transgenic rescue from embryonic lethality and renal carcinogenesis in the Nihon rat model by introduction of a wild-type Bhd gene. *Oncogene* 25:2885-9.
- Tomlinson IP, Alam NA, Rowan AJ, Barclay E, Jaeger EE, Kelsell D, Leigh I, Gorman P, Lamlum H, Rahman S and others. 2002. Germline mutations in FH predispose to dominantly inherited uterine fibroids, skin leiomyomata and papillary renal cell cancer. *Nature genetics* 30:406-10.
- Toro JR, Glenn G, Duray P, Darling T, Weirich G, Zbar B, Linehan M, Turner ML. 1999. Birt-Hogg-Dube syndrome: a novel marker of kidney neoplasia. *Archives of dermatology* 135:1195-202.
- Toro JR, Pautler SE, Stewart L, Glenn GM, Weinreich M, Toure O, Wei MH, Schmidt LS, Davis L, Zbar B and others. 2007. Lung cysts, spontaneous pneumothorax, and genetic associations in 89 families with Birt-Hogg-Dube syndrome. *American journal of respiratory and critical care medicine* 175:1044-53.
- Toro JR, Wei MH, Glenn GM, Weinreich M, Toure O, Vocke C, Turner M, Choyke P, Merino MJ, Pinto PA and others. 2008. BHD mutations, clinical and molecular genetic investigations of Birt-Hogg-Dube syndrome: a new series of 50 families and a review of published reports. *J Med Genet* 45:321-31.
- Umemura K, Takagi S, Ishigaki Y, Iwabuchi M, Kuroki S, Kinouchi Y, Shimosegawa T. 2008. Gastrointestinal polyposis with esophageal

- polyposis is useful for early diagnosis of Cowden's disease. *World J Gastroenterol* 14:5755-9.
- Valastyan S, Weinberg RA. 2011. Tumor metastasis: molecular insights and evolving paradigms. *Cell* 147:275-92.
- Valentino L, Pierre J. 2006. JAK/STAT signal transduction: regulators and implication in hematological malignancies. *Biochem Pharmacol* 71:713-21.
- van Slegtenhorst M, de Hoogt R, Hermans C, Nellist M, Janssen B, Verhoef S, Lindhout D, van den Ouweland A, Halley D, Young J and others. 1997. Identification of the tuberous sclerosis gene TSC1 on chromosome 9q34. *Science (New York, N.Y)* 277:805-8.
- van Slegtenhorst M, Khabibullin D, Hartman TR, Nicolas E, Kruger WD, Henske EP. 2007. The Birt-Hogg-Dube and tuberous sclerosis complex homologs have opposing roles in amino acid homeostasis in *Schizosaccharomyces pombe*. *The Journal of biological chemistry* 282:24583-90.
- van Steensel MA, Verstraeten VL, Frank J, Kelleners-Smeets NW, Poblete-Gutierrez P, Marcus-Soekarman D, Bladergroen RS, Steijlen PM, van Geel M. 2007. Novel mutations in the BHD gene and absence of loss of heterozygosity in fibrofolliculomas of Birt-Hogg-Dube patients. *J Invest Dermatol* 127:588-93.
- Vivanco I, Sawyers CL. 2002. The phosphatidylinositol 3-Kinase AKT pathway in human cancer. *Nat Rev Cancer* 2:489-501.
- Vocke CD, Yang Y, Pavlovich CP, Schmidt LS, Nickerson ML, Torres-Cabala CA, Merino MJ, Walther MM, Zbar B, Linehan WM. 2005. High frequency of somatic frameshift BHD gene mutations in Birt-Hogg-Dube-associated renal tumors. *Journal of the National Cancer Institute* 97:931-5.
- Wang Z, Moulton J. 2001. SNPs, protein structure, and disease. *Human mutation* 17:263-70.
- Warren MB, Torres-Cabala CA, Turner ML, Merino MJ, Matrosova VY, Nickerson ML, Ma W, Linehan WM, Zbar B, Schmidt LS. 2004. Expression of Birt-Hogg-Dube gene mRNA in normal and neoplastic human tissues. *Mod Pathol* 17:998-1011.
- Watanabe N, Madaule P, Reid T, Ishizaki T, Watanabe G, Kakizuka A, Saito Y, Nakao K, Jockusch BM, Narumiya S. 1997. p140mDia, a

- mammalian homolog of *Drosophila diaphanous*, is a target protein for Rho small GTPase and is a ligand for profilin. *EMBO J* 16:3044-56.
- Woerner SM, Benner A, Sutter C, Schiller M, Yuan YP, Keller G, Bork P, Doeberitz MK, Gebert JF. 2003. Pathogenesis of DNA repair-deficient cancers: a statistical meta-analysis of putative Real Common Target genes. *Oncogene* 22:2226-35.
- Wolf A, Keil R, Gotzl O, Mun A, Schwarze K, Lederer M, Huttelmaier S, Hatzfeld M. 2006. The armadillo protein p0071 regulates Rho signalling during cytokinesis. *Nature cell biology* 8:1432-40.
- Wood LD, Parsons DW, Jones S, Lin J, Sjoblom T, Leary RJ, Shen D, Boca SM, Barber T, Ptak J and others. 2007. The genomic landscapes of human breast and colorectal cancers. *Science (New York, N.Y)* 318:1108-13.
- Woodward ER, Maher ER. 2006. Von Hippel-Lindau disease and endocrine tumour susceptibility. *Endocr Relat Cancer* 13:415-25.
- Woodward ER, Ricketts C, Killick P, Gad S, Morris MR, Kavalier F, Hodgson SV, Giraud S, Bressac-de Paillerets B, Chapman C and others. 2008. Familial non-VHL clear cell (conventional) renal cell carcinoma: clinical features, segregation analysis, and mutation analysis of FLCN. *Clin Cancer Res* 14:5925-30.
- Woodward ER, Skytte AB, Cruger DG, Maher ER. 2010. Population-based survey of cancer risks in chromosome 3 translocation carriers. *Genes Chromosomes Cancer* 49:52-8.
- Wyckoff JB, Pinner SE, Gschmeissner S, Condeelis JS, Sahai E. 2006. ROCK- and myosin-dependent matrix deformation enables protease-independent tumor-cell invasion in vivo. *Curr Biol* 16:1515-23.
- Yim KL. 2011. Microsatellite instability in metastatic colorectal cancer: a review of pathology, response to chemotherapy and clinical outcome. *Med Oncol*
- Zbar B, Alvord WG, Glenn G, Turner M, Pavlovich CP, Schmidt L, Walther M, Choyke P, Weirich G, Hewitt SM and others. 2002. Risk of renal and colonic neoplasms and spontaneous pneumothorax in the Birt-Hogg-Dube syndrome. *Cancer Epidemiol Biomarkers Prev* 11:393-400.
- Zheng Y. 2001. Dbl family guanine nucleotide exchange factors. *Trends Biochem Sci* 26:724-32.

Zuckerkandl E. 1976. Evolutionary processes and evolutionary noise at the molecular level. I. Functional density in proteins. *J Mol Evol* 7:167-83.

Chapter 9 Peer Reviewed Publications

1. Investigation of the Birt-Hogg-Dube tumour suppressor gene (FLCN) in familial and sporadic colorectal cancer.

Nahorski MS, Lim DH, Martin L, Gille JJ, McKay K, Rehal PK, Ploeger HM, van Steensel M, Tomlinson IP, Latif F, Menko FH, Maher ER.
J Med Genet. 2010 Jun;47(6):385-90

2. Birt Hogg-Dubé syndrome-associated FLCN mutations disrupt protein stability.

Nahorski MS, Reiman A, Lim DH, Nookala RK, Seabra L, Lu X, Fenton J, Boora U, Nordenskjöld M, Latif F, Hurst LD, Maher ER.
Hum Mutat. 2011 Aug;32(8):921-9. doi: 10.1002/humu.21519. Epub 2011 Jul 12

3. A new locus-specific database (LSDB) for mutations in the folliculin (FLCN) gene.

Lim DH, Rehal PK, **Nahorski MS**, Macdonald F, Claessens T, Van Geel M, Gijezen L, Gille JJ, Giraud S, Richard S, van Steensel M, Menko FH, Maher ER.
Hum Mutat. 2010 Jan;31(1):E1043-51

4. Therapeutic targeting the loss of the birt-hogg-dube suppressor gene.

Lu X, Wei W, Fenton J, **Nahorski MS**, Rabai E, Reiman A, Seabra L, Nagy Z, Latif F, Maher ER.
Mol Cancer Ther. 2011 Jan;10(1):80-9.

5. Folliculin interacts with p0071 and regulates RhoA signalling, cell polarisation and cytokinesis

Michael S Nahorski, Laurence Seabra, AniaStraatman-Iwanowska, Aileen Wingefeld, Anne Reiman, Xiaohong Lu, Paul Gissen, Mechthild Hatzfeld, Eamonn R Maher (in preparation for re-submission to J Cell Biol)